UNIVERSITÀ DEGLI STUDI DI TRIESTE

SEDE AMMINISTRATIVA DEL DOTTORATO DI RICERCA

SCUOLA DI DOTTORATO D'INGEGNERIA DELL'INFORMAZIONE

XXV CICLO

VALIDATION AND APPLICATION OF A SHOULDER AMBULATORY MOTION ANALYSIS PROTOCOL

(SSD ING-INF/06 Bioingegneria Elettronica ed Informatica)

Dottoranda

ILARIA PAREL

Direttore della Scuola

CHIAR.MO PROF. WALTER UKOVICH

UNIVERSITÀ DEGLI STUDI DI TRIESTE

Supervisore

CHIAR.MO PROF. AGOSTINO ACCARDO

UNIVERSITÀ DEGLI STUDI DI TRIESTE

Co-Supervisore

PHD ING. ANDREA GIOVANNI CUTTI

CENTRO PROTESI INAIL (BUDRIO)

ANNO ACCADEMICO 2011/2012

Ilaria Parel:
Validation and application of a shoulder ambulatory motion analysis protocol, 2013

Email:
ilariaparel@gmail.com

Contents

GENERAL INTRODUCTION

The shoulder is a complex of joints that allows the relative motion of the humerus respect to the thorax. The main bones forming this structure are: clavicle, humerus, scapula and thorax. These bones form five joints, namely: sternoclavicular, between sternum and clavicle; acromioclavicular, between acromion (i.e. scapula) and clavicle; glenohumeral, between the glenoid fossa (i.e. scapula) and the humerus; under-deltoid, between acromion and humerus; scapulothoracic, between scapula and thorax. Only the fist three joints are in the anatomical sense (i.e. two surfaces covered by cartilage), while the last two are in the physiological sense (i.e. two surfaces which slide one with respect to the other without any interposed cartilage) [1].

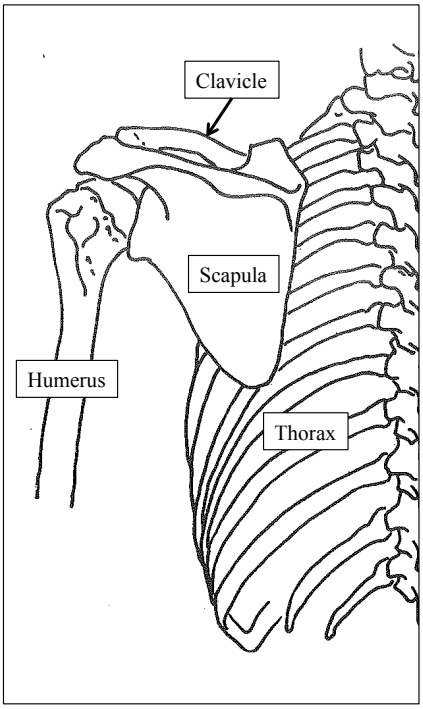

FIGURE 1. Shoulder bones: clavicle, humerus, scapula and thorax [1].

Among the five joints, the glenohumeral is one of the most complex articulations. This structure is a ball and socket joint, characterized by a small ratio between the articular surfaces of the humeral head and the glenoid fossa of the scapula. The glenoid fossa has an elliptical shape and is about 1/3-1/4 of the humeral head. This small congruence is increased by the labrum, which is the fibrous attachment of the gleno-humeral ligaments and capsule to the glenoid fossa. The relatively loose fitting of the humerus into the scapula glenoid permits a wide range of motion, but it also makes the structure vulnerable to injury. The stability of the joint is ensured by arm's and rotator cuff muscles, 2 ligaments (coraco-humeral and glenohumeral ligaments), the acromion and the subacromial bursa, which prevent from dislocations keeping the humeral head in contact with the glenoid fossa during

movements. In particular, the rotator cuff is formed by a group of 4 muscles and tendons, which stabilize the shoulder: supraspinatus, infraspinatus, teres minor and subscapularis [1].

The coordinated movement between scapula and humerus, when this latter is elevated, is called "scapulo-humeral rhythm" (SHR). From the clinical viewpoint, the SHR is typically analyzed during humerus elevation in the sagittal plane (humerus flexion) and in the scapular and frontal planes (humerus abduction) [2]. In particular, examining the shoulder elevation in the frontal and sagittal plane, it was found that 2/3 of the movements (120°) was due to glenohumeral mobility, while the left third was due to the scapulothoracic mobility (60°) [3].

Flexion movement can be divided in three phases, based on muscles recruited (Figure 2):

- From 0° to 50°-60°: anterior deltoid (1), coracobrachialis (2), greater pectoralis (3);
- From 60° to 120° the SHR starts: trapezius (4 and 5) and latissimus dorsi (6) take place in the movement;
- From 120° to 180°: the scapulo-thoracic and gleno-humeral movements interrupt and spinal muscles (7) are activated.

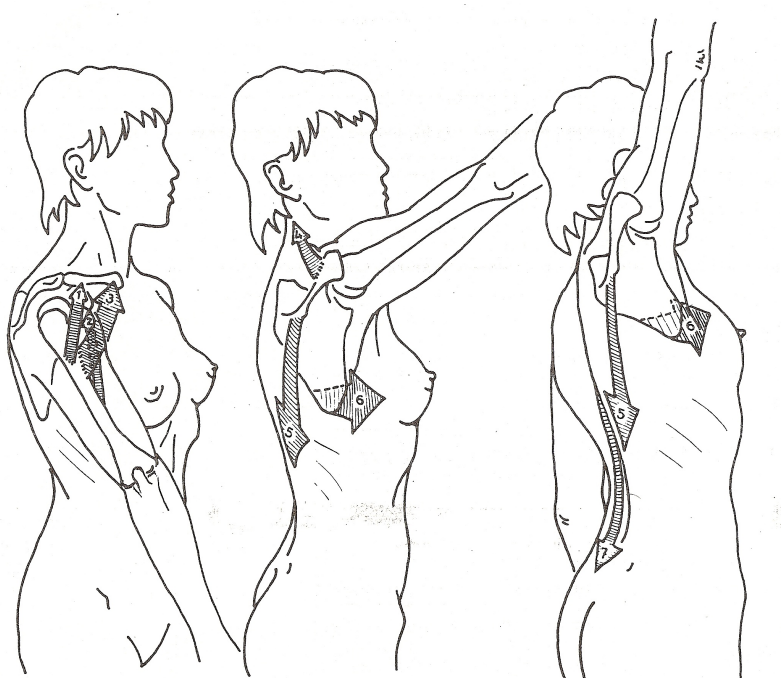

FIGURE 2. Muscles involved in shoulder flexion [1].

Abduction movement can be divided in three phases, based on muscles recruited:

- From 0° to 90°: deltoid (1), supraspinatus (2);
- From 90° to 150° the scapulo-humeral joint is blocked and the movement can proceed thanks to the shoulder girdle: trapezius (3 and 4) and latissimus dorsi (5);
- From 150° to 180°: the spinal muscles (6) are activated.

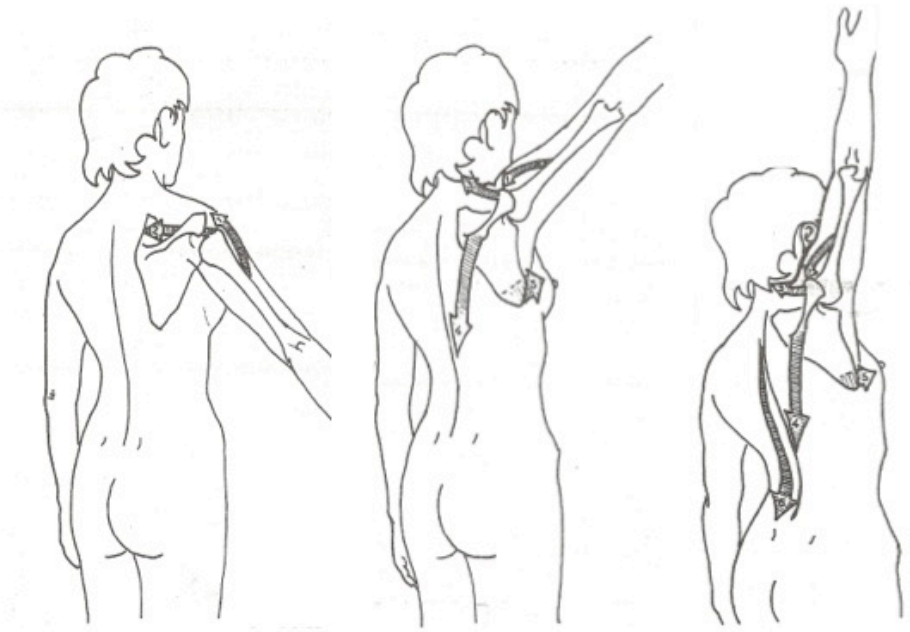

FIGURE 3 Muscles involved in shoulder abduction [1].

Traumatic events or degenerative pathologies can cause an improper balance of shoulder structures leading to musculoskeletal diseases.

Some of the most relevant individual factors that are known to increase the risk of shoulder pain and rotator cuff disease are gender, age and obesity [4]. Furthermore, literature shows that there are several work-related biomechanical factors associated with shoulder pain and rotator cuff syndromes, i.e. heavy lifting, forceful manual exertion, repetitive movements and the use of vibrating hand tools [4].

Nowadays, shoulder pathologies are an increasingly problem among workers and overhead athletes [4,5]. In particular, rotator cuff tear represents the most common shoulder pathology and was shown as the principal source of morbidity in working population [6-9]. Spigno et al [8] reports a retrospective study about shoulder accidents at work, conducted by the Genoa office of the Italian

Worker Compensation Authority (INAIL) during a period of two years (2006-2007). In this study rotator cuff tear is addressed as the most frequent pathology occurring among employees, indicating manual workers as the most affected category.

A dysfunction of the rotator cuff anatomical structures generally causes pain, lack of force and variations of shoulder kinematics, in particular in the scapulo-humeral rhythm (SHR) [10], which is defined as the coordinated movement between the scapula and humerus, when this latter is elevated. The alteration of the SHR can be drawn back to two primary causes [11]:

- protection factor: a pain adaptation model can be considered in light of a reorganization in muscles activity and scapula kinematics that can occurs in response to pain, in order to minimize disturbances. The increased scapula movements can be interpreted as a protection factor, moving the acromion away from the humeral head to avoid impingement syndrome, which occurs when there is an inflammation of tendons of the rotator cuff muscles as they pass through the subacromial space (passage beneath the acromion);
- muscles dysfunction: a reduction of scapula motion in persons with shoulder disorders can be interpreted as a primary cause of shoulder syndrome. A delayed, an inhibited or less active serratus anterior muscle and trapezius muscle can cause alterations inducing muscles imbalances and subsequent shoulder pathologies. In this case scapula motion alterations do not preserve the optimal kinematics and contribute to the development of pain and pathology.

Shoulder pain together with upper limb dysfunctions reduces self-care and functional autonomy. Rehabilitation treatments generally aim at recover arm function and reduce shoulder pain, in order to increase the quality of life of patients [11].

To better understand the role of scapular kinematics in relation to shoulder pathologies, accurate in-vivo measurements are necessary, possibly in real-life conditions. The quantitative analysis of the SHR has been considered as a basic aspect for a complete evaluation of shoulder performance [10-12], but, unfortunately, so far, the quantitative measure of SHR has been limited to few highly advanced medical centers, where dedicated motion analysis laboratories featuring expensive optoelectronic systems are available. A few years ago a new technology, based on inertial and magnetic measurement systems (IMMSs), was presented for motion analysis applications. Thanks to its low-cost and portable features, this new technology potentially permits a broader diffusion.

A motion analysis protocol was developed at INAIL Prostheses Center, named ISEO (INAIL Shoulder & Elbow Outpatient-clinic protocol). ISEO uses inertial and magnetic sensors to measure the kinematics of the upper limb. ISEO is the only peer-reviewed published protocol currently available to measure the SHR with IMMSs. To measure the SHR, the protocol uses the Xbus kit (Xsens Technologies NL), composed of 4 MTx sensor units, a Xbus master, a Bluetooth transceiver and cables. Each MTx is a small (38x53x21mm) and lightweight (30g) box, containing a 3D gyroscope, accelerometer and magnetometer, which together provide the orientation of the technical coordinate system of the MTx relative to a global, earth-based coordinate system (Xsens Technical Manual).

FIGURE 4. Xsens Xbus kit (Xsens Technologies NL).

For the application of ISEO, the following steps must then be followed [15]:

- Sensor placement on thorax, scapula, humerus and forearm (Figure 5). The thorax MTx is placed on the flat portion of the sternum. The scapular MTx is placed on the skin, just above the scapular spine, over the central third between the angulus acromialis and the trigonum spinae, aligning the MTx with the upper edge of the scapular spine. The upper arm MTx sensors are placed on elastic cuffs, respectively over the central third of the humerus, slightly posterior and over the distal third of the forearm.
- Defining the anatomical coordinate systems. For this purpose, a static measure is performed with the subject standing in a pre-defined posture to complete the sensor-to-segment

calibration: upright position, elbow flexed at 90°, neutral forearm rotation, humerus perpendicular to the ground and in neutral rotation;

- Defining functional axes. For this purpose, elbow flexion-extension and pronation-supination are executed, in order to define respectively the flexion-extension axis of the elbow and the pronation-supination axis of the forearm.
- Calculation of joint kinematics. The scapula and humerus orientations are expressed relative to the thorax. The scapula orientation is expressed in terms of protraction-retraction (PR-RE), medio-lateral rotation (ME-LA) and posterior-anterior tilting (P-A), while the humerus orientation in terms of flexion-extension (FL-EX), abduction-adduction (AB-AD) and internal-external rotation (IN-EX) for sagittal plane movements; AB-AD, FL-EX and IN-EX for the scapular plane movements.

ISEO is based on a MATLAB (The MathWorks, USA) custom made software and the MTx software development kit.

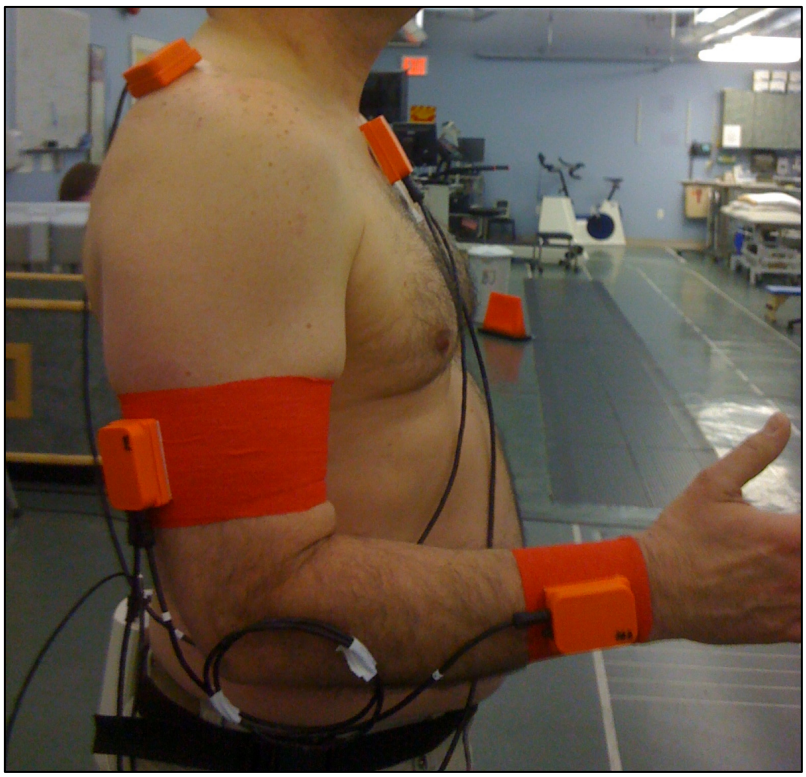

FIGURE 5. ISEO setup: sensors placement on a subject standing in the predefined-posture.

Preliminary results have confirmed the validity of ISEO to measure upper-limb kinematics [13], but, in order to investigate the applicability of ISEO for shoulder assessments, further investigations were needed to assess the influence of different operators in the application of the protocol and to support the applicability of ISEO in clinical surveys.

Therefore, the aim of this dissertation can be split in three main parts.

The first part is the validation of ISEO in terms of operator agreement, inter-protocol agreement for the scapulo-humeral coordination tracking and definition of prediction bands, in particular:

- evaluation of the intra- and inter-operator agreement in measuring the scapulo-humeral coordination;
- definition of prediction bands and intervals for the scapulo-humeral coordination, based on asymptomatic subjects;
- assessment of the agreement between ISEO and a reference protocol currently in use at different motion analysis laboratories.

The second part is about the application of ISEO for clinical assessments:

- a longitudinal study aimed at analyze the recovery of the shoulder for patients surgically treated for rotator cuff tear;
- the analysis of changes in shoulder kinematics of transradial amputees following the use of multi-grip prosthetic hands.

The third part is about the application of ISEO for performance assessments:

- a feasibility study for the assessment of the upper limb kinematics of a Formula 1 pit-crew during the pit-stop;
- upper limb functional evaluations on baseball pitchers.

The subsequent chapters summarize the results obtained for each theme reported above, providing scientific manuscripts published or submitted to scientific journals or national and international conferences.

REFERENCES

1. Kapandji I.A. Fisiologia articolare. 2010. Mailone. Monduzzi Editore
2. Ludewig PM, Reynolds JF. The Association of Scapular Kinematics and Glenohumeral Joint Pathologies. J Orthop Sports Phys Ther 2009; 39(2): 90-104
3. Nordin, M. and Frankel, V.H. Basic Biomechanics of the Musculoskeletal System. 1989. Lea & Febiger, Philadelphia, London.
4. Bodin J., Ha C., Chastang J.F., Descada A., Leclerc A., Goldberg M., Imbernon E., Roquelaure Y. Comparison of risk factors for shoulder pain and rotator cuff syndrome in the working population. Am J Ind Med 2012; 55: 605-615
5. Moen T.C, Babatunde O.M., Hsu S.H., Ahmad C.S., Levine W.N. Suprascapular neuropathy: what does the literature show? J Shoulder Elbow Surg 2012. 21: 835-846
6. Mell A.G., LaScalza S., Guffey P., Ray J., Maciejewski M., Carpenter J.E., Hughes R.E., Arbor A. Effect of rotator cuff pathology on shoulder rhythm. J Shoulder Elbow Surg 2005. 14:58S-64S
7. Melchior M., Roquelaure Y., Evanoff B.A., Chastang J. F., C. Ha C. Why are manual workers at high risk of upper limb disorders? The role of physical work factors in a random sample of workers in France (the Pays de la Loire study). Occup Environ Med 2006. 63: 754-761
8. Spigno F, Galli R., Casali C., Lagattolla N., De Lucchi M. La patologia della cuffia dei rotatori in Medicina del Lavoro tra tecnopatia ed infortunio: considerazioni medico-legali. G Ital Med Lav Erg 2010; 32:1, 68-73
9. Seo S.S., Choi J.S., An K.C., Kim J.H., Kim S.B. The factors affecting stiffness occurring with rotator cuff tear. J Shoulder Elbow Surg 2012. 21: 304-309
10. Ludewig PM, Reynolds JF. The Association of Scapular Kinematics and Glenohumeral Joint Pathologies. J Orthop Sports Phys Ther 2009; 39(2): 90-104
11. De Baets L., Jaspers E., Desloovere K., Van Deun S. A systematic review of 3D scapular kinematics and muscle activity during elevation in stroke subjects and controls. J Electromyogr Kinesiol. http://dx.doi.org/10.1016/j.jelekin.2012.06.007
12. Kibler W.B., Sciascia A. Current concepts: scapular dyskinesis. Br J Sports Med 2010. 44:300-305
13. Cutti AG, Cutti AG, Giovanardi A, Rocchi L, Davalli A, Sacchetti R. Ambulatory measurement of shoulder and elbow kinematics through inertial and magnetic sensors. Med Bio Eng Comput 2008; 46(2): 169-78

PART 1

Characterization and validation of ISEO

(INAIL Shoulder and Elbow Outpatient protocol)

In this section the studies about operator agreement, inter-protocol agreement for the scapulo-humeral coordination tracking and the definition of prediction bands are reported.
The aim of this section is to assess ISEO in order to validate and characterize its applicability in clinical and ambulatory contexts.

Chapter 1 reports the investigation about the operator agreement permits to quantify the error in scapulo-humeral coordination measure due to the re-application of the protocol by both the same operator and two different operators.

Chapter 2 reports the study about definition of prediction bands for the scapulo-humeral coordination provides reference data that would allow classifying a patient as either symptomatic or asymptomatic.

Chapter 3 reports a study about the analysis of the inter-protocol agreement comparing ISEO with a reference protocol. The aim was to assess the possibility to conduct multi-center clinical and research studies on shoulder kinematics.

Chapter 1

Ambulatory measurement of the scapulohumeral rhythm: intra- and inter operator agreement of a protocol based on inertial and magnetic sensors

Parel I, Cutti AG, Fiumana G, Porcellini G, Verni G, Accardo AP.
Gait & Posture 2012, 35: 636–640.

ABSTRACT

To measure the scapulohumeral rhythm (SHR) in outpatient settings, the motion analysis protocol named ISEO (INAIL Shoulder and Elbow Outpatient protocol) was developed, based on inertial and magnetic sensors. To complete the sensor-to-segment calibration, ISEO requires the involvement of an operator for sensor placement and for positioning the patient's arm in a predefined posture. Since this can affect the measure, this study aimed at quantifying ISEO intra- and inter-operator agreement. Forty subjects were considered, together with two operators, A and B. Three measurement sessions were completed for each subject: two by A and one by B. In each session, the humerus and scapula rotations were measured during sagittal and scapular plane elevation movements. ISEO intra- and inter-operator agreement were assessed by computing, between sessions, the: 1) similarity of the scapulohumeral patterns through the Coefficient of Multiple Correlation (CMC_2), both considering and excluding the difference of the initial value of the scapula rotations between two sessions (inter-session offset); 2) 95% Smallest Detectable Difference (SDD_{95}) in scapula range of motion.

Results for CMC_2 showed that the intra- and inter-operator agreement is acceptable (median$\geq$0.85, lower-whisker $\geq$0.75) for most of the scapula rotations, independently from the movement and the inter-session offset. The only exception is the agreement for scapula protraction-retraction and for scapula medio-lateral rotation during abduction (inter-operator), which is acceptable only if the inter-session offset is removed. SDD_{95} values ranged from 4.4° to 8.6° for the inter-operator and between 4.9° to 8.5° for the intra-operator agreement.

In conclusion, ISEO presents a high intra- and inter-operator agreement, particularly with the scapula inter-session offset removed.

1. INTRODUCTION

A clinical parameter heavily affected in most shoulder disorders is the scapulohumeral rhythm (SHR) [1], which is the coordinated movement between scapula and humerus, when the latter is elevated [2]. From the clinical viewpoint, the SHR is mainly analyzed during humerus elevations in the sagittal, scapular and frontal plane [1]. For each elevation plane, the SHR can be visualized by means of three angle-angle plots [3-6], whereby the scapulothoracic protraction-retraction (PR-RE), the medio-lateral rotation (ME-LA), and the posterior-anterior tilting (P-A) are plotted against the humerothoracic elevation.

Several methods have been developed to measure the SHR, which can be differentiated based on the scapular tracking technique. The current gold standard procedure requires fixing cortical pins

into the scapular bone, removing all soft-tissue artifacts [7]. This method is however highly invasive, and thus of limited applicability in routine practice. Consequently, non-invasive approaches have been developed, namely the palpation technique [8,9], the scapula locator [10,11], the scapular tracker [7] and the acromion marker cluster [5,12,13,14]. Another recent, non-invasive and easy-to-use technique is the one proposed by Cutti et al. [15], as part of the "INAIL Shoulder & Elbow Outpatient protocol" (ISEO), which is based on an Inertial and Magnetic Measurement System (IMMS, Xsens Technologies, NL). The tracking of the scapula is performed using a sensor positioned directly on the skin, just above the scapular spine.

Preliminary results have confirmed the validity of ISEO to measure upper-limb kinematics [15]. However, since ISEO requires the intervention of an operator for positioning the sensors and for guiding the anatomical calibration trial, the aim of this work was to assess the intra- and inter-operator agreement [16] of ISEO in measuring the SHR.

2. METHODS

2.1 SUBJECTS

Twenty healthy subjects with no history of shoulder pathology (7 female and 13 male, age: 28.3 ± 5.5, BMI: 22.4 ± 1.8) and 20 pathologic subjects (8 female and 12 male, age: 43.9 ± 19.9, BMI: 23.9 ± 4.8) were involved in the experiments, together with two operators (A and B) familiar with the protocol. Pathologic subjects were recovering from different shoulder pathologies and they were able to actively and repeatedly elevate the humerus to a minimum of 70° in the sagittal plane and 45° in the scapular plane.

Since agreement between measurements does not depend on the population in which measurements are made (being a characteristic of the measurement method involved) [16, 17], for the aim of the study healthy and pathologic subjects were considered as a single group of 40 individuals.

All subjects gave their informed consent.

2.2 INSTRUMENTATION AND UPPER EXTREMITY MOTION ANALYSIS PROTOCOL

To measure the SHR, ISEO uses 3 MTx sensor units (Xsens Technologies, NL). Each MTx is a small (38x53x21mm) and lightweight (30g) box, containing a 3D-gyroscope, accelerometer and magnetometer, which together provide the orientation of the technical coordinate system of the MTx relative to a global, earth-based coordinate system (Xsens Technical Manual).

For the application of ISEO, the following steps must then be followed [15]:

- Sensor placement on thorax, scapula and humerus (Figure 1). The thorax MTx is placed on the flat portion of the sternum. The scapular MTx is placed on the skin, just above the scapular spine, over the central third between the angulus acromialis and the trigonum spinae, aligning the MTx with the upper edge of the scapular spine. The upper arm MTx is placed on an elastic cuff, over the central third of the humerus, slightly posterior.
- Static calibration measure. A static measure is performed with the subject standing in a pre-defined posture to complete the sensor-to-segment calibration, i.e. the calculation of the anatomical coordinate systems: upright position, elbow flexed at 90°, neutral forearm rotation, humerus perpendicular to the ground and in neutral rotation;
- Calculation of joint kinematics. The scapula and humerus orientations are expressed relative to the thorax. The scapula orientation is expressed in terms of protraction-retraction (PR-RE), medio-lateral rotation (ME-LA) and posterior-anterior tilting (P-A), while the humerus orientation in terms of flexion-extension (FL-EX), abduction-adduction (AB-AD) and internal-external rotation (IN-EX) for sagittal plane movements; AB-AD, FL-EX and IN-EX for the scapular plane movements.

A MATLAB (The MathWorks, USA) custom made software, based on the MTx software development kit, was used to guide the operators in the step-by-step execution of the anatomical calibrations and to calculate joint kinematics in real-time.

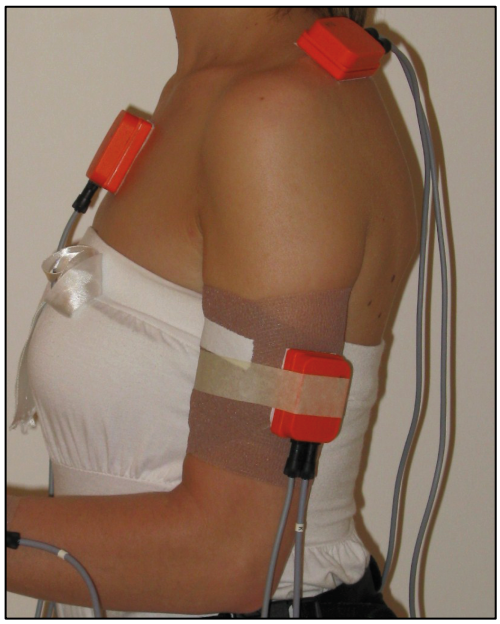

FIGURE 1. To measure the SHR, 3 sensors are required: thorax, scapula and humerus.

2.3 DATA COLLECTION

Three SHR measurement sessions were completed for each subject: two by operator A (named sessions A_1 and A_2) and one by operator B (named session B), following the $A_1 – B – A_2$ sequence. The actual operator assigned to the role of A or B was randomized for each patient. Sessions were planned on the same day, approximately 20 minutes apart to minimize the within-subject biological variability. Between sessions, MTx sensors were removed by the operator and re-applied by the second, who also repeated the static calibration, i.e. repositioned the subject in the calibration posture. Each operator made sure that no specific marks of the sensor placement remained on the skin of the subjects.

During each session, subjects performed two movements, i.e. humeral elevation in the sagittal (flex-extension; FL-EX) and scapular (ab-adduction; AB-AD) plane: starting from a resting position with the arms alongside the body and the thumb up, the subject was asked to elevate the humerus until maximum elevation without pain was reached and to return to the resting position. Each movement was repeated 8 times in a row, but only the central 5 were considered for subsequent calculations.

2.4 DATA PROCESSING

For each subject data processing consisted of two steps.

Firstly, each movement was split in an upward (from resting position to maximum elevation, hereinafter referred to as FL and AB) and a downward (from maximum elevation to resting position, hereinafter referred to as EX and AD) phase that can feature different kinematic patterns [18]. For this purpose, the segmentation algorithm described in Annex 1 was used.

Secondly, a total of 12 angle-angle plots were obtained, each containing 15 curves, i.e. 5 curves per session: 1) PR-RE vs. FL-EX, upward; 2) PR-RE vs. FL-EX, downward; 3) ME-LA vs. FL-EX, upward; 4) ME-LA vs. FL-EX, downward; 5) P-A vs. FL-EX, upward; 6) P-A vs. FL-EX downward; 7) PR-RE vs. AB-AD, upward; 8) PR-RE vs. AB-AD, downward; 9) ME-LA vs. AB-AD, upward; 10) ME-LA vs. AB-AD, downward; 11) P-A vs. AB-AD, upward; 12) P-A vs. AB-AD, downward.

2.5 ASSESSMENT OF THE PROTOCOL AGREEMENT

The intra- and inter-operator agreement of ISEO was assessed by means of the Coefficient of Multiple Correlation (CMC, *section 2.5.1*) [19] and the 95% Smallest Detectable Difference (SDD_{95}) for the scapular range of motion (ROM, *section 2.5.2*) [17].

2.5.1 Coefficient of Multiple Correlation

The intra- and inter-operator agreement for the curves reported in each of the 12 angle-angle plots was computed by means of the Coefficient of Multiple Correlation (CMC) [19-21].

For each subject, the CMC-analysis was conducted in two steps [20]. Firstly, the subject intra-session consistency was assessed by computing the CMC in the formulation named "within-day" by Kadaba and co-workers in [19], hereinafter referred to as CMC_1. Secondly, only if the subject presented a high intra-session consistency (CMC_1>0.85), the intra- and inter-operator agreement was assessed by computing the CMC between sessions, using the CMC formulation named "between-day" [19], hereinafter referred to as CMC_2. This two-step procedure was followed since the "ideal assessment" of a protocol intra- and inter-operator agreement should require a complete absence of biological variability of the subjects, which is a confounding factor [20] since it introduces a source of variability, which can be falsely attributed to the protocol application. The "filter" over CMC_1 values allows to just include subjects who have a limited "confounding effect" over the protocol assessment, i.e. it allows to limit the negative effect of the humans biological variability which is not excludable in real life. Please refer to Annex 2 for a detailed description of CMC_1 and CMC_2 computations.

The distributions of the CMC_2 over subjects both for the intra- and inter-operator agreement, were reported in terms of box-and-whiskers plots, similarly to Garofalo et al. [20]; the acceptability of the intra- and inter-operator agreement was interpreted based on the median value (MV) and lower whisker (LW). For all scapula angles the acceptability condition was:

- Median value ≥ 0.85;
- For a good agreement: $0.75 \leq$ lower-whisker < 0.85;
- For a very good agreement: $0.85 \leq$ lower-whisker ≤ 1.

Lower values for the median or for the lower-whisker were interpreted as "unacceptable agreement".

In addition, although the CMC distributions are not normal (thus the most appropriate method for their description is through median and interquartile values), to compare our results to previous literature [21], means and standard deviations were also computed for the CMC_2 distributions of the intra-operator analysis.

Since for each subject the PR-RE, ME-LA ad P-A values at rest can change between the three sessions due to intra-subject biological variability and scapula sensor placement during the subject preparation, the CMC_2 calculations were repeated twice, firstly considering and then removing these resting values, following the algorithm reported by Garofalo et al. [20]. The second analysis

thus takes into account only the similarity of the shape of the curves excluding the inter-session offset, as reported previously [19,20].

2.5.2 Smallest Detectable Difference

The scapula ROMs associated to the maximum ROM of humerus elevation are important parameters for the evaluation of the SHR in clinics [1]. Therefore, it seemed desirable to quantify for each scapula rotation (PR-RE, ME-LA and P-A), the SDD_{95} that can be detected by ISEO, also considering the effect of the operator on the measurement.

For each subject, three pairs of sessions were analyzed: A_1 vs. A_2 for the intra-operator analysis; A_1 vs. B and A_2 vs. B for the inter-operator analysis. For each pair, only the upward phases of FL-EX and AB-AD movements were considered (FL and AB). Considering FL:

- a common ROM of humeral flexion (ROM_{FL}) was identified for the 10 repetitions of the two sessions;
- within each of the two sessions, the ROM of PR-RE, ME-LA and P-A correspondent to the ROM_{FL} was computed, by considering the mean scapula ROMs over the five movement repetitions.

As such, per subject and scapula rotation, two associated ROM values became available, each from a single session. The same investigation was performed for the AB movement.

Considering all subjects, for each movement (FL, AB), scapula rotation (PR-RE, ME-LA, P-A) and pair of sessions (A_1 vs. A_2; A_1 vs. B; A_2 vs. B), a dataset of 40 couples of scapular ROMs was thus obtained (Figure 2).

For each dataset, a one-way repeated measures ANOVA was used to verify the existence of statistically significant differences due to the operator. Then, the Standard Error of Measurement was computed from the ANOVA within-subject mean square (MS_w) [17]:

$$\mathrm{SEM} = \sqrt{\mathrm{MS_W}}$$

Finally, the SDD_{95} was computed [20]:

$$\mathrm{SDD_{95}} = \mathrm{SEM} * 1.96 * \sqrt{2}$$

SEM and SDD_{95} for sessions A_1 vs. B and A_2 vs. B were then averaged to have a single estimation of the inter-operator agreement, similarly to the procedure followed for the CMC_2 (Annex 2).

To compare the results of this study with those reported by van Andel et al. [12], the analysis for the inter-operator SEM was repeated for the scapula rotations at specific humerus elevation angles, i.e.

at rest, 90° and 120°. Sessions A_1 vs. B and A_2 vs. B were considered and results were averaged as previously described. It is important to notice that this alternative SEM analysis was only possible for the healthy subjects, since patients did not generally reached 120° humeral elevation.

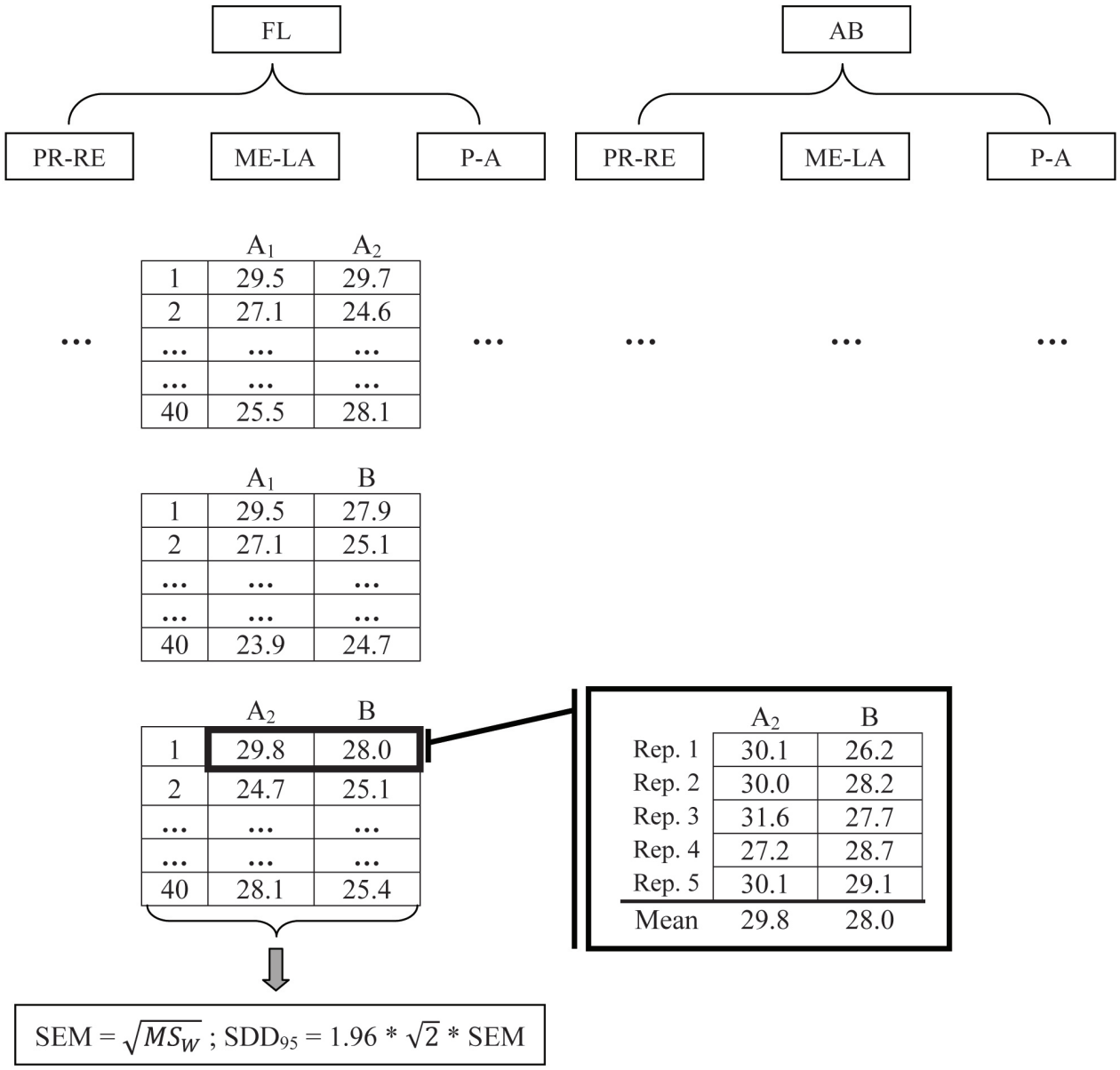

FIGURE 2. Summary of the processing to prepare the data for the SEM and SDD_{95} computation.

3. RESULTS

3.1 COEFFICIENT OF MULTIPLE CORRELATION

For the intra-operator analysis, 25 subjects were found highly consistent *intra-session* (CMC_1>0.85); for the inter-operator analysis, this was true for 28 subjects. Considering these two subgroups, the box-and-whiskers plots for CMC_2 are reported in Figure 3 and comparisons with the acceptability condition are summarized in Table 1.

To support the acceptability conditions, Figure 4 presents, for each scapula rotation, an example of SHR patterns classified as having an unacceptable, good and very good agreement, based on the CMC_2 value.

Mean and standard deviations of CMC_2 distributions for the intra-operator analysis (*considering* the scapula angle values at rest) are reported in Table 2

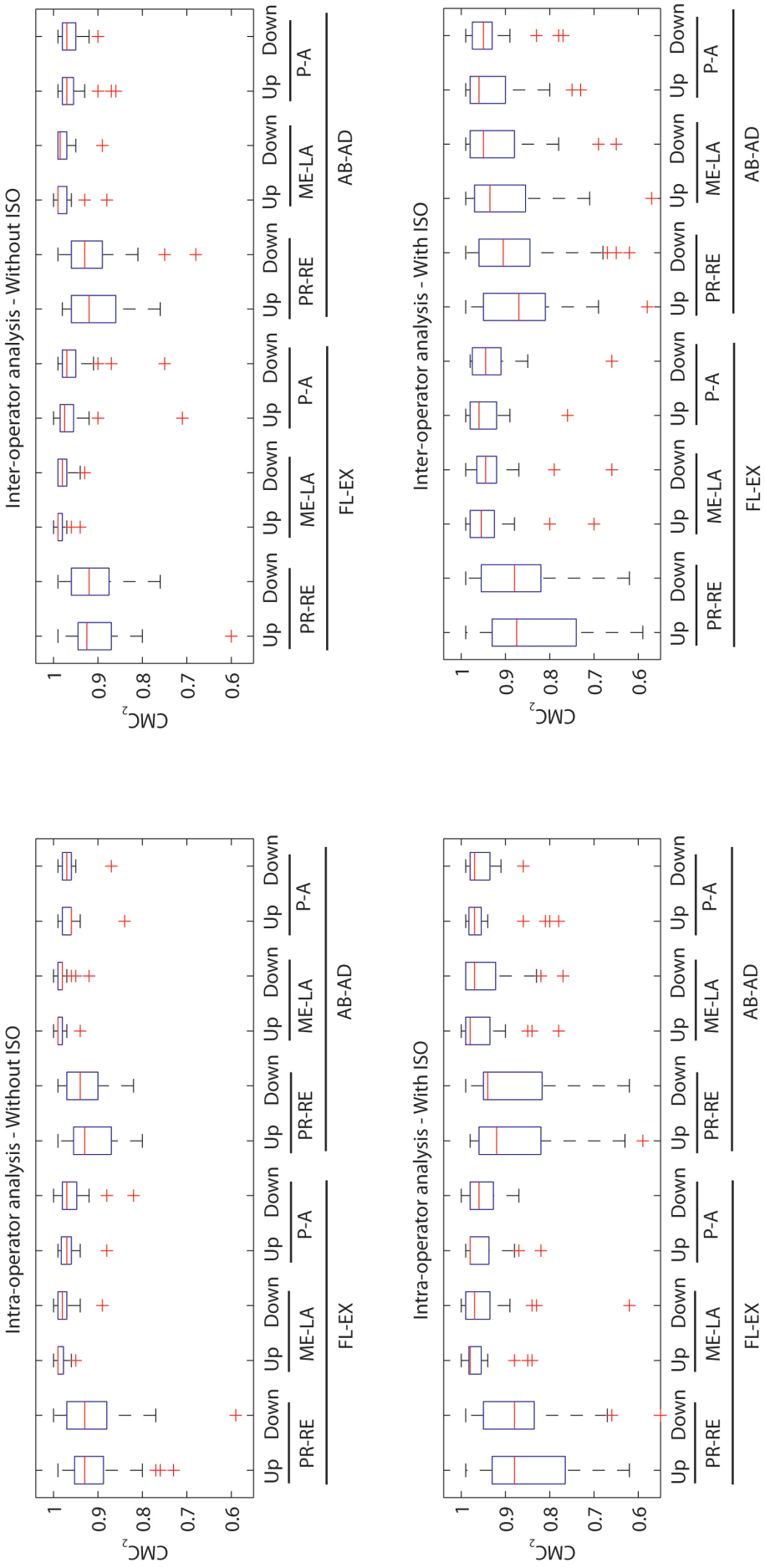

FIGURE 3. Box-&-whiskers plots for the CMC_2 divided per intra- and inter-operator agreement, both considering and excluding the inter-session offset (ISO)

Humerus movement	Scapular movement	Phase	INTRA**	INTER**	INTRA*	INTER*
FL-EX	PR-RE	Upward				
		Downward				
	ME-LA	Upward				
		Downward				
	P-A	Upward				
		Downward				
AB-AD	PR-RE	Upward				
		Downward				
	ME-LA	Upward				
		Downward				
	P-A	Upward				
		Downward				

TABLE 1. Results from the CMC_2 analysis considering the intra and inter-operator analysis with (*) and without (**) inter-session offset. White: very-good; Gray: good; Black: unacceptable.

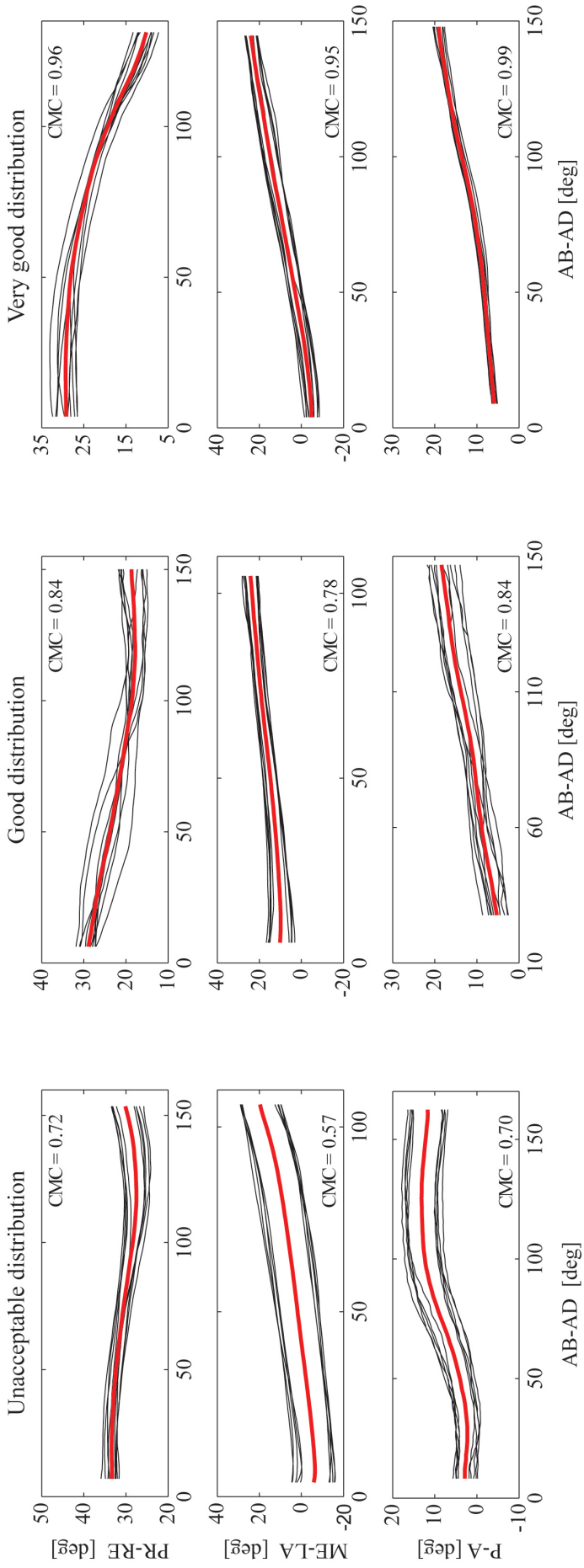

FIGURE 4. An example of angle-angle plots for the 3 scapula rotations (PR-RE, ME-LA and P-A) during the AB-AD movement, with indication of the correspondent CMC_2 values. Based on 1) the previous literature, 2) observation of the individual subjects' pattern, and 3) discussion with the clinical team, curves agreement was classified as unacceptable, good or excellent. Ranges for the interpretation of the CMC_2 distributions over subjects were then defined.

Humerus movement	Scapular movement	This study		Thigpen et al.[21]	
		Mean	***SD***	**Mean**	***SD***
FL	**PR-RE**	0.85	*0.11*	0.82	*0.20*
	ME-LA	0.96	*0.04*	0.94	*0.08*
	P-A	0.95	*0.05*	0.85	*0.24*
AB	**PR-RE**	0.87	*0.11*	0.74	*0.27*
	ME-LA	0.95	*0.06*	0.91	*0.12*
	P-A	0.94	*0.06*	0.83	*0.24*

TABLE 2. Mean and standard deviations of CMC_2 distributions for the intra-operator analysis with inter-session offset. For ease of comparison, results from this study are reported alongside the results from Thigpen et al. [21].

3.2 SMALLEST DETECTABLE DIFFERENCE

Results from the repeated measures ANOVA indicated no systematic effect of the operator for none of the humeral movements and scapula rotations ($p>0.05$). Table 3 reports the results for SEM and SDD_{95} for each of the scapula rotations.

Humerus movement	Scapular movement	INTRA		INTER	
		SEM	***SDD*$_{95}$**	**SEM**	***SDD*$_{95}$**
FL	**PR-RE**	2,6°	*7,1°*	2,5°	*6,8°*
	ME-LA	2,2°	*6,2°*	1,9°	*5,2°*
	P-A	3,1°	*8,5°*	2,8°	*7,7°*
AB	**PR-RE**	3,0°	*8,3°*	3,1°	*8,6°*
	ME-LA	1,8°	*4,9°*	1,6°	*4,4°*
	P-A	2,7°	*7,4°*	2,4°	*6,6°*

TABLE 3. SEM and SDD_{95} values for the scapular ROMs, both for the intra- (INTRA) and inter-operator (INTER) agreement.

The results for the analysis of the inter-operator SEM for healthy subjects, as performed by van Andel et al. [12], are reported in Table 4.

Scapular movement	Humerus elevation	This study	Van Andel et al. [12]
PR-RE	At rest	2,6°	4,3°
	90° humeral AB	2,7°	6,3°
	120° humeral AB	3,0°	7,7°
	90° humeral FL	2,8°	6,1°
	120° humeral FL	3,2°	8,0°
ME-LA	At rest	3,9°	3,4°
	90° humeral AB	4,5°	4,2°
	120° humeral AB	3,7°	3,9°
	90° humeral FL	3,4°	3,8°
	120° humeral FL	3,7°	4,1°
P-A	At rest	1,3°	7,7°
	90° humeral AB	2,3°	7,0°
	120° humeral AB	2,8°	7,3°
	90° humeral FL	2,5°	6,6°
	120° humeral FL	3,1°	8,4°

TABLE 4. SEM values for each scapula rotation, at specific humerus elevation angles, similarly to [12].

4. DISCUSSION AND CONCLUSIONS

This study describes the intra- and inter-operator agreement of ISEO, which is a motion analysis protocol designed for the quantitative measure of the SHR in outpatient settings. The CMC_2 and the SDD_{95} were used in conjunctions as agreement parameters, as recommended by McGinley et al. [22], since both parameters assess different aspects of the intra- and inter-operator agreement. The former takes into account the similarity of the SHR curves as a whole and summarizes the concurrent effects of the similarity in shape, offset, correlation and ROM [23]. The latter provides a specific evaluation of the smallest change in scapula ROMs of a subject "for the difference in the measures to be considered real" [17], i.e. not due to the re-application of ISEO by the same or a different operator. In other words, when differences recorded for a subject between two sessions are greater than SDD_{95}, then these differences can be due to the natural day-to-day variability of the

subject or to the effect of the therapy (if any), but at 95% probability they are not due to the re-application of ISEO itself. It should be noticed that CMC_2 and SDD_{95} have been previously referred to as "reliability" parameters [20,22], while they should be referred to as agreement parameters, since none of the two "relates the magnitude of the *measurement error* in observed measurements to the inherent *variability* in the underlying level of the quantity *between subjects*" [16].

Results for CMC_2 (Table 1) showed that the intra- and inter-operator agreement is generally acceptable for all scapula rotations, both considering and removing the inter-session offset. Limitations exist however for PR-RE, which appeared the most critical scapula angle; for the inter-operator analysis including the inter-session offset also ME-LA upward during AB-AD movement became unacceptable.

If the CMC_2 mean values and standard deviations (Table 2) are considered, ISEO appears to have a better intra-operator agreement compared to the acromion method for scapula tracking [21]. Thigpen et al. [21] reported a range of CMC_2 mean values from 0.82 to 0.94 for the sagittal plane and from 0.74 to 0.91 for the scapular plane, with standard deviation varying from 0.08 to 0.28. In this study, CMC_2 mean values ranged from 0.85 to 0.96 for the sagittal plane and from 0.87 to 0.95 for the scapular plane, with a standard deviation varying from 0.04 to 0.11. Based on the comparison with Thigpen et al. [21], we might have concluded the acceptability of the intra-operator agreement for PR-RE including the inter-session offset. However, we do think that the stricter acceptability conditions considered in this study more closely represent clinically acceptable values, as graphically presented in Figure 4.

Results from the ANOVA confirmed that the operator did not introduce a systematic bias in the measurement of the ROM of scapula rotations. SDD_{95} values ranged from 4.4° to 8.6° for the inter-operator agreement and between 4.9° to 8.5° for the intra-operator agreement. Lowest values were obtained for ME-LA, both for FL-EX (5.2°) and AB-AD (4.4°).

It should be noticed that the inter-operator agreement showed SDD_{95} values slightly lower than the intra-operator values. A possible explanation could be that the intra-operator sessions were the first and the last in each subject assessment day, resulting in a possible fatigue effect.

The comparison of the SEM values for the acromion cluster method, as reported by van Andel et al. [12], shows that ISEO inter-operator agreement (*considering* the inter-session offset), generally features lower values and concurrent lower SDD_{95}, with the only exception of ME-LA at rest and at 90° of humeral AB-AD; the associated 0.5° difference, however, does not appear to be clinically significant. For ISEO, the SEM values ranged from 1.3° to 4.5°, while for the acromion cluster

method values ranged from 3.4° to 8.4°. Longitudinal studies on specific patient populations will clarify if the SDD_{95} values reported for ISEO are small enough to detect clinically significant changes.

One of the possible limitations of the present study was the inclusion of just two operators. However, the application of the protocol by more operators in consecutive sessions would have considerably increased the risk of fatigue of the subjects. Therefore we think that the inclusion of two operators was the best possible compromise between the applicability of the study "in-vivo" and fatigue.

The two operators received training in the application of ISEO by the protocol developers, consisting in the application of ISEO on three subjects, which were not included in this study. Until specific assessments on the minimum skill of the operators will be conducted, we think that three training subjects should be assessed to acquire confidence with ISEO.

In conclusion, we found that ISEO has potentials for an every-day clinical application thanks to its high intra- and inter-operator agreement, in particular when the inter-session offset is removed.

REFERENCES

1. Ludewig PM, Reynolds JF. The Association of Scapular Kinematics and Glenohumeral Joint
2. Pathologies. J Orthop Sports Phys Ther 2009; 39(2): 90-104
3. Veeger DJ, van der Helm FCT. Shoulder function: The perfect compromise between mobility and stability. J Biomech 2007; 40: 2119-2129
4. Ebaugh DD, McClure PW, Karduna AR. Three-dimensional scapulothoracic motion during active and passive arm elevation. Clin Biomech 2005; 20(7): 700-9
5. McClure PW, Michener LA, Sennett BJ, Karduna AR. Direct 3-dimensional measurement of scapular kinematics during dynamic movements in vivo. J Shoulder Elbow Surg 2001; 10(3): 269-77
6. Ludewig PM, Cook TM. Alterations in shoulder kinematics and associated muscle activity in people with symptoms of shoulder impingements. Phys Ther 2000; 80(3): 276-291
7. Kontaxis A, Johnson GR. Adaptation of scapula lateral rotation after reverse anatomy shoulder replacement. Comput Methods Biomech Biomed Engin 2008; 11(1): 73-80.
8. Karduna AR, McClure PW, Michener LA, Sennett B. Dynamic measurements of three-dimensional scapular kinematics: a validation study. J Biomech 2001; 123(2): 184-190
9. van der Helm FC, Pronk GM. Three-Dimensional Recording and description of motions of the shoulder mechanism. J Biomech Eng 1995; 117(1): 27-40
10. Roy JS, Moffet H, Hébert LJ, St-Vincent G, McFadyen BJ. The reliability of three-dimensional scapular attitudes in healthy people with shoulder impingement syndrome. BMC Muscoloskelet Disord 2007; 21: 8-49
11. Johnson GR, Stuart PS, Mitchell S. A method for the measurement of three dimensional scapular movement. Clin Biomech 1993; 8(5): 269-273

12. Meskers CG, Vermeulen HM, de Groot JH, van Der Helm FC, Rozing PM. 3D shoulder position measurements using a six degree-of-freedom electromagnetic tracking device. Clin Biomech 1998; 13(4-5): 280-292
13. van Andel C, van Hutten K, Eversdijk M, Veeger D, Harlaar J. Recording scapular motion using an acromion marker cluster. Gait Posture 2009; 29(1): 123-8
14. Meskers CG, van de Sande MA, de Groot JH. Comparison between tripod and skin-fixed recording of scapular motion. J Biomech 2007; 40(4): 941-6
15. Prinold JAI, Shaheen AF, Bull AMJ. Skin-fixed scapula trackers: a comparison of two dynamic J Biomech 2011; 44: 2004-07
16. Cutti AG, Giovanardi A, Rocchi L, Davalli A, Sacchetti R. Ambulatory measurement of shoulder and elbow kinematics through inertial and magnetic sensors. Med Bio Eng Comput 2008; 46(2): 169-78
17. Bartlett JW, Frost C. Reliability, repeatability and reproducibility: analysis of measurement errors in continuous variables. Ultrasound Obstet Gynecol 2008; 31(4): 466-75
18. Weir JP. Quantifying test-retest reliability using the intraclass correlation coefficient and the SEM. J Strength Cond Res 2005; 19(1): 231-240
19. Borstad JD, Ludewig PM. Comparison of scapular kinematics between elevation and lowering of the arm in the scapular plane. Clin Biomech 2002; 17(9-10): 650-9.
20. Kadaba MP, Ramakrishnan HK, Wootten E, Gainey J, Gorton G, Cochran GVB. Repeatability and electromiographic data in normal adult gait. J Orthop Res 1989; 7: 849-860
21. Garofalo P, Cutti AG, Filippi MV, Cavazza S, Ferrari A , Cappello A, Davalli A. Inter-operator reliability and prediction bands of a novel protocol to measure the coordinated movements of shoulder-girdle and humerus in clinical settings. Med Bio Eng Comput 2009; 47(5): 475-86
22. Thigpen CA et al. (2005) The repeatability of scapular rotations across three planes of humeral elevation. Res Sports Med, 3(3):181-98
23. McGinley JL et al. (2009) The reliability of three-dimensional kinematic gait measurements: a systematic review. Gait Posture, 29(3):360-9
24. Ferrari A, Cutti AG, Cappello A (2010) A new formulation of the coefficient of multiple correlation to assess the similarity of waveforms measured synchronously by different motion analysis protocols. Gait Posture 31:540–542

ANNEX 1

SEGMENTATION ALGORITHM

Acronyms

SHR: Scapulohumeral rhythm

FL: humeral flexion

EX: humeral extension

AB: humeral abduction

AD: humeral adduction

PR-RE: scapula protraction-retraction

ME-LA: scapula medio-lateral rotation

P-A: scapula posterior-anterior tilting

HT: high-threshold for FL-EX(t) and AB-AD(t)

LT: low-threshold for FL-EX(t) and AB-AD(t)

t_{EUP}: time sample correspondent to the *End of an Upward Phase* of a movement

t_{OUP}: time sample correspondent to the *Onset of an Upward Phase* of a movement

t_{EDP}: time sample correspondent to the *End of an Downward Phase* of a movement

t_{ODP}: time sample correspondent to the *Onset of an Downward Phase* of a movement

INTRODUCTION

For a detailed analysis of the SHR, a segmentation algorithm was implemented to divide the upward (FL and AB) and downward (EX and AD) phases of FL-EX and AB-AD movements. This allowed to obtain a total of 12 angle-angle plots for each session: 1) PR-RE vs. FL-EX, upward; 2) PR-RE vs. FL-EX, downward; 3) ME-LA vs. FL-EX, upward; 4) ME-LA vs. FL-EX, downward; 5) P-A vs FL-EX, upward; 6) P-A vs. FL-EX, downward; 7) PR-RE vs. AB-AD, upward; 8) PR-RE vs. AB-AD, downward; 9) ME-LA vs. AB-AD, upward; 10) ME-LA vs. AB-AD, downward; 11) P-A vs. AB-AD, upward; 12) P-A vs. AB-AD, downward. The aim of this document is to describe the segmentation algorithm.

ALGORITHM

The segmentation algorithm derives from the one developed by Garofalo et al. (2008) [15] and entails 3 steps (Figure 1-3).

In step 1 (Figure 1) high and low thresholds are determined for FL-EX(t):

1.1) Local maxima are determined and those higher than 70° (reference value) are selected. The lowest maximum is then computed and is defined as the high threshold (HT).

1.2) Local minima are determined and those below 20° (reference value) are selected. The highest minimum is then computed and is defined as the low threshold (LT).

1.3) Starting from the first sample, FL-EX(t) is scanned forward until a time sample is found where FL-EX(t_i) > HT. That time sample is then classified as the end of the first upward phase, t_{EUP}.

1.4) Starting from FL-EX(t_{EUP}), FL-EX(t) is scanned backward until a time sample is found where FL-EX(t_i) < LT. That time sample is then classified as the onset of the first upward phase, t_{OUP}.

1.5) An upward phase check is run in order to verify the presence of minima in the extracted curve. If any are found, the curve is discarded; otherwise t_{OUP} and t_{EUP} are stored in a vector of time samples T.

1.6) Starting from FL-EX(t_{EUP}), FL-EX(t) is scanned forward until a time sample is found where FL-EX(t_i) < LT. That time sample is then classified as the end of the first downward phase, t_{EDP}.

1.7) Starting from FL-EX(t_{EDP}), FL-EX(t) is scanned backward until a time sample is found where FL-EX(t_i) > HT. That time sample is then classified as the onset of the first backward phase, t_{ODP}.

1.8) A downward phase check is run in order to verify the presence of minima in the extracted curve. If any are found, the curve is discarded; otherwise t_{ODP} and t_{EDP} are stored in T.

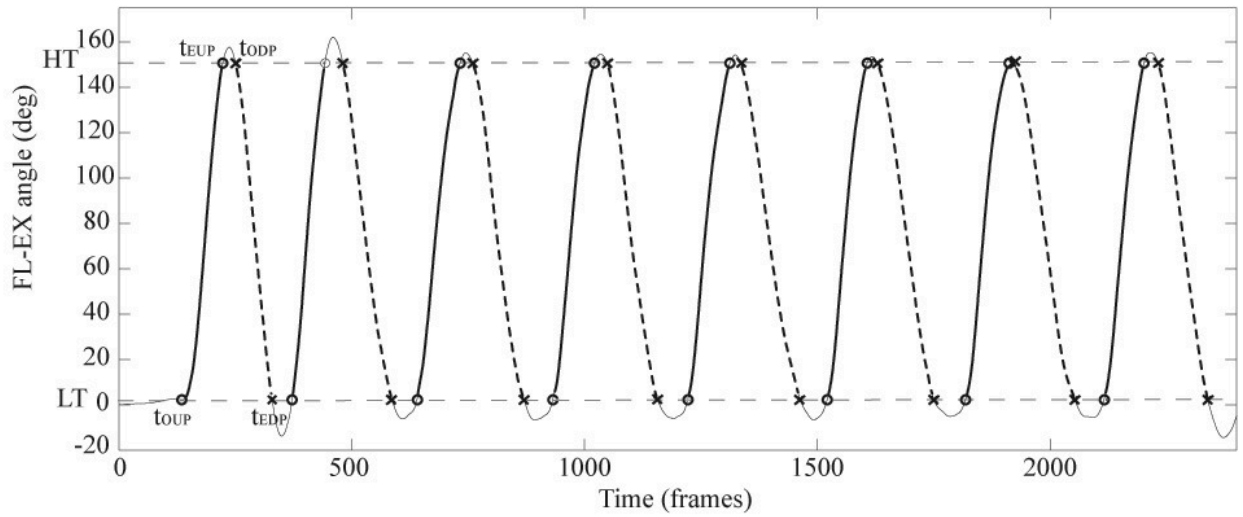

FIGURE 1. Visual description of step 1

In step 2 (Fig. 2), the time samples in T are used to segment also ME-LA(t) in its upward and downward phases. Next, corresponding upward and downward phases of FL-EX and ME-LA are plotted to obtain two angle-angle plots: ME-LA vs. FL-EX, upward phase (Fig. 1c); ME-LA vs. FL-EX, downward phase (Fig. 1d).

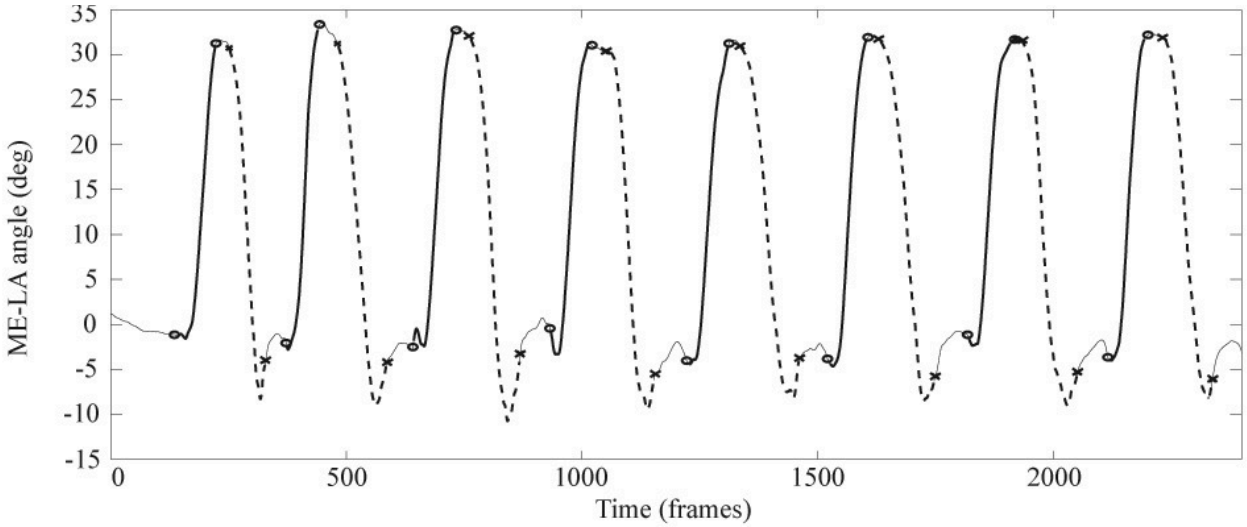

FIGURE 2. Visual description of step 2

In step 3 five upward and downward phases of FE(t) vs. ME-LA(t) are selected and considered for further computations.

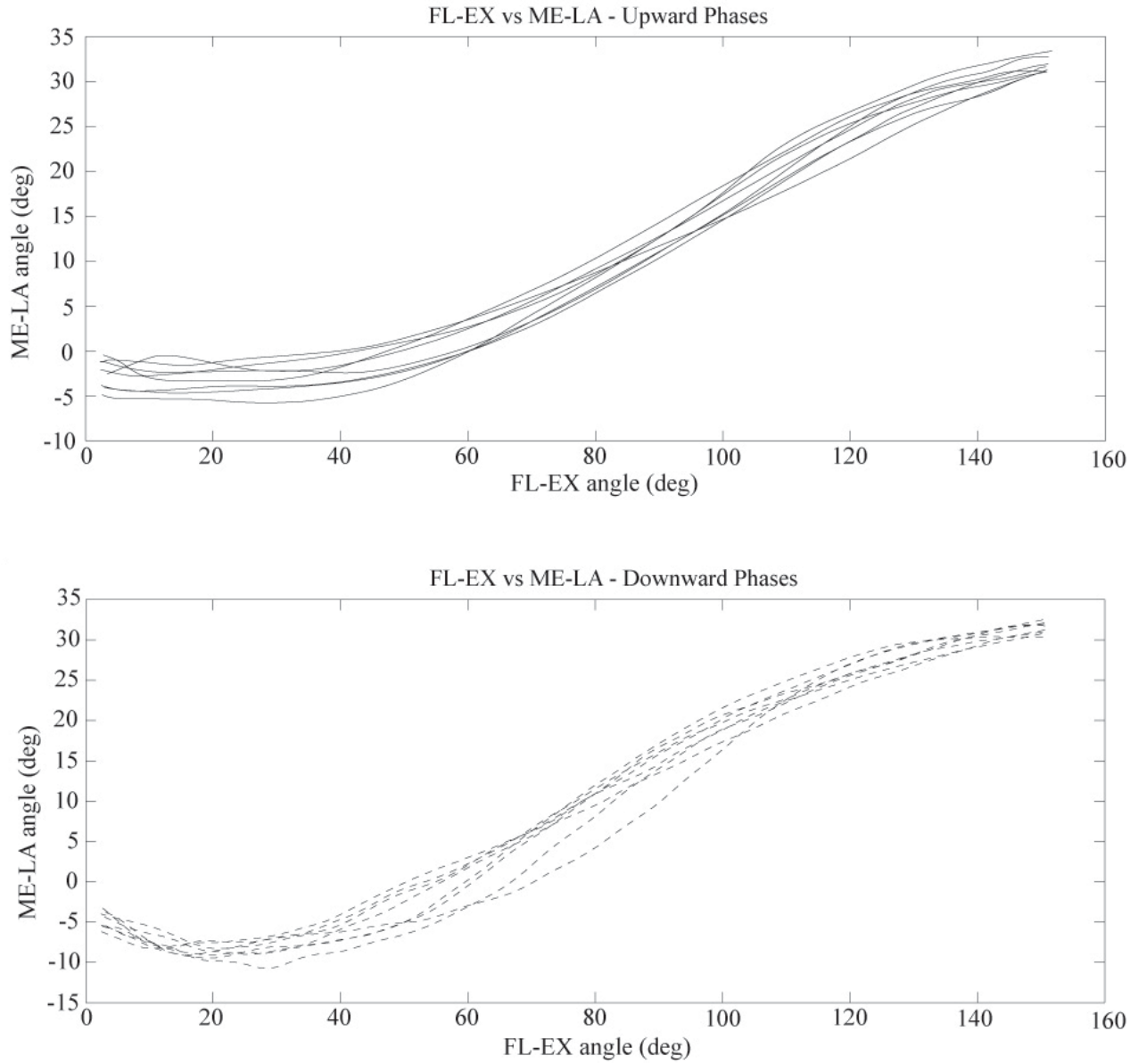

FIGURE 3. Visual description of step 3

The same steps are applied for PR-RE(t) and P-A(t).

The algorithm is also applied for the segmentation of AB-AD(t). For this movement the reference value to identify the local maxima and minima are 55° and 20°, respectively.

ANNEX 2

DETAILS OF THE DATA PROCESSING FOR THE CMC COMPUTATION

INTRODUCTION

The intra- and inter-operator agreement of ISEO was assessed by means of the Coefficient of Multiple Correlation (CMC). The summary of the data processing is provided in the main text. In this Annex, the computational details are provided.

METHODS

The agreement analysis was split in two parts: *Part 1* addressing the intra-operator agreement and *Part 2* the inter-operator agreement.

Part 1. As described in Figure 1, for the evaluation of the intra-operator agreement, the data acquired in the two sessions by operator A were considered (5 + 5 waveforms for each subject).
Firstly, the variability of each subject in the execution of the movements was considered (intra-subject variability). To check for the intra-subject variability, the CMC_1 was computed for every angle-angle plot:

$$CMC_1 = \sqrt{1-\frac{\sum_{i=1}^{O}\sum_{j=1}^{M}\sum_{t=1}^{S}(Y_{ijt}-\overline{Y}_{it})^2/OS(M-1)}{\sum_{i=1}^{O}\sum_{j=1}^{M}\sum_{t=1}^{S}(Y_{ijt}-\overline{Y}_{i})^2/O(MS-1)}} \quad (1)$$

where:
t = 1, …, S (S = 80) differentiates the 80 samples of the angle on the X-axis.
j = 1, …, M (M = 5) differentiates the 5 repetitions of each movement, in order of execution.
i = 1, …, O (O = 2) differentiates the waveforms obtained by operator A_1 from those of A_2.
Y_{ijt} is the Y-axis angle correspondent to the t-th X-axis angle, of the j-th waveforms, obtained by the i-th operator;
$\overline{Y}_{it}$ is the average among the M waveforms of the subject at the t-th X-axis angle of the i-th operator;

$\overline{Y}_i$ is the average among the M*S waveforms of the subject obtained by the i-th operator.

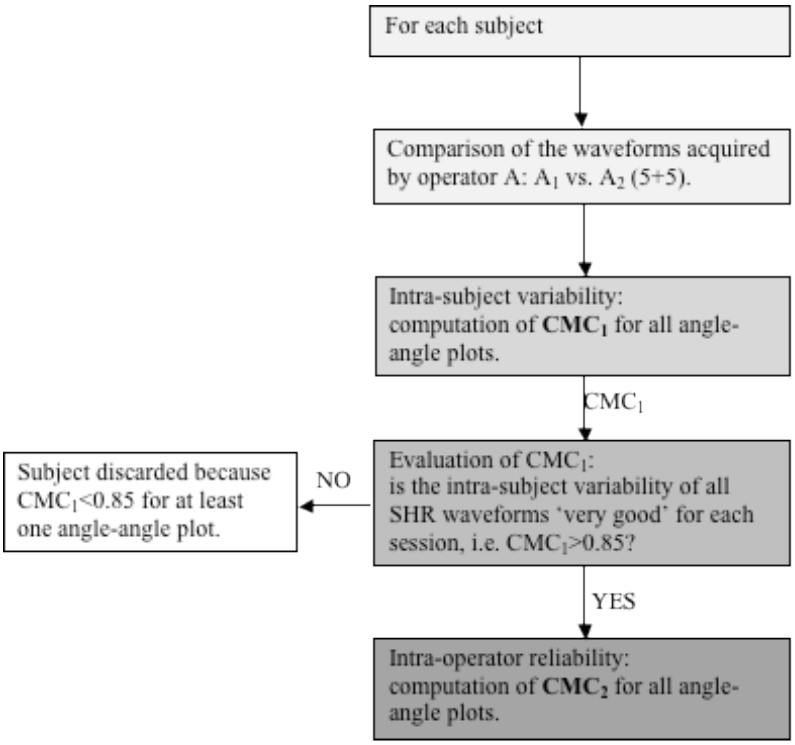

FIGURE 1. Flow-chart of the intra-operator reliability

As previously done by Garofalo et al. [13], only for those subjects with a very good CMC_1 (≥0.85) the intra-operator agreement was computed through the CMC in the between-day formulation (CMC_2), for all angle-angle plots. Subjects with CMC_1<0.85 were discarded as their high biological variability can alter the estimation of the protocol agreement, which is the focus of the analysis. The CMC_2 equation is:

$$CMC_2 = \sqrt{1 - \frac{\sum_{i=1}^{O}\sum_{j=1}^{M}\sum_{t=1}^{S}(Y_{ijt}-\overline{Y}_t)^2/S(OM-1)}{\sum_{i=1}^{O}\sum_{j=1}^{M}\sum_{t=1}^{S}(Y_{ijt}-\overline{Y})^2/(OMS-1)}} \qquad (2)$$

where:

$\overline{Y}_t$ is the average among all the M*O waveforms of the subjects at the t-th X-axis angle;

$\overline{Y}$ is the grand mean of all the waveforms from all the operator.

Part 2. As described in Figure 2, for each subject the waveforms acquired by operator A and B were considered. Two parallel investigations were carried out: A_1 vs. B (*Investigation 1*) and A_2 vs.

B (*Investigation 2*). The CMC_1 and the CMC_2 were computed for both investigations applying the same rules of *Part 1*. Finally, for the analysis of CMC_2 over the subjects, a merged group of values for CMC_2 was created respecting the following rules:

- if there was a subject reliable both for *Investigation 1* and *Investigation 2*, the mean value of both CMC_2 was considered;
- if there was a subject reliable only for one investigation, the correspondent CMC_2 was considered.

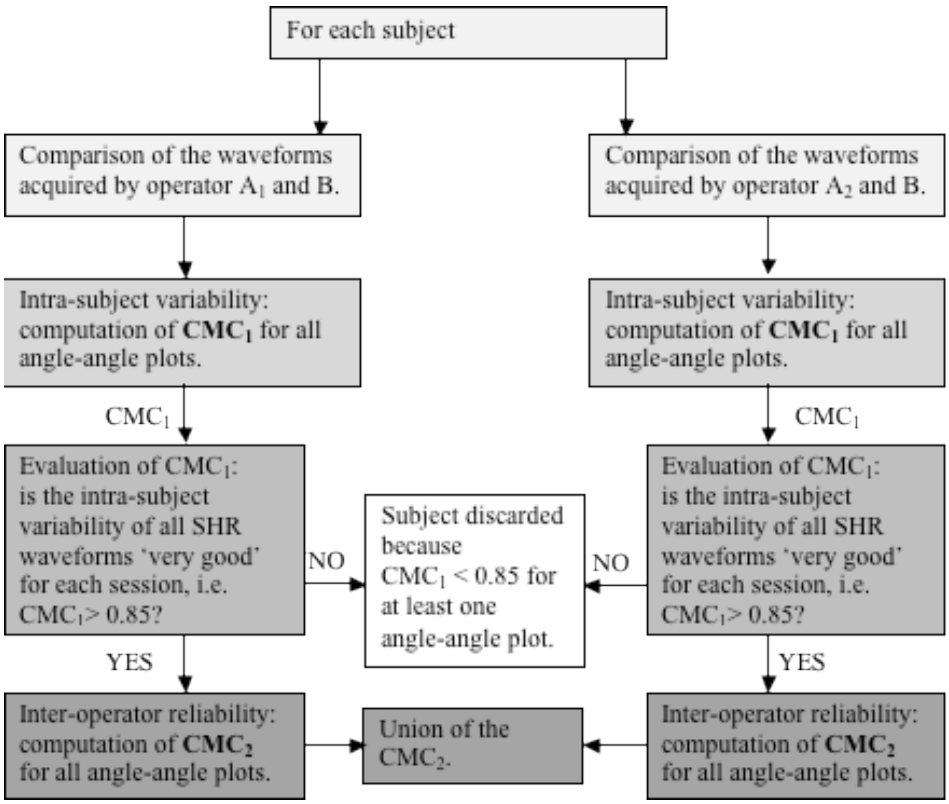

FIGURE 2. Flow-chart of the inter-operator reliability analysis.

Chapter 2

Prediction bands and intervals for the scapulo-humeral coordination based on Bootstrap and Gaussian theories

Cutti AG, Parel I, Raggi M, Petracci E, Pellegrini A, Porcellini G, Accardo AP, Verni G.
Gait & Posture Submitted.

ABSTRACT

Quantitative motion analysis protocols have been developed to assess the coordination between scapula and humerus. However, their use in clinical examinations is still limited by the unavailability of prediction bands and intervals that would allow classifying a patient as either symptomatic or asymptomatic. The aim of this study was to present such prediction bands and intervals for the "ISEO" protocol, by using one non-parametric (Bootstrap) and two Gaussian parametric methods (based on the Student's T and Normal distributions).

One hundred and eleven asymptomatic subjects were divided into three groups based on their age (18-30, 31-50, 51-70). For each group, "monolateral" prediction bands and intervals were computed for the scapulo-humeral patterns and the scapula resting orientation, respectively. A forth group included the 36 subjects (42±13 year-old) for whom the scapulo-humeral coordination was measured bilaterally, and "differential" prediction bands and intervals were computed, which describe right-to-left side differences.

Bootstrap and Gaussian-based methods were compared using cross-validation analyses, by evaluating the coverage probability in comparison to a 90% target. Results showed a mean coverage for Bootstrap from 86% to 90%, compared to 67%-70% for parametric bands and 87-88% for parametric intervals. Bootstrap prediction bands showed a distinctive change in amplitude and mean pattern related to age, with an increase toward scapula retraction, lateral rotation and posterior tilt.

In conclusion, Bootstrap ensures an optimal coverage and should be preferred over parametric methods. Moreover, the stratification of "monolateral" prediction bands and intervals by age appears relevant for the correct classification of patients.

ABBREVIATIONS

PBI	Prediction Bands and Intervals
PB	Prediction Band
PI	Prediction Interval
MP	Monolateral Pattern
MO	Monolateral Offset
DP	Differential Pattern
DO	Differential Offset

1. INTRODUCTION

The assessment of scapula kinematics relative to humerus elevation, i.e. the scapulo-humeral coordination, is relevant in the clinical examination of patients with shoulder disorders [1-4]. To overcome the limitations of observational scales [1,5], quantitative motion analysis protocols [6] that rely on electromagnetic, optoelectronic or, more recently, inertial sensors have been developed [2,7-9]. The clinical application of these protocols would be facilitated via the availability of prediction bands (PBs) and intervals (PIs). Such prediction bands and intervals (PBI) allow to measure the "distance" between the scapulo-humeral coordination of a new patient and that of asymptomatic control subjects [10-11]. Unfortunately, "monolateral" PBI, i.e. obtained by assessing a single side of each control subject, have never been directly reported: most of the literature focused on confidence intervals for the mean pattern of scapula rotations [12-16] or reported the mean patterns ± 1 standard deviation, typically for selected humerus elevation angles [3,17-19]. The calculation of PBI from the available results would suffer from three main limitations. Firstly, a limited number of subjects was typically involved in the studies, ranging from 10 to 20 [2]. Secondly, subjects were usually young adults (35 year-old average [2]) or spanned a wide age-range [13,20], which questions the applicability of possible PBI for the classification of older patients [20-23]. Thirdly, current mean patterns and related uncertainty intervals were established using a point-by-point method based on the Gaussian theory. Such theory assumes a normal distribution of subjects' data and ignores the correlation between the points of the curve. In gait analysis, these assumptions led to narrow prediction bands with a reduced "coverage probability", i.e. including fewer curves than expected of known asymptomatic subjects. For instance, Lenhoff et al. reported an actual coverage probability of 54% instead of 90% for the knee flexion-extension [10].

Furthermore, "differential" PBI, i.e. PBI obtained from assessing the difference in scapulo-humeral coordination of the right and left side of control subjects, have also never been reported, despite the relevance of side-to-side analyses [3,5]. This lack of knowledge limits the possibility of within-patient evaluations, since a "normal variability range" is missing when assessing the difference between a patient's own sound and affected side.

The aim of this study was to overcome the state-of-the-art, by generating age-stratified "monolateral" PBI as well as "differential" PBI for the scapulo-humeral coordination, based on the non-parametric Bootstrap technique [24,25]. To the authors' knowledge, this methodology has never been applied to upper limb kinematics. To verify if the Bootstrap method is a superior tool for the calculation of PBI in shoulder motion analysis, as in gait analysis [10,11], a further aim of this

study was to calculate PBI based on the Gaussian theory and to compare the coverage probability of both methods. An example of clinical application of the PBI is provided in Section 3.4.

2. METHODS

2.1 SUBJECTS

Asymptomatic subjects (N = 111; mean age ± SD: 38 ± 14) were recruited for this study after giving their informed consent. Subjects were split in three age-groups:

- group 1 (G1): from 18 to 30 year-old (mean 24), including 46 subjects (35 male);
- group 2 (G2): from 31 to 50 year-old (mean 40), including 35 subjects (22 male);
- group 3 (G3): from 51 to 70 year-old (mean 60), including 30 subjects (13 male).

A forth group (GD) included all subjects for whom the scapulo-humeral coordination of both sides was measured (N = 36; mean age ± SD: 42 ± 13): 10 subjects from G1 (6 male), 13 from G2 (9 male), and 13 from G3 (6 male).

2.2 MOTION ANALYSIS PROTOCOL

To measure the scapulo-humeral coordination, the ISEO protocol was used [9], with 3 MTx sensors (Xsens Technologies, NL), positioned over thorax, scapula and humerus. Each MTx is a small (38x53x21mm) and lightweight (30g) inertial and magnetic measurement unit, which provides the orientation of its embedded technical coordinate system relative to a global, earth-based coordinate system (Xsens Technical Manual). The ISEO procedure for the subject-specific sensor-to-segment calibration has been previously reported, as well as the intra- and inter-operator agreement [26].

2.3 DATA COLLECTION

For each subject, the humerus elevation in the sagittal (FL-EX) and in the scapular (AB-AD) plane was measured together with the scapula protraction-retraction (PR-RE), medio-lateral rotation (ME-LA) and posterior-anterior tilting (P-A). Starting with the arms alongside the body, each subject was asked to elevate the humerus, with the thumb up, until his/her maximum elevation was reached and then to return to the starting position. Each movement was repeated five times in a row, but only the middle three were considered for subsequent calculations [6].

2.4 DATA PROCESSING

The following data processing was applied to each subject (Figure 1).

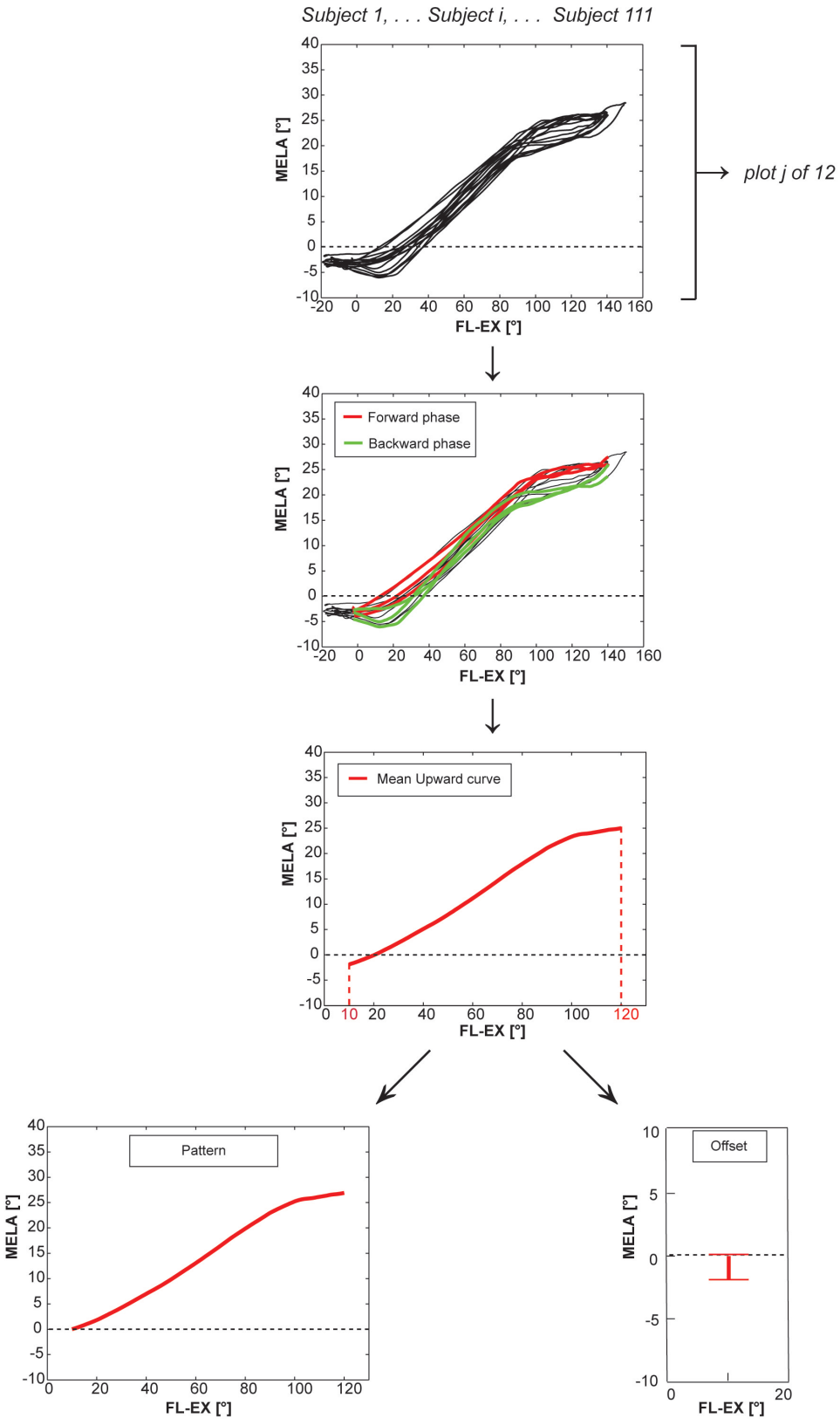

FIGURE 1. Graphical representation of the data processing applied to each subject.

Each movement was split in an upward and a downward phase [26,15] and a total of 12 angle-angle plots was obtained, each plot containing three curves: 1-2) PR-RE vs. FL-EX, upward, downward; 3-4) ME-LA vs. FL-EX, upward, downward; 5-6) P-A vs. FL-EX, upward, downward; 7-8) PR-RE vs. AB-AD, upward, downward; 9-10) ME-LA vs. AB-AD, upward, downward; 11-12) P-A vs. AB-AD, upward, downward. A common range of humerus elevation was considered for all curves, from 10° to 120°. In this interval, curves were resampled to feature 111 equally spaced points.

Next, for each angle-angle plot, the mean curve from the three was computed and two types of information were extracted:

- the scapula rotation at 10° of humerus elevation (scapular offset), i.e. a single scalar value for PR-RE, ME-LA or P-A, depending on the angle-angle plot considered;
- the scapular "monolateral pattern" (MP), obtained by subtracting the scapular offset from the mean curve: this pattern can be interpreted as the variation of "range of motion" of scapula rotation during humerus elevation.

For the subsequent statistical analysis, all 12 MPs together with the three scapular offsets of the forward flexion movement were considered. These offsets will be referred to as "monolateral offsets" (MO): one for PR-RE, one for ME-LA and one for P-A.

Finally, if the subject was included in GD, differential offsets (DOs) and differential patterns (DPs) were also calculated:

- DO: subtracting the left side MO for PR-RE/ME-LA/P-A from the respective right MOs;
- DP: point-by-point subtraction of corresponding left-side MPs from the right-side MPs.

In summary, for each subject in G1-G3, 3 MO scalar values and 12 MPs were computed. In addition, 3 DOs and 12 DPs were computed for each subject in GD.

2.5 STATISTICAL PROCEDURE

For each group (G1-G3) and angle-angle plot, three distinct 90% PBs around the group mean curve were calculated, based on the subjects' MPs. Similarly, for each group and MO, three distinct 90% PIs were calculated. The same approach was followed for GD, considering DPs and DOs.

The first PB was established through the non-parametric Bootstrap method [10,25]. A padding of 100 points was implemented to obtain periodic waveforms from MPs and DPs. Subsequently, 13 Fourier coefficients were calculated [25] to extract a parametric description of each MP/DP. PB was finally calculated through 500 Bootstrap replications.

The second PB was established through a parametric procedure based on the Gaussian theory and assuming a Normal distribution, as commonly done in the literature [11]. In particular, the PB was

obtained by considering point-by-point intervals with amplitude of ±1.6449 standard deviations around the subjects' mean curve.

Finally, the third PB was also established through a Gaussian approach, though by considering the Student's T distribution [10]. In the calculation of PB the inverse of the cumulative distribution function is of interest, and thus the Normal distribution closely approximates T only for samples > 300. Hence, the coefficient 1.6449 must be replaced with specific critical values that depend on the number of subjects included in each group. Following this approach, the resulting critical values were 1.6794 for G1, 1.6909 for G2, 1.6991 for G3 and 1.6896 for GD.

The calculation of PIs for MOs and DOs was based on the same three methods, applied on scalar values instead of waveforms [11].

To compare the three PBs of each angle-angle plot and the three PIs, we calculated the coverage probability of each method, through a leave-one-out cross-validation procedure [10]. If methods are equivalent, they should return a coverage as close as possible to 90% for each angle-angle plot or interval. In particular, we hypothesized that no statistically significant differences should be observed between the three methods when comparing the distributions obtained from pooling the coverage probabilities of the:

- H1: angle-angle plots (12) and groups (3), for the monolateral PBs;
- H2: intervals (3) and groups (3), for the monolateral PIs;
- H3: angle-angle plots (12) of GD, for the differential PBs.

No statistical analysis was performed for the differential PIs, since just three values per method would have been included.

The calculations of PBI were implemented in MATLAB 2011a (The MathWorks, USA). To test hypotheses H1-H3, one-way repeated-measures ANOVA (1 factor, 3 levels) was used after checking for normality (p=0.05) using SPSS Statistics 20 (IBM Corporation, USA). Post-hoc tests were carried out with Bonferroni adjustments.

3. RESULTS

3.1 MONOLATERAL PBI

Figures 2-3-4 report the monolateral PBs, respectively for G1, G2 and G3. For all angle-angle plots of G1-G3, the Bootstrap method generated the widest PBs. Comparison of the Bootstrap PBs for G1, G2 and G3 is presented in Figure 5.

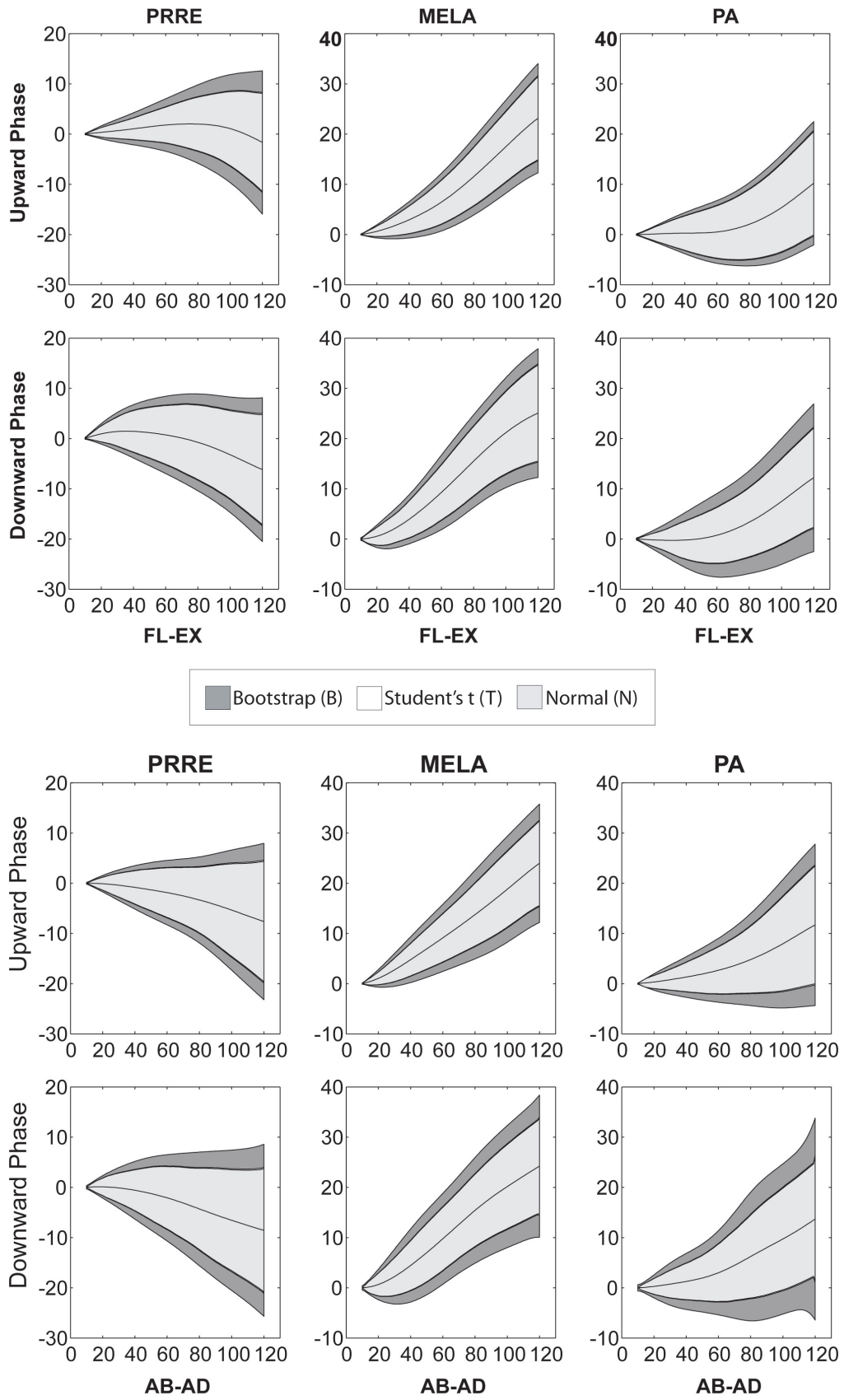

FIGURE 2. Monolateral prediction bands for G1. Bands were computed considering the Bootstrap (dark grey), Student's T distribution (white), and the Normal distribution (light grey) methods. Bands of T and Normal distributions are almost overlapping.

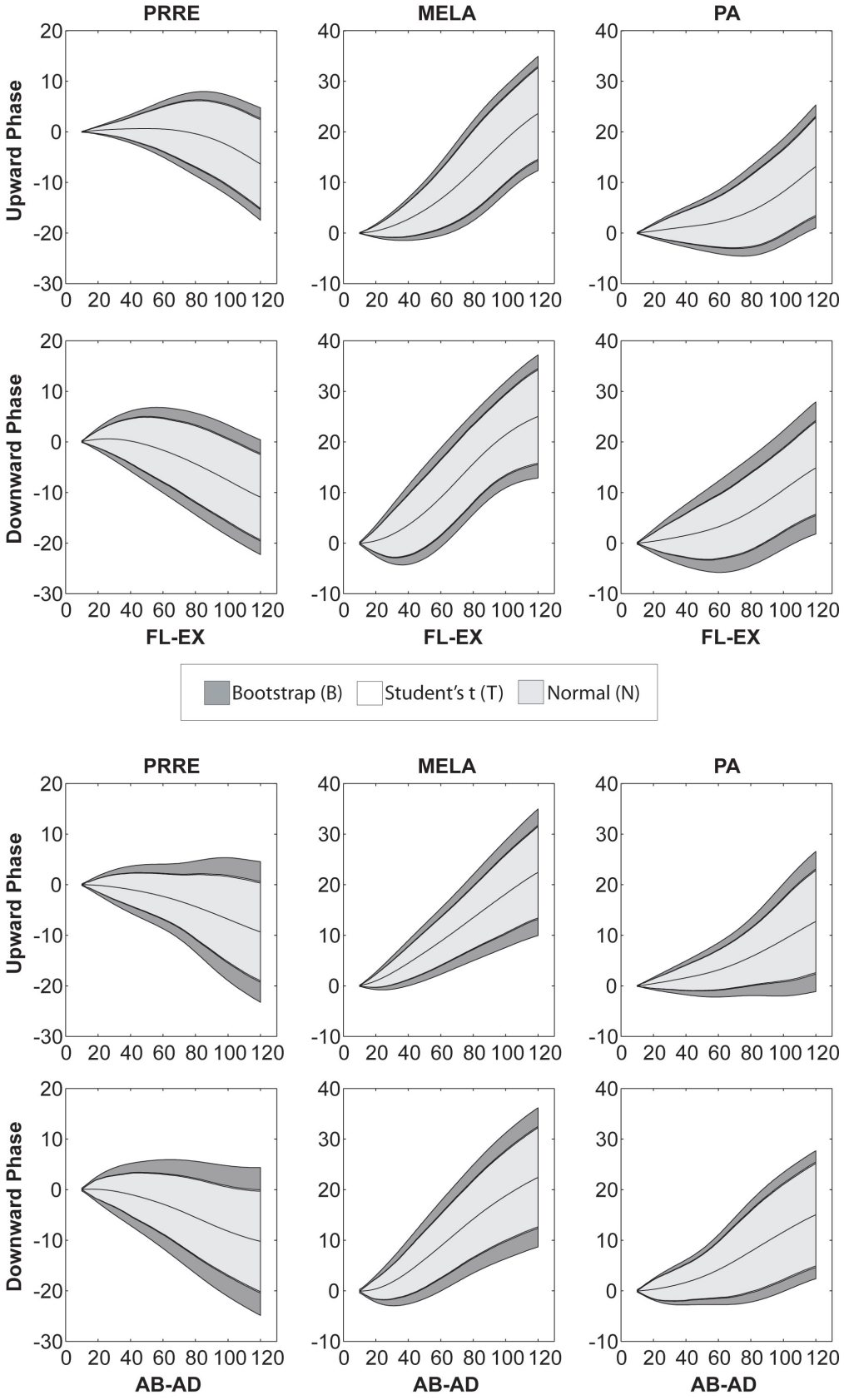

FIGURE 3. Monolateral prediction bands for G2. Bands were computed considering the Bootstrap (dark grey), Student's T distribution (white), and the Normal distribution (light grey) methods. Bands of T and Normal distributions are almost overlapping.

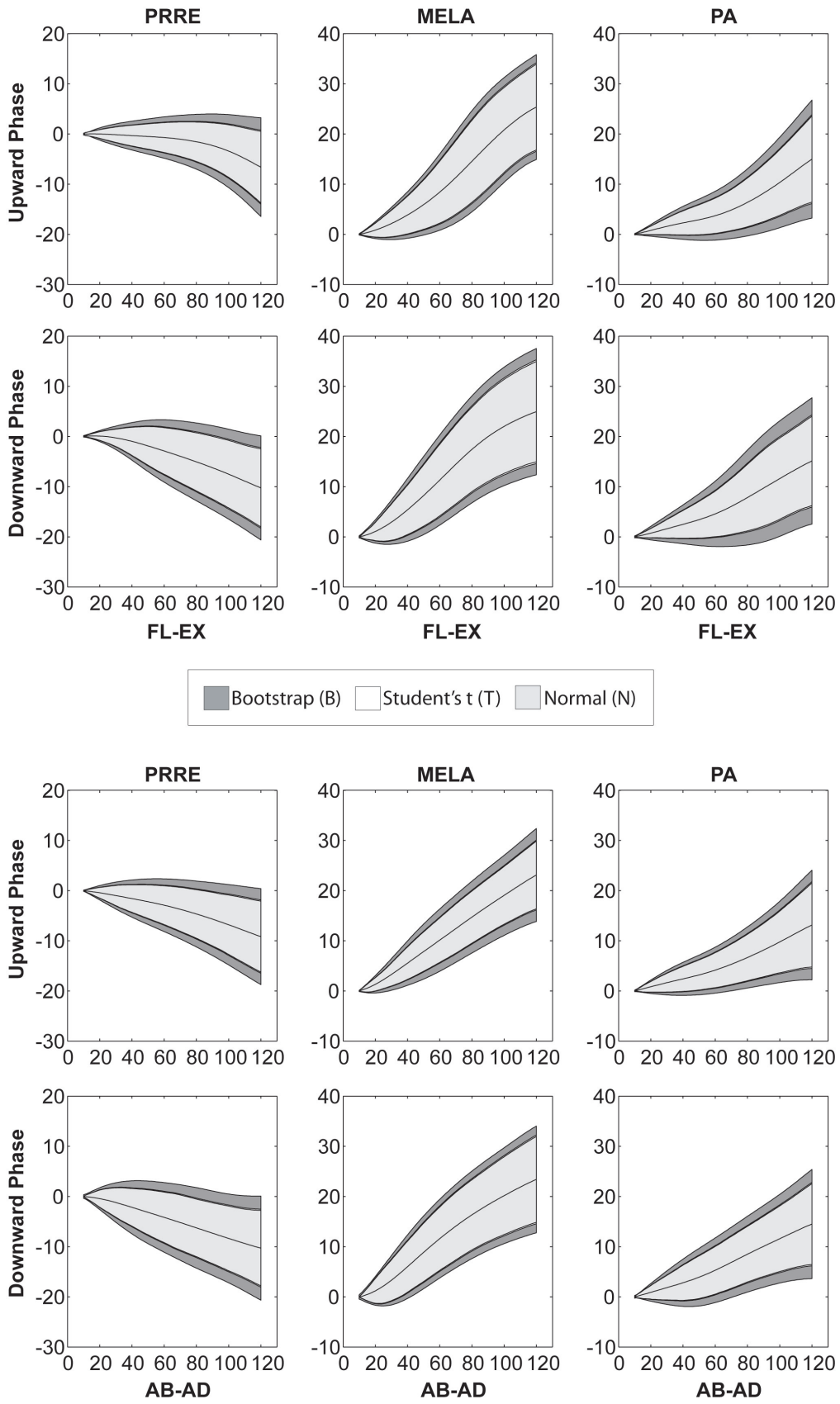

FIGURE 4. Monolateral prediction bands for G3. Bands were computed considering the Bootstrap (dark grey), Student's T distribution (white), and the Normal distribution (light grey) methods. Bands of T and Normal distributions are almost overlapping.

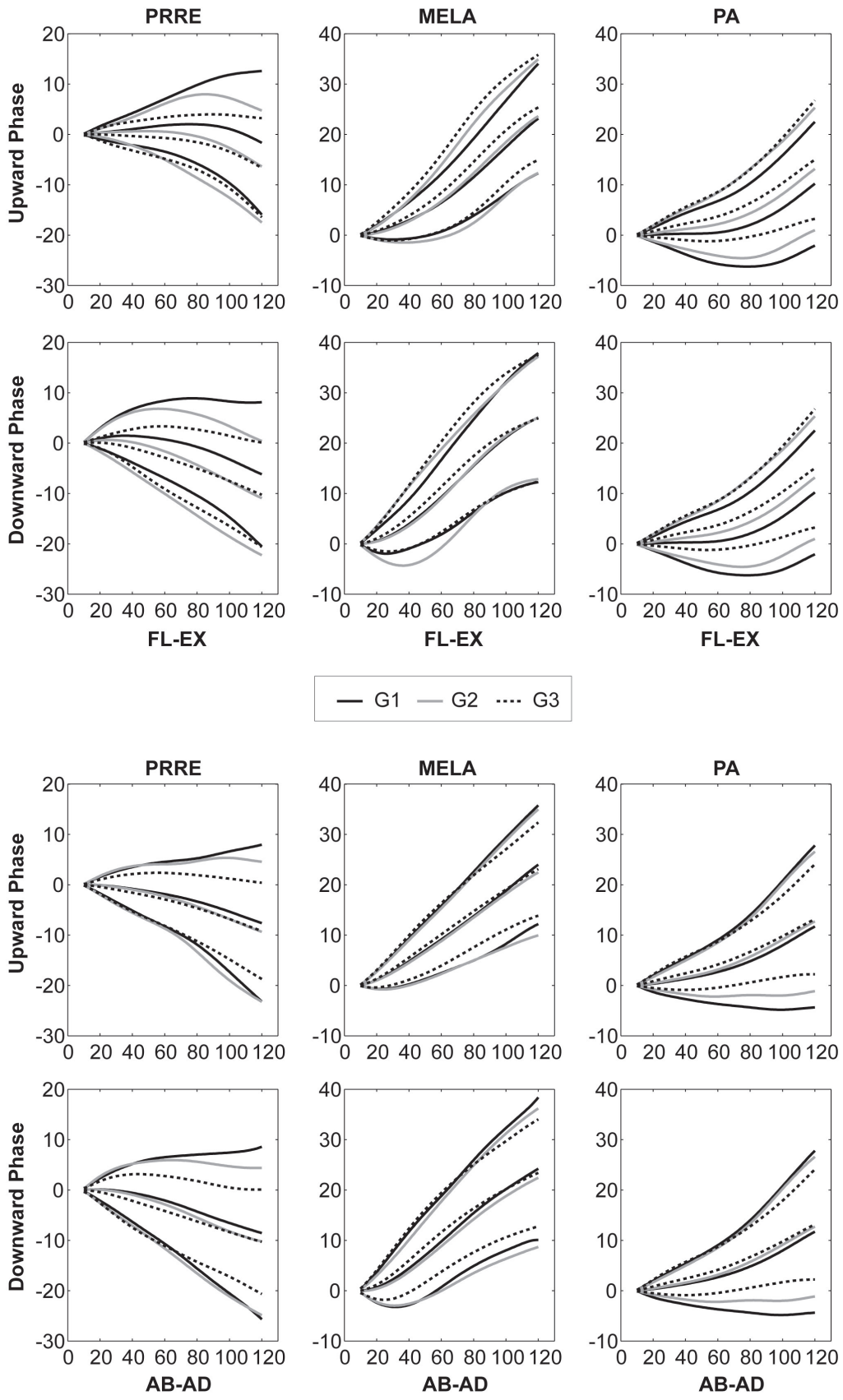

FIGURE 5. Comparison of the Bootstrap monolateral prediction bands of groups G1 (black), G2 (grey) and G3 (dotted). For each group, three lines are reported: the central is the mean, while the other two are the upper and lower prediction bands.

Figure 6 reports the monolateral PIs for G1, G2 and G3. The Bootstrap method also generated wider PIs for 7 out of 9 angles (3 scapular angles per group), i.e. all but PR-RE and ME-LA of G1. Figure 7 reports the graphical comparison of the Bootstrap PIs for G1-G3.

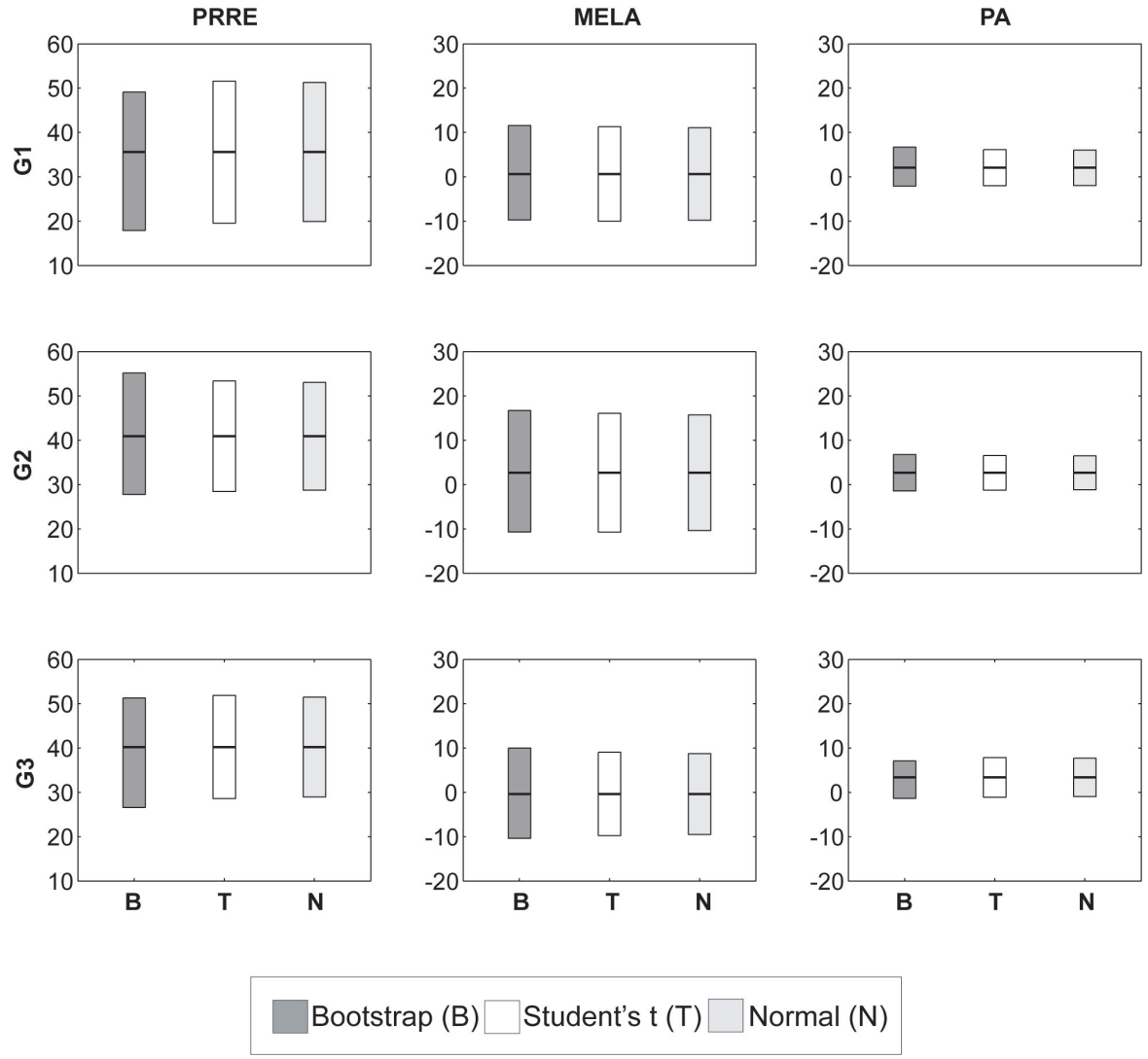

FIGURE 6. Comparison of the Bootstrap monolateral prediction intervals (b) of groups G1 (black), G2 (grey) and G3 (dotted). For each group, three lines are reported: the central is the mean, while the other two are the upper and lower prediction bands.

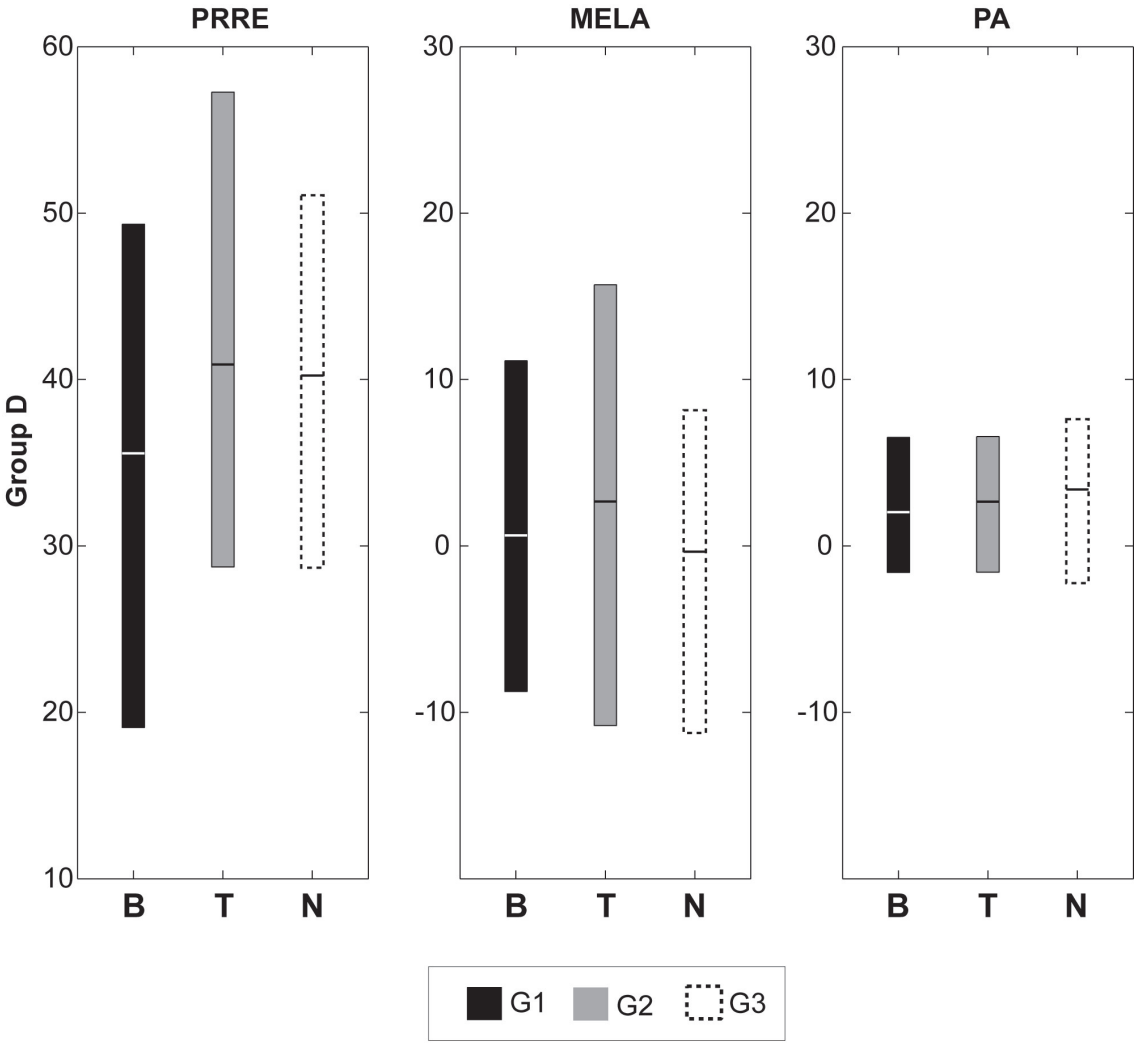

FIGURE 7. Comparison of the Bootstrap monolateral prediction intervals (b) of groups G1 (black), G2 (grey) and G3 (dotted). For each group, three lines are reported: the central is the mean, while the other two are the upper and lower prediction bands.

3.2 DIFFERENTIAL PBI

Figures 8 and 9 report, respectively, the PBs and PIs for GD. As for the monolateral case, the Bootstrap method generated the widest PBs, while the amplitude of the differential PIs was very close between methods (maximum difference of 1.8° for PR-RE, 0.8° for ME-LA and 0.3 for P-A).

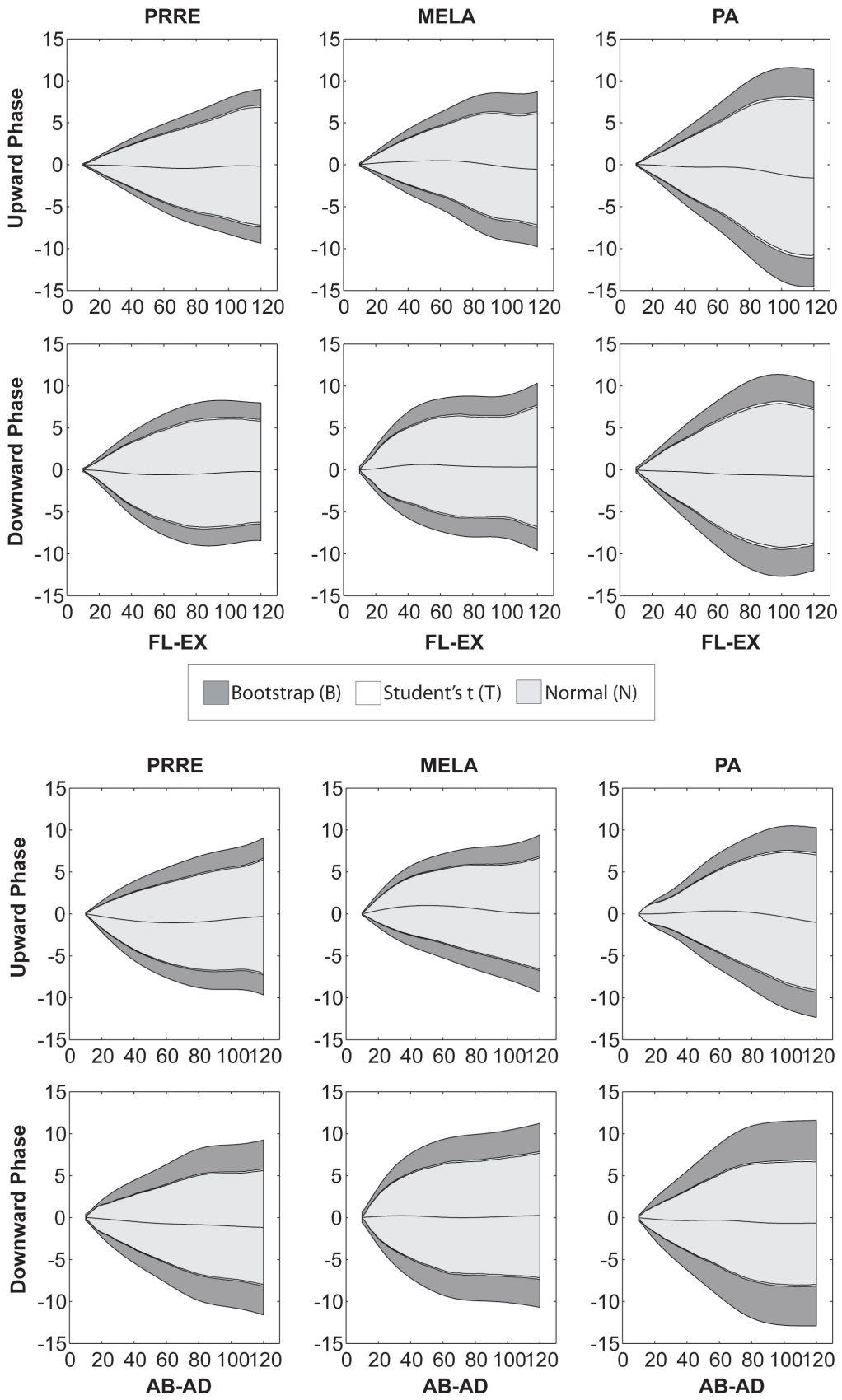

FIGURE 8. Differential prediction bands for GD. Bands were computed considering the Bootstrap (dark grey), Student's T (white), and the Normal (light grey) methods. Bands of T and Normal distributions are almost overlapping.

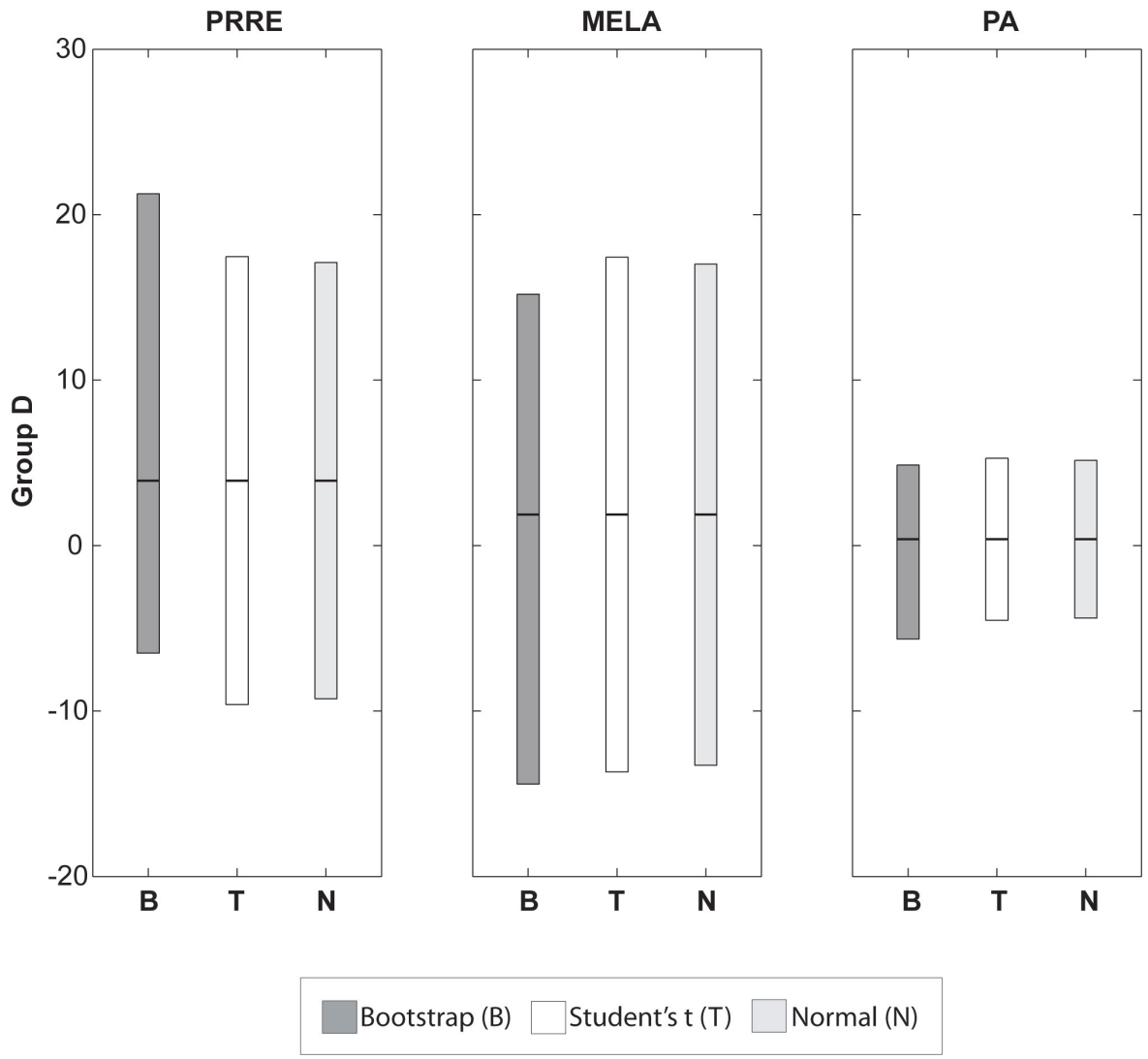

FIGURE 9. Differential prediction intervals for GD. Bands were computed considering the Bootstrap (dark grey), Student's T (white), and the Normal (light grey) methods.

3.3 ANALYSIS OF THE COVERAGE PROBABILITY

All numerical values for the coverage probabilities of the three methods are reported in Tables 1-4. Figures 8a, 8b and 8c report the distributions of the coverage probabilities for hypotheses H1-H3.

			G 1			G 2			G 3		
			PRRE	MELA	PA	PRRE	MELA	PA	PRRE	MELA	PA
FE	FW	B	0.85	0.85	0.89	0.89	0.89	0.86	0.87	0.87	0.87
		T	0.67	0.72	0.83	0.74	0.77	0.66	0.77	0.73	0.70
		N	0.67	0.70	0.83	0.74	0.71	0.66	0.77	0.70	0.70
	BW	B	0.87	0.87	0.87	0.89	0.86	0.89	0.83	0.80	0.83
		T	0.65	0.67	0.72	0.69	0.66	0.71	0.80	0.70	0.57
		N	0.63	0.65	0.65	0.66	0.66	0.69	0.77	0.63	0.53
AA	FW	B	0.89	0.89	0.89	0.86	0.89	0.86	0.83	0.87	0.83
		T	0.80	0.63	0.83	0.77	0.77	0.77	0.67	0.63	0.77
		N	0.78	0.61	0.83	0.77	0.74	0.71	0.67	0.60	0.73
	BW	B	0.89	0.87	0.89	0.86	0.86	0.86	0.83	0.90	0.87
		T	0.65	0.65	0.72	0.69	0.63	0.63	0.63	0.67	0.67
		N	0.65	0.63	0.72	0.69	0.63	0.60	0.60	0.60	0.63

TABLE 1. Coverage probabilities of monolateral prediction bands of the Bootstrap (B), Student's T (T), and Normal (N) methods.

	G 1			G 2			G 3		
	PRRE	MELA	PA	PRRE	MELA	PA	PRRE	MELA	PA
B	0.91	0.89	0.89	0.89	0.89	0.91	0.87	0.87	0.93
T	0.93	0.89	0.85	0.86	0.89	0.89	0.87	0.83	0.90
N	0.93	0.89	0.83	0.86	0.89	0.80	0.87	0.83	0.90

TABLE 2. Coverage probabilities of monolateral prediction intervals of the Bootstrap (B), Student's T (T), and Normal (N) methods.

			G D		
			PRRE	MELA	PA
FE	FW	B	0.83	0.81	0.92
		T	0.67	0.69	0.61
		N	0.64	0.67	0.58
	BW	B	0.89	0.86	0.83
		T	0.75	0.53	0.72
		N	0.75	0.53	0.72
AA	FW	B	0.89	0.86	0.89
		T	0.72	0.69	0.81
		N	0.72	0.67	0.75
	BW	B	0.86	0.83	0.83
		T	0.67	0.67	0.64
		N	0.64	0.67	0.64

TABLE 3. Coverage probabilities of differential prediction bands of the Bootstrap (B), Student's T (T), and Normal (N) methods.

	G D		
	PRRE	MELA	PA
B	0.94	0.94	0.89
T	0.86	0.89	0.86
N	0.86	0.89	0.86

TABLE 4. Coverage probabilities of differential prediction intervals of the Bootstrap (B), Student's T (T), and Normal (N) methods.

Considering H1 (monolateral PBs), statistically significant differences exist between the mean coverage for Bootstrap (87%) and both other methods: 70% for Student's T and 68% for Normal (maximum differences up to 30%). Moreover, a small but statistically significant difference also exists between Student's T and Normal (-2%) coverage probabilities. For H2 (monolateral PIs), the mean coverage was 90% for Bootstrap, 88% for T and 87% for Normal, with no statistically significant differences. Finally, results for H3 (differential PBs) were similar to H1, with statistically significant differences between the Bootstrap mean coverage (86%) and all other methods: 68% for T and 66% for Normal (maximum differences up to 33%). Figure 8d reports the distributions for the differential PIs, with results for Bootstrap always greater or equal to the other two methods.

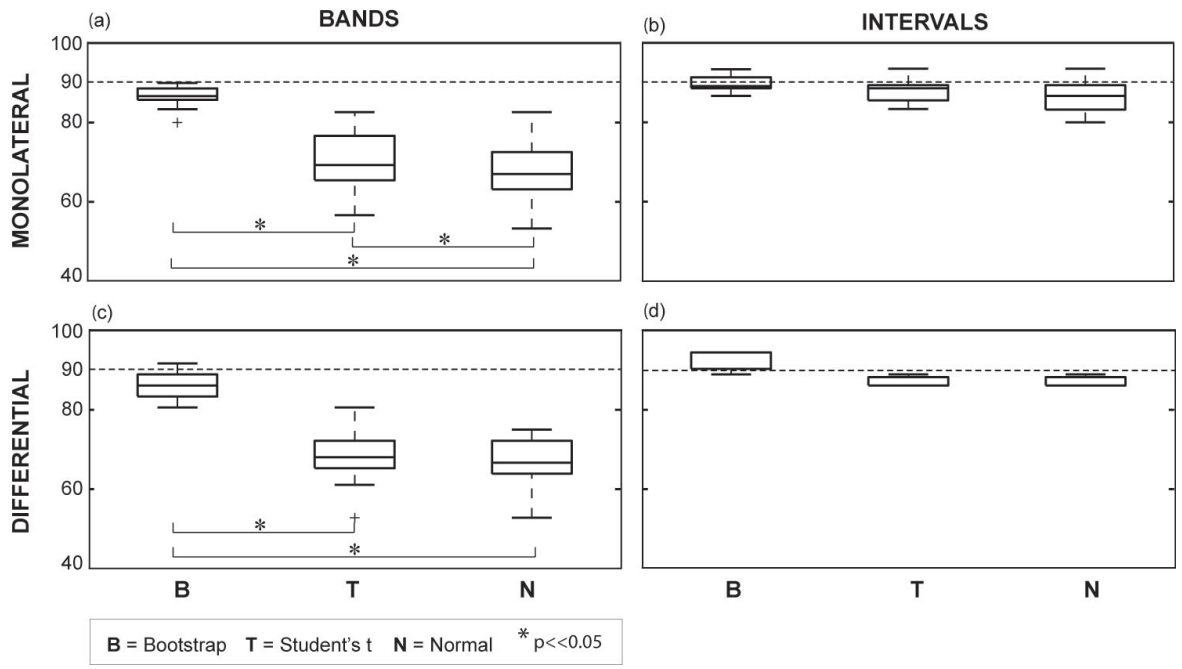

FIGURE 8. Distributions of the coverage probabilities of the Bootstrap (B), Student's T (T), and Normal (N) methods: (a) monolateral prediction bands (H1); (b) monolateral prediction intervals (H2); (c) differential prediction bands (H3); (d) differential prediction intervals. Results are reported as percentages of coverage (mean ± 2SD).

3.4 CLINICAL APPLICATION

This section is intended to illustrate, through a case study:

- the possible misclassifications caused by the use of Gaussian PBI;
- how differential PBI can clarify doubts in the classification of the scapulo-humeral coordination of a patient, by including within-subject left-to-right side comparisons.

Let us consider the case of TN, a 52 year-old woman, arthroscopically treated for a lesion of the supraspinatus on the right side. TN was longitudinally evaluated with ISEO at 45, 70, 90 days after surgery, with an additional 1-year follow-up evaluation of both sides. Figure 9 reports the comparison of TN's scapulo-humeral coordination with the Bootstrap and Gaussian PBI of G3, limited to the upward phase of the FL-EX movement.

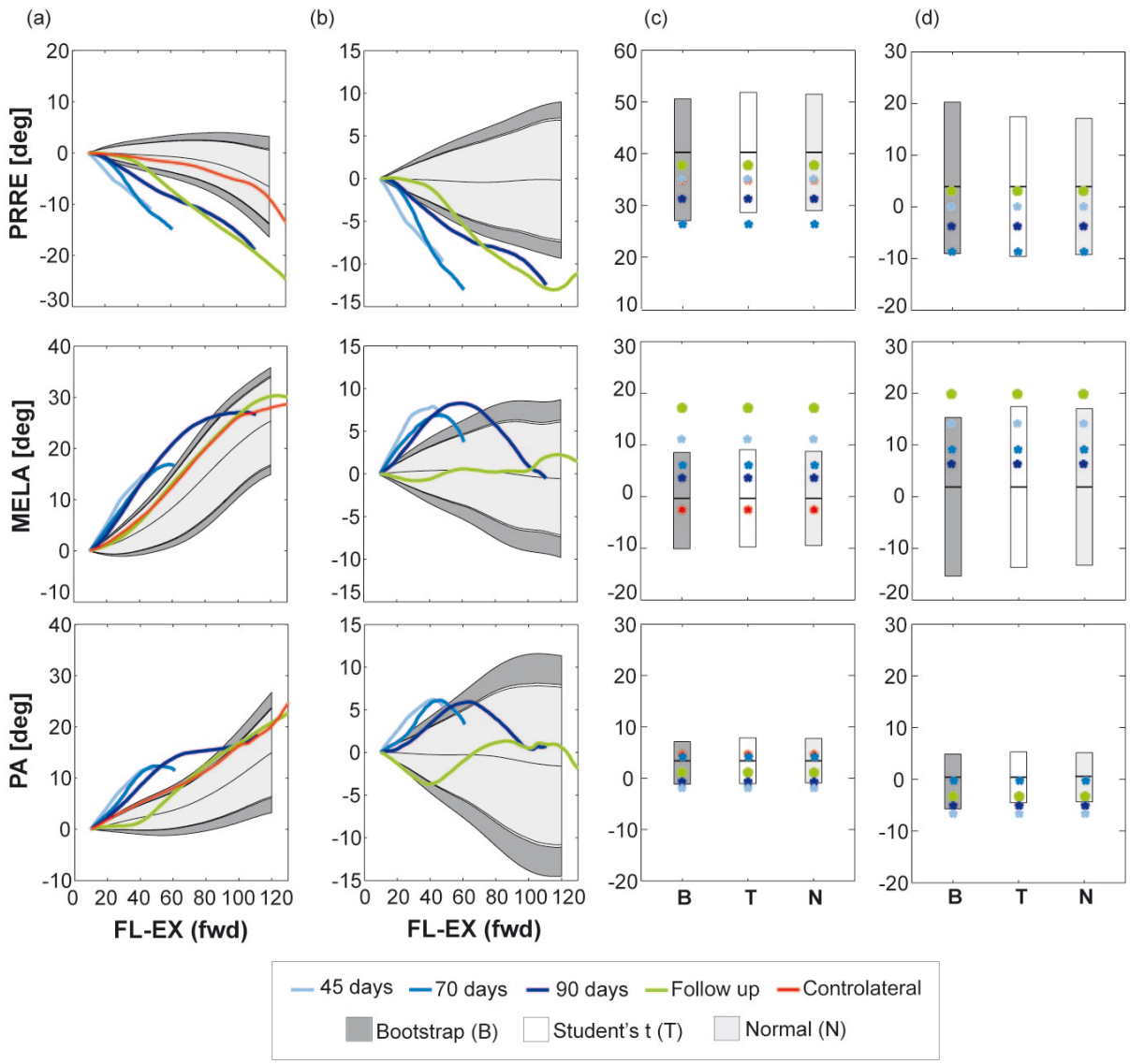

FIGURE 9. Case study. Longitudinal assessment of the scapulo-humeral coordination for the upward phase of the FL-EX movement. The treated side (right, R) was evaluated at 45 (light blue), 70 (blue), 90 (dark blue) days after surgery, and at 1-year follow-up (green). The coordination for the controlateral left side (L-red) is also reported, as well as the PBI computed through the Bootstrap and the Gaussian methods (group G3): (a) Monolateral prediction bands; (b) Differential prediction bands; (c) Monolateral prediction intervals; (d) Differential prediction intervals.

TN has never suffered from relevant pain or disorders on the left side, that was clinically evaluated as asymptomatic. However, the Gaussian methods identified this side as symptomatic when looking at the P-A angle-angle plot. The Bootstrap PB did correctly classify it as asymptomatic, though at the limit of the 90% probability range.

The right side scapulo-humeral coordination shows a progression towards the monolateral PBs, from 45 days to follow-up (Figure 9a). While the Bootstrap and Gaussian methods both classify the follow-up for PR-RE as symptomatic and ME-LA as asymptomatic, they diverge when classifying P-A, whereby the Gaussian methods misidentified this pattern as symptomatic.

Based on these monolateral PBs, the pattern for P-A appears critical. The P-A differential PB can hereby serve as an additional within-subject evaluation. In particular, the differential P-A pattern at 90 days (Figure 9b) is within the Bootstrap PB, and should therefore be classified as asymptomatic (though at the extreme of the acceptability range), which is opposite to what was highlighted by the monolateral analysis. This stresses the importance of performing, whenever possible, side-to-side comparisons [3].

The analysis of the monolateral and differential offsets shows a single case of misclassification by the Gaussian method in the P-A differential PIs at 90 days.

From the clinical standpoint, the analysis of the scapula offsets provides complementary information to the analysis of the patterns. While patterns for PR-RE appear symptomatic, the offsets are generally within the asymptomatic range of Bootstrap PIs. On the contrary, while ME-LA patterns at follow-up are classified as asymptomatic, the offsets are clearly out of the range. Clinicians should consider both patterns and offsets when planning the treatment.

4. DISCUSSION AND CONCLUSIONS

This study describes, for the first time, the application of the Bootstrap method for the calculation of PBI for the scapulo-humeral coordination. To facilitate the clinical application, we extracted and separately analyzed two features of the scapulo-humeral coordination: the scapula orientation in a specific reference posture (offset) and the patterns (curves) of coordination. This should allow the clinician to concentrate on the subject's posture and movement separately, as commonly reported in literature [7,3,18]. Of course these factors will interact during rehabilitation, emphasizing the importance of the longitudinal analysis of both. The reference posture selected for the analysis of scapula orientation was with the subject in 10° humerus flexion relative to the thorax. This posture was selected since it represents the closest approximation to the scapula resting position, at a humerus elevation *common to all subjects* and strictly within the setting phase of scapula motion [15].

Both for scapula patterns and offsets, we reported monolateral and differential PBI. The mean pattern associated with the monolateral PBs is consistent with previous findings [2]: during humerus elevation the scapula moves into slight protraction and then retraction, lateral rotation and

posterior tilting. Also the intervals for the scapula resting orientation are consistent with previous findings [7].

While monolateral reference data are relatively common in biomechanics, differentials PBI have never been reported for the upper limb. Compared to monolateral, differential PBI are less affected by personal factors between subjects, e.g. age, sex, working activity [21,23,27] or soft tissue artifact [28], since these factors will affect both sides in a similar way. Hence, differential PBI do not need to be stratified by age, as opposed to monolateral PBI. Figure 5 and 7 clearly showed that the monolateral Bootstrap PBI for the age groups (G1-G3) do not overlap, so that the use of non-age-matched PBI can lead to misclassifications. Interestingly, there seems to be a consistent trend in the scapulo-humeral pattern from younger subjects (G1) to older adults (G3): PR-RE patterns move toward retraction, ME-LA toward lateral rotation and P-A toward posterior tilting. This is similar to a compensatory motion to avoid shoulder impingement, which can be present in asymptomatic older adults [29], by moving the acromion away from the humeral head [2]; moreover, increased lateral rotation can be consistent with restricted capsule [22]. Our findings are complementary to Endo et al., who reported "pain-causative" scapular motions [2] in elderly subjects, that remained partly unexplained [20]. Dayandhi et al. [30] already reported a difference in scapula movements between children and adults. The scapular behavior described for the children is similar to the result of the elderly in the current study. This suggests optimal scapula stabilization during adulthood, which warrants further investigation. As additional element of interest, the amplitude of PBI also decreases from G1 to G3, i.e. differences between young adults are larger than between older subjects. These findings may be explained by the increased stiffness of the glenohumeral joint with age and the related constraint on motion.

Results from the analysis of the coverage probability highlighted the superiority of Bootstrap PBI compared to the Gaussian approaches, with percentages very close to the nominal 90%, as in gait analysis [10]. In particular for PB (hypotheses H1 and H3), the use of the Normal distribution provided the worst coverage, on average. The use of the T distribution ensured modestly superior results, with differences with respect to Bootstrap of about 17%, and in worst cases up to 30%. Results imply that up to one patient in 5 could be misclassified for what concerns the scapulo-humeral coordination, using the Normal or T distribution PBs.

A limitation of this study was that monolateral PBI could not be stratified based on sex, due to the reduction in the number of subjects in each subgroup. In addition, a sensitivity analysis regarding the misclassifications rate due to the use of non-age-matched PBI for the classification of a new patient was beyond the scope of the study and deserves a specific analysis.

In conclusion, Bootstrap PBI for the scapulo-humeral coordination ensure an optimal coverage and should always be preferred over standard parametric methods. Moreover, the stratification of monolateral PBI by age appears relevant for the correct classification of patients.

5. REFERENCES

1. Ludewig PM, Reynolds JF. The Association of Scapular Kinematics and Glenohumeral Joint Pathologies. J Orthop Sports Phys Ther 2009; 39(2): 90-104
2. De Baets L, Jaspers E, Desloovere K, Van Deun S. A systematic review of 3D scapular kinematics and muscle activity during elevation in stroke subjects and controls. J Electromyogr Kinesiol. 2012 Jul 26. http://dx.doi.org/10.1016/j.jelekin.2012.06.007
3. Morais NV, Pascoal AG. Scapular positioning assessment: Is side-to-side comparison clinically acceptable? Man Ther. 2012 Jul 23. http://dx.doi.org/10.1016/j.math.2012.07.001
4. Kibler WB, Sciascia A, Wilkes T. Scapular dyskinesis and its relation to shoulder injury. J Am Acad Orthop Surg. 2012 Jun;20(6):364-72.
5. Hickey BW, Milosavljevic S, Bell ML, Milburn PD. Accuracy and reliability of observational motion analysis in identifying shoulder symptoms. Man Ther. 2007 Aug;12(3):263-70.
6. Kontaxis A, Cutti AG, Johnson GR, Veeger HE. A framework for the definition of standardized protocols for measuring upper-extremity kinematics. Clin Biomech (Bristol, Avon). 2009 Mar;24(3):246-53.
7. Struyf F, Nijs J, Baeyens JP, Mottram S, Meeusen R. Scapular positioning and movement in unimpaired shoulders, shoulder impingement syndrome, and glenohumeral instability. Scand J Med Sci Sports. 2011 Jun;21(3):352-8.
8. Garofalo P, Cutti AG, Filippi MV, Cavazza S, Ferrari A , Cappello A, Davalli A. Inter-operator reliability and prediction bands of a novel protocol to measure the coordinated movements of shoulder-girdle and humerus in clinical settings. Med Bio Eng Comput 2009; 47(5): 475-86
9. Cutti AG, Giovanardi A, Rocchi L, Davalli A, Sacchetti R. Ambulatory measurement of shoulder and elbow kinematics through inertial and magnetic sensors. Med Bio Eng Comput 2008; 46(2): 169-78
10. Lenhoff MW, Santner TJ, Otis JC, Peterson MG, Williams BJ, Backus SI. Bootstrap prediction and confidence bands: a superior statistical method for analysis of gait data. Gait Posture. 1999 Mar;9(1):10-7.
11. Duhamel A, Bourriez JL, Devos P, Krystkowiak P, Destée A, Derambure P, Defebvre L. Statistical tools for clinical gait analysis. Gait Posture. 2004 Oct;20(2):204-12.
12. Borstad JD, Ludewig PM. The effect of long versus short pectoralis minor resting length on scapular kinematics in healthy individuals. J Orthop Sports Phys Ther. 2005 Apr;35(4):227-38.
13. Crosbie J, Kilbreath SL, Hollmann L, York S. Scapulohumeral rhythm and associated spinal motion. Clin Biomech (Bristol, Avon). 2008 Feb;23(2):184-92.
14. Ludewig PM, Phadke V, Braman JP, Hassett DR, Cieminski CJ, LaPrade RF. Motion of the shoulder complex during multiplanar humeral elevation. J Bone Joint Surg Am. 2009 Feb;91(2):378-89.

15. McClure PW, Michener LA, Sennett BJ, Karduna AR. Direct 3-dimensional measurement of scapular kinematics during dynamic movements in vivo. J Shoulder Elbow Surg. 2001 May-Jun;10(3):269-77.
16. Fayad F, Hoffmann G, Hanneton S, Yazbeck C, Lefevre-Colau MM, Poiraudeau S, Revel M, Roby-Brami A. 3-D scapular kinematics during arm elevation: effect of motion velocity. Clin Biomech (Bristol, Avon). 2006 Nov;21(9):932-41.
17. van Andel C, van Hutten K, Eversdijk M, Veeger D, Harlaar J. Recording scapular motion using an acromion marker cluster. Gait Posture 2009; 29(1): 123-8
18. Yano Y, Hamada J, Tamai K, Yoshizaki K, Sahara R, Fujiwara T, Nohara Y. Different scapular kinematics in healthy subjects during arm elevation and lowering: glenohumeral and scapulothoracic patterns. J Shoulder Elbow Surg. 2010 Mar;19(2):209-15.
19. Pascoal AG, van der Helm FF, Pezarat Correia P, Carita I. Effects of different arm external loads on the scapulo-humeral rhythm. Clin Biomech (Bristol, Avon). 2000;15 Suppl 1:S21-4.
20. Endo K, Yukata K, Yasui N. Influence of age on scapulo-thoracic orientation. Clin Biomech (Bristol, Avon). 2004 Dec;19(10):1009-13.
21. Tempelhof S, Rupp S, Seil R. Age-related prevalence of rotator cuff tears in asymptomatic shoulders. J Shoulder Elbow Surg 1999;8:296-9.
22. Lin JJ, Hanten WP, Olson SL, Roddey TS, Soto-Quijano DA, Lim HK, Sherwood AM. Functional activities characteristics of shoulder complex movements: Exploration with a 3-D electromagnetic measurement system. J Rehabil Res Dev. 2005 Mar-Apr;42(2):199-210.
23. Downie BK, Miller BS. Treatment of rotator cuff tears in older individuals: a systematic review. J Shoulder Elbow Surg. 2012 Sep;21(9):1255-61.
24. Efron B, Tibshirani RJ. An Introduction to the Bootstrap. London: Chapman and Hall, 1993.
25. Olshen RA, Biden EN, Wyatt MP, Sutherland DH. Gait analysis and the bootstrap. Ann Statist 1989;17:1419–40.
26. Parel I, Cutti AG, Fiumana G, Porcellini G, Verni G, Accardo AP. Ambulatory measurement of the scapulohumeral rhythm: intra- and inter-operator agreement of a protocol based on inertial and magnetic sensors. Gait Posture. 2012 Apr;35(4):636-40.
27. Bodin J, Ha C, Chastang JF, Descatha A, Leclerc A, Goldberg M, Imbernon E, Roquelaure Y. Comparison of risk factors for shoulder pain and rotator cuff syndrome in the working population. Am J Ind Med. 2012 Jul;55(7):605-15.
28. Cutti AG, Paolini G, Troncossi M, Cappello A, Davalli A. Soft tissue artefact assessment in humeral axial rotation. Gait Posture. 2005 Apr;21(3):341-9.
29. Yamamoto A., Takagishi K, Osawa T, Yanagawa T, Nakajima D, Shitara H, Kobayashi T. Prevalence and risk factors of a rotator cuff tear in the general population. J Shoulder Elbow Surg. 2010 Jan; 19(1):116-20.
30. Dayanidhi S, Orlin M, Kozin S, Duff S, Karduna A. Scapular kinematics during humeral elevation in adults and children. Clin Biomech (Bristol, Avon). 2005 Jul;20(6):600-6.

Chapter 3

Within-protocol repeatability and agreement of two protocols for the analysis of scapulo-humeral coordination

Parel I, Cutti AG, Kraszewski A, Verni G, Hillstrom H, Kontaxis A.
Medical & Biological Engineering & Computing Submitted

ABSTRACT

Multi-center clinical and research studies on shoulder kinematics are currently uncommon. The availability of agreement studies of between-center motion analysis protocols is lacking and work in this area would foster standardization and dataset compatibility. The aim of this work was to evaluate the kinematic agreement between two upper extremity protocols at different laboratories: one based on the scapula tracker and the ISB recommendations (ST) and the other based on the spine tracker and the ISEO protocol (ISEO). First, in-vivo within-protocol repeatability for each protocol was assessed on a group of 23 healthy subjects. Then, the between-protocol agreement was evaluated, both through comparisons with the literature (RMSE) and with the within-protocol repeatability (Limits of Agreement).

The within-protocol repeatability resulted sufficient both for ST and ISEO. Assuming the within-protocol repeatability as threshold for agreement, ST and ISEO resulted interchangeable for scapula protraction-retraction up to 50° and scapula medio-lateral rotation up to 120° for flexion-extension and 100° for ab-adduction movements. Depending on the aim of a clinical study, the threshold might be narrowed or enlarged, leading to different results for agreement.

INTRODUCTION

Multi-center clinical and research studies focusing on shoulder kinematics are currently uncommon, mainly due to the diversity of methodologies adopted by each center, which include non-invasive devices for dynamic scapula-tracking and, to some extent, anatomical coordinate systems.

In particular, four tracking methods are commonly used in the literature to measure scapula kinematics non-invasively and dynamically [5]: i) the scapula tracker [8,14], ii) the acromion tracker [10,12,17], iii) skin-markers [9,20], and iv) the scapula spine tracker [4,13]. The *scapula tracker* was designed to track the scapula motion by following the scapula spine and acromion. It usually consists of a base that has a hinge joint that allows it to conform to the scapula spine and height adjustable footpad that rests on the acromion and connects to the base through an also adjustable arm. The *acromion tracker* consists of a magnetic sensor or marker cluster placed on the skin over the acromial plate of the scapula. The *skin-marker method* is a straightforward placement of markers over the main anatomical landmarks of the scapula [19]. Finally, the *spine tracker* collects scapula kinematics via a calibrated inertial and magnetic sensor positioned over the central third between the angulus acromialis and the trigonum spinae, aligned with the upper edge of the

scapula spine. Since these methods differ based on the sensor placement, it is reasonable to expect each to be influenced by soft-tissue artifact differently.

The advent of inertial and magnetic measurement systems (IMMS) contributes to the diversity of measurement techniques among laboratories. With IMMS the direct identification of anatomical landmarks is not practical and therefore the application of the ISB/ISG recommendations is not feasible. Functional and static-reference posture approaches are recommended instead [4,6].

The execution of multi-center clinical motion analysis trials would benefit from studies measuring the agreement between the different protocols to establish the interchangeability of the kinematic data. At present, however, such analyses are not available. The aim of this work was to assess the agreement between the protocols currently in use at two different motion analysis laboratories of the authors, i.e. one based on the scapula tracker and the ISB recommendations (ST) and the other based on the spine tracker and the ISEO protocol (ISEO). Specifically, the within-protocol repeatability for both protocols was assessed on the same group of subjects because acceptable levels of within-protocol repeatability are a precondition for a between-protocol agreement analysis [1,3]. Then the between-protocol agreement was evaluated, both through comparisons with values from the literature and through comparison with the within-protocol repeatability.

METHODS

SUBJECTS

Twenty-three asymptomatic subjects (13 male and 10 female, 29 ± 8 year-old) with no history of shoulder pathology were recruited for the study. Before collecting data, all subjects signed an informed consent approved by the Institutional Review Board. The kinematics of the right (dominant) shoulder was collected for all subjects by a single investigator, familiar with both protocols.

UPPER LIMB PROTOCOLS

The kinematics of each subject was collected by means of ST and ISEO protocols at the Leon Root, MD Motion Analysis Laboratory of the Hospital for Special Surgery. The ST protocol used a scapula tracker built following the recommendations provided in [8] and fabricated through rapid prototyping (Figure 1A). Data were collected using a 12-camera optical motion tracking system (Motion Analysis Corporation; Santa Rosa, CA USA) with individual and clusters of passive reflective markers (12.7mm diameter). The anatomical frames of thorax, scapula and humerus were constructed by implementing the ISB recommendations [19]. Bony anatomical landmarks were

located using a digitizing pointer (C-Motion), and Visual3D® software (C-Motion Inc; Germantown, MD USA) was used for the visualization and computation of the coordinate systems and kinematics. Cyclic glenohumeral circumductions were used to calculate the glenohumeral joint center, based on a functional method [15].

The ISEO protocol is based on three inertial and magnetic sensors (Xsens Technologies; Enschede, The Netherlands) positioned on the thorax, scapula (Figure 1B) and humerus [4]. To create the anatomical coordinate systems, ISEO requires an acquisition in a static reference posture with the subject standing upright and the humerus positioned alongside the body in neutral rotation and the elbow flexed at 90° in neutral pronation-supination. A MATLAB® (The MathWorks; Natick, MD USA) custom-written code, based on the MTx (Xsens) software development kit, was used to collect data and calculate joint kinematics in real-time.

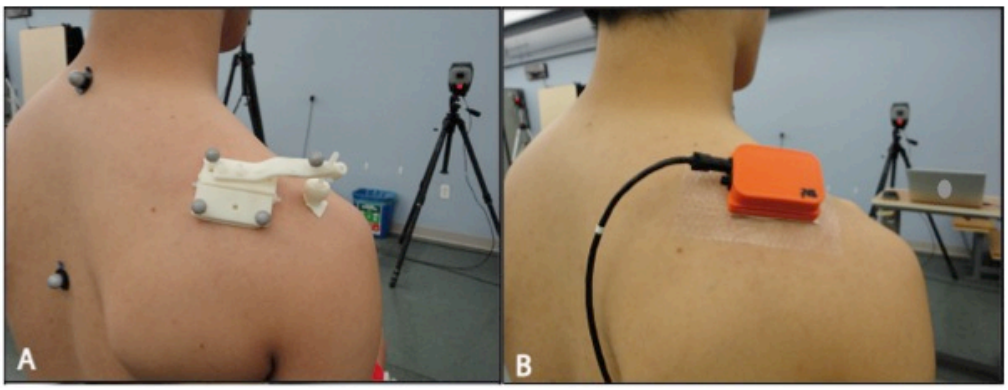

FIGURE 1 A-B. Position of the scapula-tracker (ST, 1A) and of the spine-tracker (ISEO, 1B) on the same subject.

EXPERIMENTAL SETUP AND MOTION DATA COLLECTION

Due to the shape and placement of the scapula trackers and to avoid any interference between setups, the ST and ISEO protocols were applied and tested separately on the same day. To assess within-protocol repeatability each protocol was applied twice, and to minimize operator bias – influenced by the positioning of sensors from the previous session – protocols were applied considering the schema A-B-A-B, where A could represent ST and B could represent ISEO or vice-versa in a random fashion. Therefore each subject underwent a total of 4 testing sessions: two ST and two ISEO protocols.

A standardized setup was adopted. All subjects were required to stand upright with their feet positioned over footprints aligned to shoulder width and parallel to the sagittal plane. Two straight

lines were drawn on the ground to identify the humerus planes of elevation, i.e. sagittal plane and scapular plane (30° anterior to the frontal plane). A vertical pole was used to control the plane of elevation during the task. Self-paced movements of flexion-extension (FL-EX) in the sagittal plane and abduction-adduction (AB-AD) in the scapular plane, starting from a resting position (arms at side) to maximum elevation and back to resting, were collected. Each movement was repeated 5 times with the arm straight and the thumb up. The middle three repetitions were considered for further data analysis. To minimize fatigue, at the end of each session each subject was asked to rest for about 15 minutes.

DATA ANALYSIS

The kinematics describing the scapulo-humeral coordination was calculated for both protocols using the following Euler decompositions:

- y – z' – x'' for the scapulothoracic joint (scapula with respect to the thorax), corresponding to protraction-retraction (PR-RE), medio-lateral rotation (ME-LA) and posterior-anterior tilting (P-A);
- x – z' – y'' for the humerothoracic joint (humerus with respect to the thorax) when elevating in the sagittal plane, corresponding to FL-EX, AB-AD and internal-external rotation;
- z – x' – y'' for the humerothoracic joint (humerus with respect to the thorax) when elevating in the scapular plane, corresponding to AB-AD, FL-EX and internal-external rotation.

The following data processing was applied to each subject and session. Each movement was split into an upward and downward phase [13] and only upward phases were analyzed, similarly to [8,14,16,17]. A total of 6 angle-angle plots were generated, each plot containing three curves: 1) PR-RE vs. FL-EX; 2) ME-LA vs. FL-EX; 3) P-A vs. FL-EX; 4) PR-RE vs. AB-AD; 5) ME-LA vs. AB-AD; 6) P-A vs. AB-AD. The minimum and maximum humerus elevation across all subjects was standardized to 20° and 130°. In this range, curves were resampled (through cubic spline interpolation) to 111 equally spaced points such that the mean curve could be computed for each plot. The entire mean curve was offset by the minimum scapula rotation value at 20° of humerus elevation (considered as the resting position) to improve visual comparison between protocols and sessions. The resulting curve, called the *mean angle-angle pattern,* was interpreted as variation of range of motion (ROM) of scapula rotation during humerus elevation. For each mean angle-angle pattern, 11 discrete humerus elevation angles (*h*) from 30° to 130° with steps of 10° were considered and the corresponding *scapula ROMs* were extracted. Any statistical analysis of scapula values at 20° humerus elevation is obviated since all angle-angle patterns are aligned at this point.

STATISTICAL ANALYSIS

The following statistical analyses apply to each angle-angle plot.

To assess the *within-protocol repeatability* and compare our study to the literature, the mean curves of the two sessions from each subject and protocol were used to calculate the following parameters:

- for each discrete humerus elevation angle *h*, the root mean square error (RMSE) comparing the data of the two sessions across all 23 subjects:

$$\mathrm{RMSE}^{h}_{\mathrm{within-protocol}} = \sqrt{\frac{\sum_{s=1}^{23}(\bar{x}_{1,s}-\bar{x}_{2,s})^{2}}{23}} \quad (1)$$

  where $\bar{x}_{1,s}$ is the scapula ROM of the sth subject extracted from the 1st session and $\bar{x}_{2,s}$ from the 2nd session

- the mean and standard deviation (SD) of the dataset obtained by polling together the scapula $\mathrm{RMSE}^{h}_{\mathrm{within-protocol}}$ of all humerus elevation angles, similarly to [16]:

$$\overline{\mathrm{RMSE}} = \frac{\sum_{h=1}^{11}\mathrm{RMSE}^{h}_{\mathrm{within-protocol}}}{11} \quad (2a)$$

$$\sigma_{\mathrm{RMSE}} = \mathrm{sd}(\mathrm{RMSE}^{1}_{\mathrm{within-protocol}}, \ldots, \mathrm{RMSE}^{11}_{\mathrm{within-protocol}}) \quad (2b)$$

- the standard error of measurement (SEM) for the scapula offset, and for the scapula ROMs at 90° and 120° of humerus elevation [17]:

$$\mathrm{SEM} = \sqrt{\mathrm{MS_W}} \quad (3)$$

where $\mathrm{MS_W}$ is the sum of squares due to the within-subject variability, computed from one-way repeated measures ANOVA [13,18];

- the 95% Limits of Agreement (LoA) for each humerus elevation angle [3]:

$$\mathrm{LoA} = \text{mean difference} \pm 1.96 * \mathrm{SD} \quad (4)$$

The Coefficient of Repeatability (CR) [3] was extracted:

$$CR = 1.96 * SD \quad (5)$$

CR is in relation to SEM (SEM = CR/(1.96*√2)) and complements the available results in the literature.

The repeatability of each protocol was considered to be acceptable based on $\overline{RMSE}$ and σ_{RMSE} as well as SEM, if their values were smaller than or equal to those available in [16] and [17], respectively.

To assess the *agreement between protocols* and compare our results to the literature, for each subject and protocol the mean curve obtained from the mean curves of the two sessions was considered to calculate the following parameters:

- for each humerus elevation angle *h*, the RMSE between-protocol, similarly to [8]:

$$RMSE^{h}_{between-protocol} = \sqrt{\frac{\sum_{s=1}^{23}(\bar{x}_{ST,s} - \bar{x}_{ISEO,s})^2}{23}} \quad (6)$$

where $\bar{x}_{ST,s}$ is the scapula value of the s^{th} subject obtained from the mean pattern of the two session of ST and $\bar{x}_{ISEO,s}$ from the two sessions of ISEO;

- the 95% LoA for each humerus elevation angle, as recommended by [3]. The within-protocol LoA were used as reference to assess the LoA between-protocol.

To establish if the between-protocol agreement was sufficient, we adopted two alternative criteria. The first states that the protocols are in agreement if the RMSE values (Eq. 6) are smaller than or equal to 5°, a value assumed in [7,8] to indicate a sufficient agreement between ST and bone-pin trackers. This criterion, however, does not take into account the within-protocol repeatability, as opposed to the most recent recommendations in agreement studies [3]. The second criterion implements these indications through a strict condition, which states that the protocols are in agreement if both the following apply:

- the between-protocol CRs are smaller than or equal to the largest within-protocol CRs;
- the LoA bias between-protocol is within 1°.

RESULTS

Figure 2(a,b,c-g,h,i) provides a visual representation of the between-protocol variability. In particular, it reports the protocols mean patterns and related standard errors.

Table 2 reports, for each scapula rotation, results about the analysis of the SEM from Eq. 3, together with the results reported in [17].

Figure 3 reports the 95% LoA (Eq. 4) of both protocols. Numerical data are provided in Table 3.

Finally, Figure 3 shows the 95% LoA for the between-protocol agreement, with CRs numerically reported in Table 3.

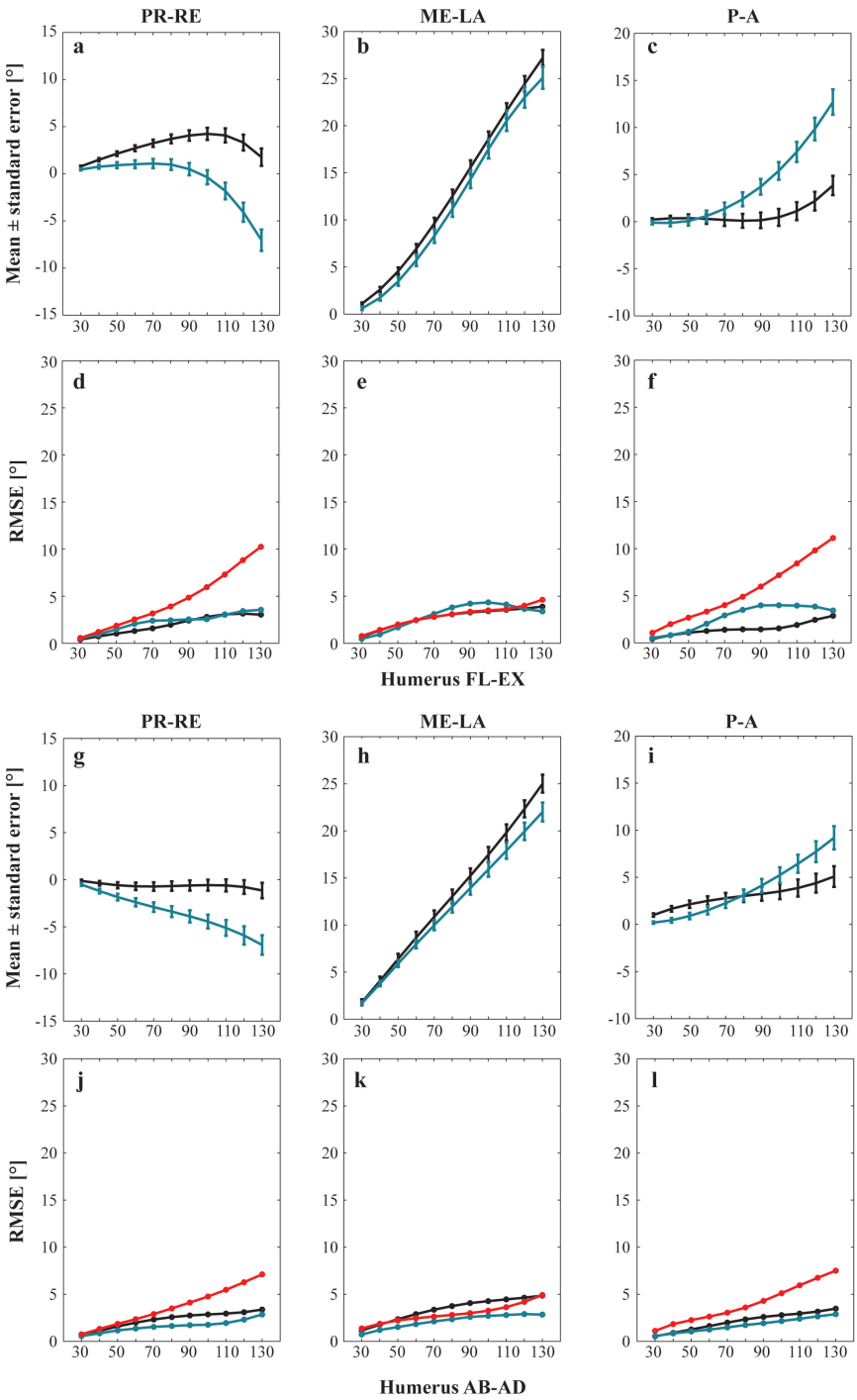

FIGURE 2. Panels (a-c, g-i) report, for each protocol and angle-angle plot, the mean pattern and related standard error, calculated at each humerus elevation angle: black lines for ST and blue lines for ISEO. Panels (d-f, j-l) report both the $RMSE_{within\text{-}protocol}$ and the $RMSE_{between\text{-}protocol}$: black lines for ST, blue lines for ISEO and red lines for the between protocols.

Regarding the within-protocol assessment, $RMSE^{h}_{\text{within}-\text{protocol}}$ values from Eq. 1 are reported in Figure 2(d,e,f-j,k,l). In addition, Table 1 reports, for each scapula rotation and protocol, $\overline{RMSE}$ and σ_{RMSE}, together with the results presented by [16].

	Sagittal plane						Scapular plane					
	ST		ISEO		Thigpen et al. [16]		ST		ISEO		Thigpen et al. [16]	
Scapula rotation	Mean	SD	Mean	SD	Mean	SD	Mean	SD	Mean	SD	Mean	SD
PR-RE	1,96	1,02	2,27	0,96	4,14	3,81	2,30	0,87	1,61	0,64	4,10	3,98
ME-LA	2,75	1,02	2,93	1,35	3,43	3,24	3,42	1,23	2,14	0,74	4,03	3,72
P-A	1,50	0,70	2,74	1,36	4,13	5,04	2,15	0,97	1,72	0,76	4,85	5,84

TABLE 1. Results for $\overline{\mathrm{RMSE}}$ and σ_{RMSE} (Eq.2a,b), that describe the within-protocol repeatability of ST and ISEO protocols compared to the within-protocol (between-session) repeatability reported in [16] for the acromion tracker.

Scapula rotation	Humerus elevation	This study: ST	This study: ISEO	Van Andel et al [17]
PR-RE	At rest	5,1	3,9	4,3
	90° humeral AB	1,9	1,2	6,3
	120° AB	2,2	1,6	7,7
	90° humeral FL	1,7	1,8	6,1
	120° humeral FL	2,2	2,4	8,0
ME-LA	At rest	2,9	3,4	3,4
	90° humeral AB	2,9	1,8	4,2
	120° AB	3,3	2,1	3,9
	90° humeral FL	2,3	3,0	3,8
	120° humeral FL	2,6	2,6	4,1
P-A	At rest	4,2	1,6	7,7
	90° humeral AB	1,8	1,4	7,0
	120° AB	2,2	1,9	7,3
	90° humeral FL	1,0	2,8	6,6
	120° humeral FL	1,7	2,7	8,4

TABLE 2. Results for SEM within-protocol for ST and ISEO, compared to the results reported in [17] for the acromion tracker. Regarding the analysis of the agreement, $\mathrm{RMSE}^{h}_{\mathrm{between-protocol}}$ values (Eq. 6) are reported in Figure 2 (d,e,f-j,k,l).

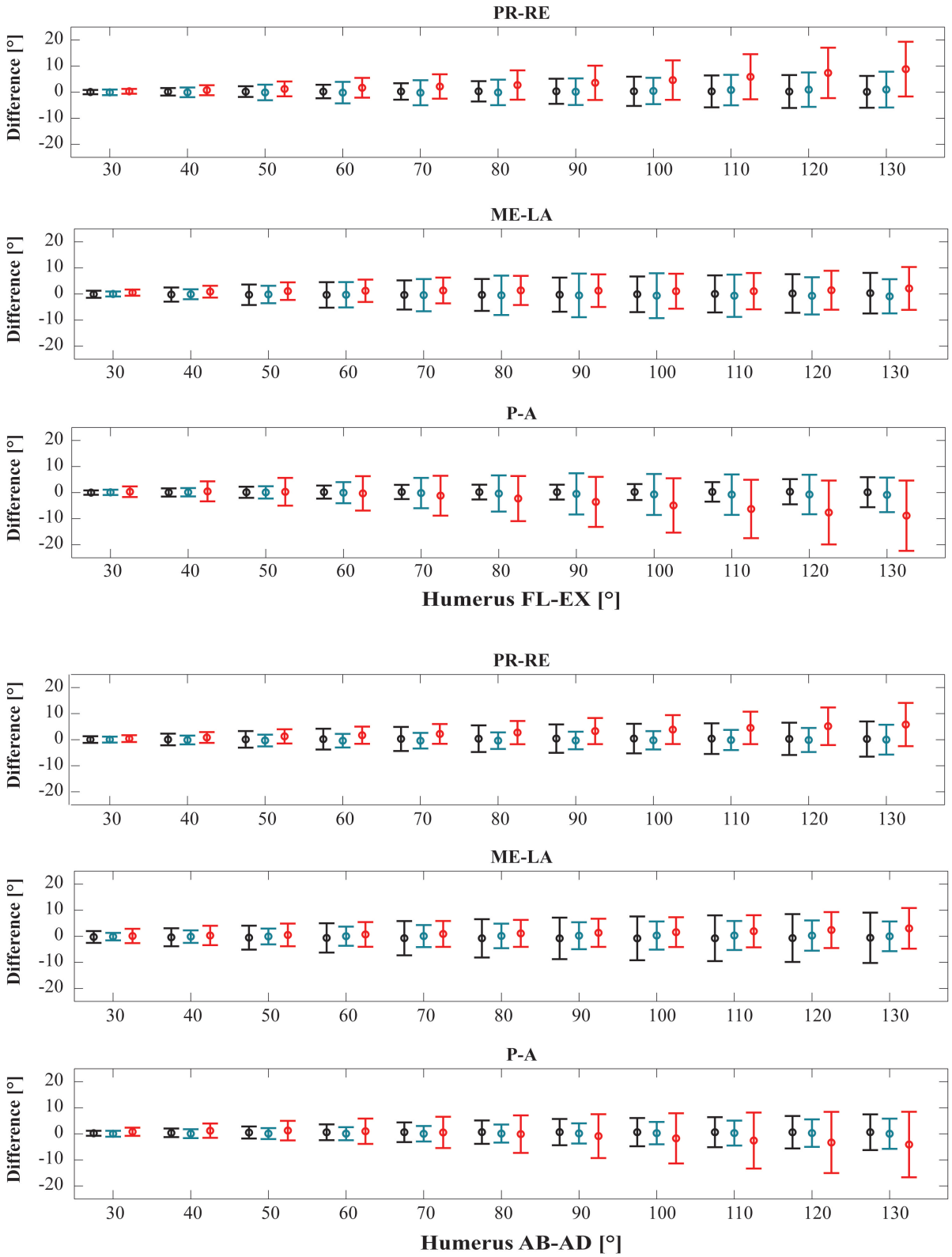

FIGURE 3. Limits of Agreement for ST (black) and ISEO (blue), within-protocol and between-protocols (red), for each angle-angle plot and humerus elevation angle. Limits of Agreements are reported in a summarized form, with the dot symbol representing the bias and bars representing ±CR. Y axes report the difference (Session 1 – Session 2) for the within-protocol repeatability and (ST - ISEO) for the between-protocol agreement.

Scapula rotation	Humerus elevation	Sagittal plane			Scapular plane		
		Within protocol		Between protocols	Within protocol		Between protocols
		ST	ISEO		ST	ISEO	
PR-RE	30	1	1	1	1	1	1
	40	1	2	2	2	2	2
	50	2	3	3	3	2	3
	60	3	4	4	4	3	3
	70	3	5	5	5	3	4
	80	4	5	6	5	3	4
	90	5	5	7	5	3	5
	100	6	5	8	6	4	6
	110	6	6	9	6	4	6
	120	6	7	10	6	5	7
	130	6	7	10	7	6	8
ME-LA	30	1	1	1	2	1	2
	40	3	2	2	3	2	3
	50	4	3	3	5	3	4
	60	5	5	4	6	4	5
	70	6	6	5	7	4	5
	80	6	8	6	7	5	5
	90	7	8	6	8	5	5
	100	7	9	7	8	5	6
	110	7	8	7	9	6	6
	120	7	7	7	9	6	7
	130	8	7	8	10	6	8
P-A	30	1	1	2	1	1	2
	40	2	2	4	2	2	3
	50	2	2	5	2	2	4
	60	2	4	7	3	3	5
	70	3	6	8	4	3	6
	80	3	7	9	4	3	7
	90	3	8	10	5	4	8
	100	3	8	10	5	4	10
	110	4	8	11	6	5	11
	120	5	8	12	6	5	12
	130	6	7	13	7	6	13

TABLE 3. Results for the CRs within and between protocols.

DISCUSSION AND CONCLUSIONS

This study was aimed at describing the agreement between the ST and ISEO protocols, which has never been reported before, to possibly support the execution of multi-center trials based on the two protocols. When comparing two measurement protocols it is ideal to capture them concurrently,

however, due to similarities in size and anatomical placement of the ST and ISEO scapula trackers it was impossible to avoid interference between setups with a concurrent measurement.

WITHIN-PROTOCOL REPEATABILITY

The within-protocol repeatability was firstly investigated. In Figure 2 (a,b,c-g,h,i) mean patterns and standard errors are plotted for each angle-angle plot and humerus elevation angle. It is interesting to notice that the maximum ROM for PR-RE and P-A is considerably smaller in ST than in ISEO (in particular in AB-AD), with results from ISEO closer to the findings previously reported in [11] using intra-cortical pins. For ME-LA (Figure 2b and 2h), the ROMs are similar between the two protocols, with ST ROMs slightly wider.

Figure 2 (d,e,f-j,k,l) also reports the values for the within-protocol RMSE (Eq. 1): RMSE patterns for ST and ISEO are very similar, except for P-A VS FL-EX (Figure 2f), which presents very low values for ST, probably due to the very limited signal in P-A up to 120° of humerus elevation recorded by this protocol. $\overline{\mathrm{RMSE}}$ and σ_{RMSE} obtained for ST and ISEO as reported in Table 1, are much smaller than those presented in [16], which assessed the between-session repeatability of the acromion tracker [10,12,17].

The SEMs found in this study (Table 2) range from 1° to 5.1° for ST and from 1.2° to 3.9° for ISEO considering all movements and scapula rotations. These results are within the values reported by Van Andel et al. [17] (3.4°-8.4°), except for PR-RE at rest for ST, which is slightly (0.8°) above the reference (4.3°).

Regarding results of the within-protocol repeatability by means of 95% LoA, the assumption of normality was checked (Lillietest – MATLAB®) and confirmed for all scapula ROM distributions of each humerus elevation angle. Figure 3 shows that the biases between the two sessions of each protocol are very low and within 1°, meaning that the two sessions are true replicates of the same measurement [3]. Analyses of the CRs for both ST and ISEO show that values increase with the humerus elevation angle (Table 3). Maxima are usually within 7°, with the only exception of ME-LA for ST in FL-EX at 130° of humerus elevation, and in AB-AD from 90°. To assess if these CRs are acceptable, the SEM reported in [17] can be considered as reference. In particular, considering the mathematical relationship between CR and SEM, it is possible to compute CRs from the values reported in Table 2, resulting in a minimum CR of 9.4° and a maximum of 23°. These values are much larger than the CRs for ST and ISEO, thus the within-protocol repeatability is considered acceptable. Moreover, it seems possible to consider, for each humerus elevation angle, the

maximum between the CR values of ST and ISEO as reference for interpreting the CR between-protocols.

Based on the analysis of the RMSE with respect to [8] and of the SEM and LoA with respect to [17], it can be conducted that the within-protocol repeatability is sufficient both for ST and ISEO, even though the repeatability of ST in PR-RE measured by SEM at rest appears slightly above the range (0.8°).

BETWEEN-PROTOCOL AGREEMENT

Regarding the between-protocol agreement, the interchangeability of the two protocols was firstly assessed comparing the $\mathrm{RMSE}^{h}_{\mathrm{between-protocol}}$ values found in the present study (Figure 2 a,b,c-g,h,i) with the 5° threshold that emerges from [7,8], based on the results reported for ST in comparison with intra-cortical pins: results for PR-RE and P-A are within the threshold up to, respectively, 90° and 80° for FL-EX and 100° for AB-AD. $\mathrm{RMSE}^{h}_{\mathrm{between-protocol}}$ values for ME-LA are always within the threshold.

Regarding the analysis of the 95% LoA between-protocol, based on CRs (Table 3 and Figure 3):

- results for PR-RE are acceptable up to 70° and 110° of humerus elevation for FL-EX and AB-AD, respectively;
- results for MELA show a good agreement both in FL-EX and AB-AD;
- between-protocol CRs are never acceptable for P-A.

The analyses of LoA biases show that:

- for PR-RE, values are acceptable up to 50° both in FL-EX and AB-AD;
- for MELA, values are acceptable up to 120° in FL-EX and 100° in AB-AD;
- for P-A, values are acceptable up to 70° in FL-EX and 90° in AB-AD.

Therefore, merging the results obtained for CRs and biases, it possible to state that, based on the analysis of the 95% LoA, the two protocols are in agreement:

- for PR-RE, up to 50° for FLEX and AB-AD;
- for ME-LA, up to 120° for FL-EX and 100° in AB-AD.

In summary, based on the available literature [7,8] it should be concluded that ISEO and ST are in agreement up to about 90° for PR-RE and P-A and always in agreement for ME-LA. However, these results appear too wide when using the LoA and the within-protocol repeatability as reference. Assuming a very strict threshold for agreement, i.e. the maximum within-protocol repeatability, ISEO and ST appear interchangeable for PR-RE up to 50° and ME-LA up to 120° for FL-EX and 100° for AB-AD. Of course, depending on the aim of a clinical study, the threshold might be

narrowed or enlarged, leading to different results for agreement. As reported by Bland et al. [3] *"How small the limits of agreement should be for us, to conclude that the methods agree sufficiently, is a clinical, not a statistical, decision"* and, *"how small* [the difference between observations] *has to be depends on the measurement and the use to which it is to be put"* [2]. For instance, by considering as thresholds the CRs of the within-protocol repeatability reported in [17] for the acromion tracker, the agreement of ST and ISEO would be much broader: the agreement would be conditioned only by the LoA biases, since all the CR values between-protocols would be acceptable.

The results presented in this study for the between-protocol agreement do not take into account the possible implementation of "calibration factors" between protocols, as previously implemented by [8], to improve the accuracy of ST compared to bone-pins. The implementation of such correction techniques can positively influence the bias between protocols, possibly widening the agreement for ME-LA above 120° (100°) for FL-EX (AB-AD), as well as for PR-RE.

REFERENCES

1. Bartlett J.W., Frost C. Reliability, repeatability and reproducibility: analysis of measurement errors in continuous variables. Ultrasound Obstet Gynecol 2010. 31: 466-475.
2. Bland M. An introduction to medical statistics. 3rd Ed, Oxford University Press, New York, p. 273.
3. Bland J.M., Altman D.G. Applying the right statistics: analyses of measurement studies. Ultrasound Obstet Gynecol 2003. 22: 85-93.
4. Cutti A.G., Giovanardi A., Rocchi L., Davalli A., Sacchetti R. Ambulatory measurement of shoulder and elbow kinematics through inertial and magnetic sensors. Med Bio Eng Comput 2008. 46(2): 169-78.
5. De Baets L., Jaspers E., Desloovere K., Van Deun S. A systematic review of 3D scapular kinematics and muscle activity during elevation in stroke subjects and controls. J Electromyogr Kinesiol http://dx.doi.org/10.1016/j.jelekin.2012.06.007
6. de Vries W.H., Veeger H.E., Cutti A.G., Baten C., van der Helm F.C. Functionally interpretable local coordinate systems for the upper extremity using inertial & magnetic measurement systems. J Biomech 2010. 43(10): 1983-1988.
7. Ebaugh D.D., McClure P.W., Karduna A.R. Three-dimensional scapulothoracic motion during active and passive arm elevation. Clin Biomech 2005. 20(7): 700-709.
8. Karduna A.R., McClure P.W., Michener L.A., Sennett B. Dynamic measurement of three-dimensional scapular kinematics: a validation study. J Biomech Eng 2001. 123(2): 184-90.
9. Lovern B., Stroud L.A., Evans R.O., Holt C.A. Dynamic tracking of the scapula using skin-mounted markers. Proc Inst Mech Eng H 2009. 223(7): 823-31.
10. Ludewig P.M., Cook T.M. Alterations in shoulder kinematics and associated muscle activity in people with symptoms of shoulder impingement. Phys Ther 2000. 80(3):276-91.

11. McClure P.W., Michener L.A., Sennett B.J., Karduna A.R. Direct 3-dimensional measurement of scapular kinematics during dynamic movements in vivo. J Shoulder Elbow Surg 2001. 10(3): 269-77.
12. Meskers C.G., van de Sande M.A., de Groot J.H. Comparison between tripod and skin-fixed recording of scapular motion. J Biomech 2007. 40(4): 941-6.
13. Parel I., Cutti A.G., Fiumana G., Porcellini G., Verni G., Accardo A.P. Ambulatory measurement of the scapulohumeral rhythm: intra- and inter-operator agreement of a protocol based on inertial and magnetic sensors. Gait Posture 2012. 35(4): 636-40.
14. Prinold J.A.I., Shaheen A.F., Bull A.M.J. Skin-fixed scapula trackers: a comparison of two dynamic methods across a range of calibration positions. J Biomech 2011. 44(10): 2004-7.
15. Schwartz M.H., Rozulmalski A. A new method for estimating joint parameters from motion data. J Biomech 2005. 38(1): 107-116.
16. Thigpen C.A., Gross M.T., Karas S.G. The repeatability of scapular rotations across three planes of humeral elevation. Res Sports Med 2005. 13(3): 181-198.
17. van Andel C., van Hutten K., Eversdijk M., Veeger D., Harlaar J. Recording scapular motion using an acromion marker cluster. Gait Posture 2009. 29(1): 123-8.
18. Weir J.P. Quantifying test-retest reliability using the intraclass correlation coefficient and the sem. J Strength Cond Res 2005. 19(1): 231-240.
19. Wu G., van der Helm F.C., Veeger H.E., Makhsous M., Van Roy P., Anglin C., Nagels J., Karduna A.R., McQuade K., Wang X., Werner F.W., Buchholz B. ISB recommendation on definitions of joint coordinate systems of various joints for the reporting of human joint motion--Part II: shoulder, elbow, wrist and hand. J Biomech 2005. 38(5): 981-992.
20. Yano Y., Hamada J., Tamai K., Yoshizaki K., Sahara R., Fujiwara T., Nohara Y. Different scapular kinematics in healthy subjects during arm elevation and lowering: glenohumeral and scapulothoracic patterns. J Shoulder Elbow Surg 2010. 19(2): 209-15.

PART 2

Application of ISEO for clinical assessments

In this section the application of ISEO for clinical surveys is reported.
The aim of these studies is to understand if ISEO is applicable in specific clinical contexts.

Chapter 4 reports data and results regarding a longitudinal study conducted in collaboration with Cervesi Hospital (Rimini, Italy). A group of patients treated for rotator cuff tear, which represents one of the most widespread upper arm pathologies in the working population (please refer to *General introduction* for references), was considered during a rehabilitation period of 6-12 months after the surgery treatment. The scapula kinematics of the patients was assessed with ISEO in order to understand if the sensitivity of the protocol is adequate for the detection of changes in scapulo-humeral coordination during rehabilitation. In particular, three studies were carried out:

- Section 4.1: the scapulo-humeral rhythm of the controlateral side of patients was assessed in order to understand if, during the rehabilitation, the acquisition of the controlateral asymptomatic side can be measured only once or should be repeated at each session;
- Section 4.2: changes in the scapulo-humeral rhythm of patients treated for rotator-cuff tear were assessed over a period of 90 days, which represent the recommended recovery period for this type of pathology;
- Section 4.3: a proposal for the modification of the Constant score is reported, in order to introduce for this scale the assessment of scapula kinematic alterations.

Chapter 5 is focused on the theme of motion analysis of upper limb kinematics in transradial amputees. A protocol for the assessment of changes introduced from new prosthetic hands was developed at INAIL Prostheses Center. This protocol comprehends both psychological and motion analysis sessions. This chapter reports the motion analysis protocol developed for this purpose, in particular:

- Section 5.1: the biomechanical assessment of upper limb and the motion analysis protocol developed for trans-radial amputees are reported in detail;
- Section 5.2: a case study of a patient using the Otto-Bock “Michelangelo” hand is reported. In this study a stereophotogrammetric system was used to collect kinematic data in order to assess the applicability of the protocol. The subsequent step will be the application of ISEO protocol for the same purpose.

Chapter 4

Longitudinal study

Section 4.1

Can the scapulo-humeral rhythm of the controlateral side of patients surgically treated for rotator-cuff tear be measured only once in longitudinal studies?

Parel I, Cutti AG, Fiumana G, Porcellini G, Verni G, Accardo AP.
International Society of Biomechanics Conference 2011, Proceeding.

ABSTRACT

A protocol, named ISEO, based on inertial and magnetic sensors, was developed to measure the scapulo-humeral rhythm (SHR). The aim of this work was to understand if and when the SHR of the controlateral side of patients surgically treated for rotator cuff tear can be measured only once (i.e. in a single session), during longitudinal studies, or should be measured, together with the affected side, in every session. Results suggest that this is possible only if a set of 3 criteria is respected with the single session that the rater would like to assume as reference.

INTRODUCTION

A protocol, named ISEO, has been developed by Centro Protesi INAIL to analyze the scapulo-humeral rhythm (SHR) in outpatient clinics [1]. ISEO is based on inertial and magnetic sensors, positioned over the thorax, scapula, humerus and forearm. For positioning the scapula sensor, specific guidelines are provided to the rater [1]. The anatomical and functional frames are defined based on a static acquisition (with the subject standing still with the elbow flexed 90° and vertical humerus in neutral intra/extra rotation) and through a pure flexion/extension and a pure pronation/supination of the elbow. ISEO accuracy in measuring the SHR has been previously analyzed [2], as well as its intra- and inter-rater reliability [3].

In the standard practice, ISEO is currently applied to evaluate the evolution of the SHR during the rehabilitation of patients surgically treated for rotator cuff tear [4]. In these patients, the controlateral side is usually considered as reference, after ensuring its anatomical and functional integrity. The SHRs of both sides are now measured during every evaluation sessions. In order to save time, however, it would be optimal to measure the controlateral side SHR only once, during the first session.

The aim of this work was therefore to:

Q1) measure the similarity of the SHR of the controlateral side of rotator cuff tear patients over time, at the same intervals used for the evaluation of the surgically treated side;

Q2) if necessary, define objective and practical criteria to consider a controlateral SHR as an appropriate reference.

METHODS

Eleven subjects (52±11 years-old) were involved in the study (after giving their informed consent), together with a rater familiar with ISEO. Subjects were all treated arthroscopically for rotator cuff

tear of the supraspinatus. All controlateral sides were clinically evaluated as fully functional for the age of the patient. Three measurement sessions of the controlateral SHR were completed for each subject at 45, 70 and 90 days from surgery of the affected side. In each acquisition, a minimum of 7 humerus flex-extension (FE) and ab-adduction (AA) movements was measured, but the central 3 were considered for subsequent computations. For every movement the three scapula rotations were measured, i.e. pro-retraction (PR-RE), medio-lateral (ME-LA) and posterior-anterior tilting (P-A) as well as the humerus-thorax FE (during FE movements) and AA (during AA movements). Only the upward movements were considered, as they required an active anti-gravitational control of the arm.

A total of 6 angle-angle plots were thus obtained for each subject, namely PR-RE/ME-LA/P-A vs FE and PR-RE/ME-LA/P-A vs AA, and on each we reported 3 groups of 3 SHR curves (3 curves per session).

To measure the between-day repeatability of each subject and answer to question 1, we used the CMC formulation named CMC_2 in [5], after removing the offset. CMC_2 expresses the similarity of the 9 curves of the 3 sessions altogether.

In order to have a further in-depth about the biological variability of each subject within-day and to have a support to answer question 2, we also computed the CMC in the CMC_1 formulation [5]. CMC_1 expresses the average biological variability of the subject within each day. CMC_1 and CMC_2 can be generally interpreted as in [5], i.e. as excellent if greater than 0.95, very good if between 0.85 and 0.95, good if between 0.75 and 0.85, moderate if between 0.65 and 0.75 and inacceptable otherwise.

In order to consider the option of measuring the SHR of the controlateral side only once, for this study we assumed that the distribution of CMC_2 over subjects must be as follows:

1) for the angle-angle plots involving ME-LA: median >0.95; lower whiskers >0.80;
2) for the angle-angle plots involving PR-RE and P-A: median >0.85; lower whiskers >0.75;

These are the same acceptability ranges for the intra-rater reliability of ISEO [3]. In other words, in this study we assumed acceptable the option of measuring the controlateral side just once, only if the between-day reliability is comparable with the intra-rater reliability, which is the minimum uncertainty intrinsic in ISEO.

RESULTS AND DISCUSSION

Results for CMC_2 over the 11 subjects are reported in the box & whiskers plot shown in Figure 1 and indicate that there is an acceptable reliability between days for ME-LA, even though 3 subjects (2 for FE and 1 for AA) were classified as outliers.

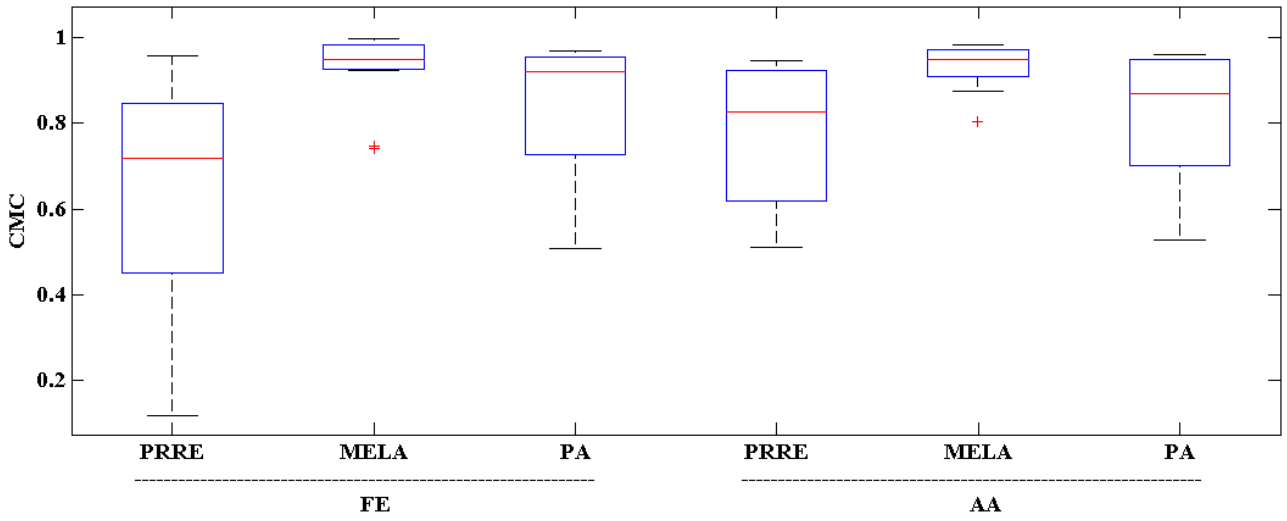

FIGURE 1. Results from the CMC_2 for all groups.

For PR-RE and P-A, instead, the reliability does not meet the criteria that were assumed.

For each angle-angle plot, if only the subjects with CMC_1>0.95 are considered (i.e. those presenting a high consistency of the SHR pattern within-day), the CMC_2 distribution becomes the one reported in Figure 2, in which the criteria are met for all angles and movements, with the exception of P-A during AA.

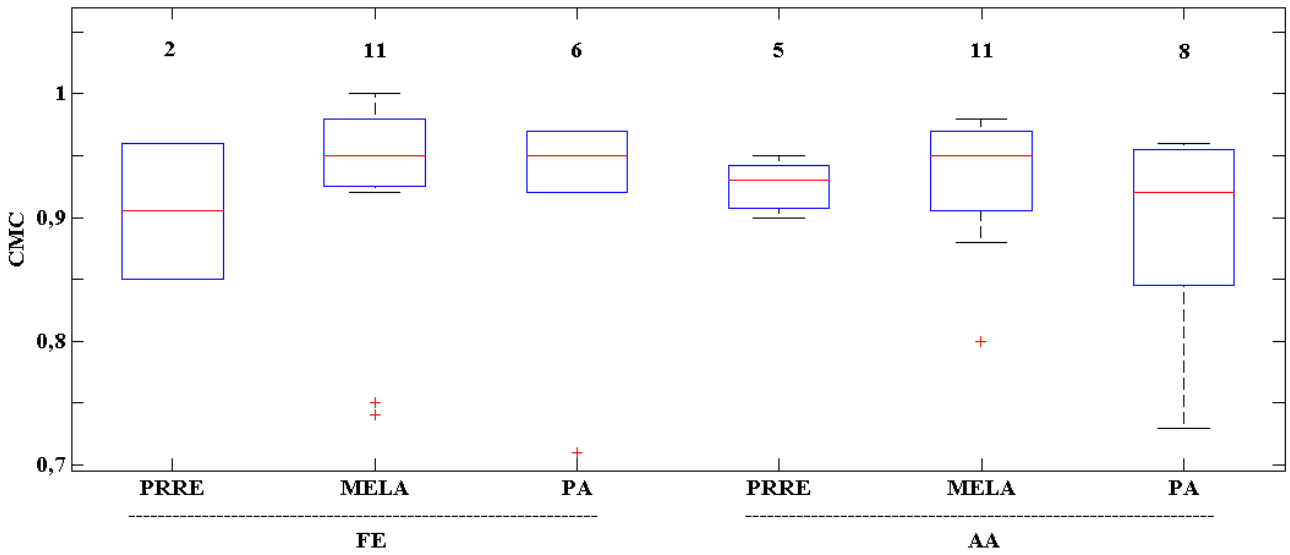

FIGURE 2. Results from the CMC_2 for reliable groups.

The outliers highlighted in Figure 2 and the additional subject who moves the whisker of P-A during AA to 0.73 and does not allow to meet the criteria for this angle, are all featured by a single session in which the *shape* of the SHR curves were dissimilar from those reported for healthy subjects [2,6].

If these sessions are removed, then the CMC_2 distributions are those reported in Figure 3, which satisfy all the criteria.

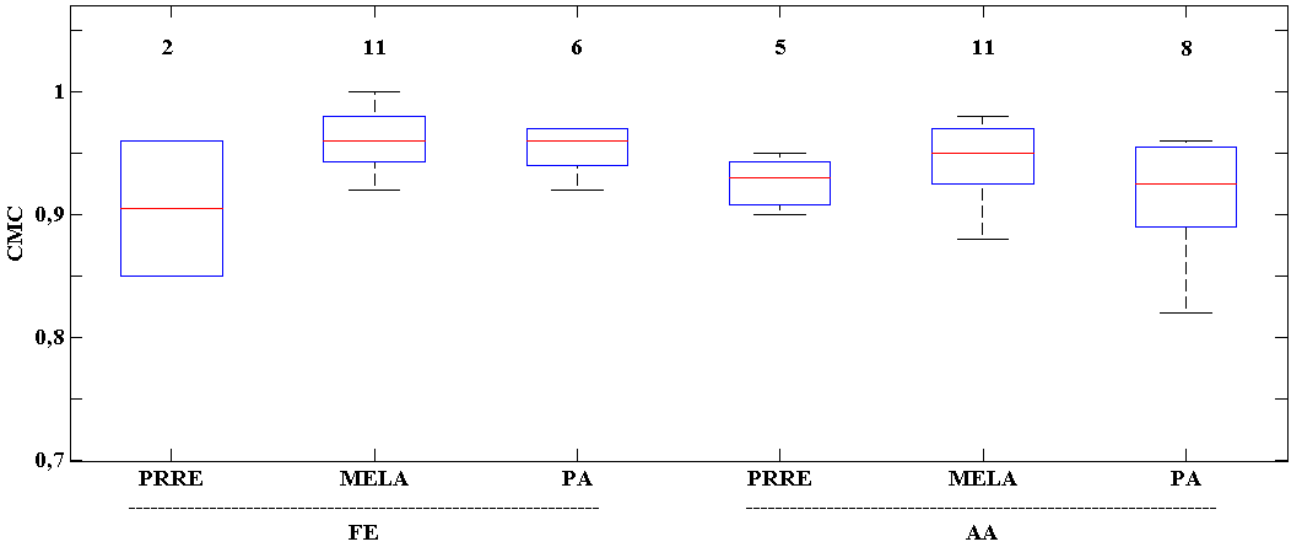

FIGURE 3. Results from the CMC_2 for reliable sessions.

It is important to notice that the condition on CMC_1 decreases the number of subjects considered. This is particularly critical for PR-RE, which appears the angle for which a sufficient between-day reliability is difficult to obtain due to its intrinsic variability *within-day*. This conclusion is consistent with previous findings [7].

CONCLUSIONS

From the results reported, the SHR of the controlateral side of patients treated for a rotator cuff-tear in their working-age present a between-day repeatability, which is always acceptable for ME-LA; therefore, a single session can be considered. For PR-RE and P-A, instead, the between-day repeatability can be critical for some subjects.

However, for those subjects that satisfy the following criteria, the SHR for all scapula angles can be measured in a single session:

1. during the acquisition the subject must reach its maximum humeral elevation.

2. the CMC_1 value must be greater than 0.95 for each angle-angle plot.
3. the pattern of the curves in the angle-angle plot should be similar in *shape* to the mean pattern of healthy controls [2,6].

For those subjects that are not able to meet the criteria, it is proposed to consider the SHR curves measured in at least two days and create a mean curve for each angle-angle plot, with subject-specific confidence bands, e.g. based on the Bootstrap technique [8]. This can be the case in particular if PR-RE is of particular interest, as PR-RE patterns versus FE (worst case) and AA are the less reliable within-day.

Results about PR-RE can explain why very few studies highlighted significant differences between pathologic populations and healthy controls for the part of the SHR involving PR-RE [9, 10].

REFERENCES

1. Cutti AG, Giovanardi A, Rocchi L, Davalli A, Sacchetti R. Ambulatory measurement of shoulder and elbow kinematics through inertial and magnetic sensors. Med Bio Eng Comput 2008; 46(2): 169-78
2. Ulrich M, Cutti AG, Van Tuijl B, Parel I, Veeger DJ. Ambulatory measurement of the scapulohumeral rhythm: accuracy of a protocol based on inertial and magnetic sensors. Gait & Posture. Submitted.
3. Parel I, Cutti AG, Fiumana G, Porcellini G, Verni G, Accardo AP. Ambulatory measurement of the scapulohumeral rhythm: intra- and inter-operator agreement of a protocol based on inertial and magnetic sensors. Gait Posture. 2012 Apr;35(4):636-40.
4. Parel I, Cutti AG, Fiumana G, Porcellini G, Verni G, Accardo AP. Changes in the scapulo-humeral rhythm of patients treated arthroscopically for rotator-cuff tear over a period of 90 days. Proceeding at ISB XXII, Brussels, Belgium, 2011.
5. Garofalo P, Cutti AG, Filippi MV, Cavazza S, Ferrari A , Cappello A, Davalli A. Inter-operator reliability and prediction bands of a novel protocol to measure the coordinated movements of shoulder-girdle and humerus in clinical settings. Med Bio Eng Comput 2009; 47(5): 475-86
6. Meskers CG, van de Sande MA, de Groot JH. Comparison between tripod and skin-fixed recording of scapular motion. J Biomech 2007; 40(4): 941-6
7. Thigpen CA et al. (2005) The repeatability of scapular rotations across three planes of humeral elevation. Res Sports Med, 3(3):181-98
8. Lenhoff MW, Santner TJ, Otis JC, Peterson MG, Williams BJ, Backus SI. Bootstrap prediction and confidence bands: a superior statistical method for analysis of gait data. Gait Posture. 1999 Mar; 9(1):10-7.
9. Meskers CG, Koppe PA, Konijnenbelt MH, Veeger DH, Janssen TW. Kinematic alterations in the ipsilateral shoulder of patients with hemiplegia due to stroke. Am J Phys Med Rehabil. 2005 Feb;84(2):97-105.
10. Ludewig PM, Reynolds JF. The association of scapular kinematics and glenohumeral joint pathologies. J Orthop Sports Phys Ther 2009; 39(2): 90-104

Section 4.2

Changes in the scapulo-humeral rhythm of patients arthroscopically treated for rotator-cuff tear over a period of 90 days

Parel I, Cutti AG, Fiumana G, Porcellini G, Verni G, Accardo AP.
International Society of Biomechanics Conference 2011, Proceeding.

ABSTRACT

A protocol, named ISEO, based on inertial and magnetic sensors, was developed to measure the scapulo-humeral rhythm (SHR). A group of patients surgically treated for rotator cuff tear was considered during a standard rehabilitation period of 90 days after surgery. The study aimed at understanding if and when the SHR of the affected side becomes close to the SHR of the controlateral side, in terms of consistency, similarity and ranges of motion. Results suggest that at 90 days most patients increase humerus elevation at the expense of scapula compensatory movements, especially during humerus flexion.

INTRODUCTION

A protocol, named ISEO, has been developed by Centro Protesi INAIL (Italian Workers' Compensation Authority) to analyze the scapulo-humeral rhythm (SHR) in outpatient clinics, based on inertial and magnetic sensors positioned over the thorax, scapula, humerus and forearm [1]. ISEO accuracy has been analyzed [2], as well as its intra- and inter-rater reliability [3].

One of the application of ISEO within the working sector, will be to support clinicians in deciding whether a patient should refrain from working and concentrate on rehabilitation or return to the standard duties.

With this ultimate goal, ISEO is currently applied to assess the evolution of the SHR during the rehabilitation of patients surgically treated for rotator cuff tear, which is the most diffused shoulder pathology among workers [4].

In particular, this study aimed at understanding if and when the SHR of the affected side becomes close to the SHR of the controlateral (reference) side, in terms of:

Q1) consistency of the curves within a day;

Q2) similarity of the curves;

Q3) ranges of motion (ROMs),

considering the standard expected recovery period of 90 days after surgery and a commonly applied rehabilitation protocol.

METHODS

Eleven subjects (52±11 years-old) were involved in the study (after giving their informed consent), together with a rater familiar with ISEO. Patients were all treated arthroscopically for rotator cuff

tear of the supraspinatus. All controlateral sides were clinically evaluated as fully functional for the age of the patient, and thus the controlateral side will be named hereinafter "sound side". After surgery, patients were asked to keep their affected arm at rest for 21 days. Then, they followed from 2 to 3 sessions of physiotherapy/week with passive mobilizations without external rotations. At 35 days, they started a water-therapy exercise program twice a week, together with passive mobilizations including rotations, twice a week. Between 65 to 70 days, they started active exercises for force recovery with elastic bands.

Three measurement sessions of the affected and sound SHRs were completed for each subject at 45, 70 and 90 days.

In each session, a minimum of 7 humerus flex-extension (FE) and ab-adduction (AA) movements was measured, but the central 3 were considered for subsequent computations. For every movement the three scapula rotations were measured, i.e. pro-retraction (PRRE), medio-lateral (MELA) and posterior-anterior tilting (PA) as well as the humerus-thorax FE (during FE movements) and AA (during AA movements). Only the upward movements were considered, as they required an active anti-gravitational control of the arm.

A total of 6 angle-angle plots were obtained for each subject and side, namely PR-RE/ME-LA/P-A vs FE and PR-RE/ME-LA/P-A vs AA, and on each we reported 3 groups of 3 SHR curves (i.e. 3 curves per session).

To have a single reference to compare the affected side's SHRs, for each subject it was chosen the most representative SHR of the sound side among the three available, following the criteria suggested in [5].

To answer to Q1, we measured the consistency of the 3 curves within each angle-angle plot for the sound side and for each session of the affected side, through the Coefficient of Multiple Correlation (CMC). In particular, we used the CMC formulation named CMC_1 [5]. We assumed that the consistency of the curves of the affected side is equivalent to that of the sound when [5]:

- $CMC_{1\text{-AFFECTED}} \geq CMC_{1\text{-SOUND}}$, when $CMC_{1\text{-SOUND}} \leq 0.95$;
- $CMC_{1\text{-AFFECTED}} \geq 0.95$ if $CMC_{1\text{-SOUND}} > 0.95$.

To answer to Q2, for each session and angle-angle plot, we measured the similarity between the 3 curves of the affected side and the 3 curves of the sound, for the common range of humerus elevation. This was done through the CMC formulation named CMC_2 [5]. We assumed that the SHR of an affected side sufficiently matches that of the sound when $CMC_2 \geq 0.95$ for ME-LA and

P-A and CMC_2 ≥0.85 for PR-RE, as these thresholds represent the maximum uncertainty in the similarity between curves due to the re-application of the protocol by the same rater [5].

To answer to Q3, for each session and angle-angle plot we computed:

1) the difference between the ROM of humerus elevation of the sound and affected side (ΔROM_H);
2) the difference between the ROMs of scapula PR-RE/ME-LA/P-A of the sound and affected side (overall referred to as ΔROM_S), for the common ROM of humerus elevation.

To assess if ΔROM_H changes over the three sessions, we performed a post-hoc Friedman test ($p<0.05$).

The scapula ROMs of the affected side are assumed to be significantly different from the associated ROMs of the sound, when ΔROM_S are above the Smallest Detectable Differences (SDD) that takes into account the intra-rater reliability of ISEO [3].

RESULTS AND DISCUSSION

Results for CMC_1 (question Q1) are reported in Figure 1 and show that the consistency of the SHR curves of the affected side tends to increase toward the sound consistency, for all scapula angles. A limited number of patients exhibit relevant differences at the third session, i.e. 3/11 for ME-LA during FE and AA, and 2/11 for P-A during AA.

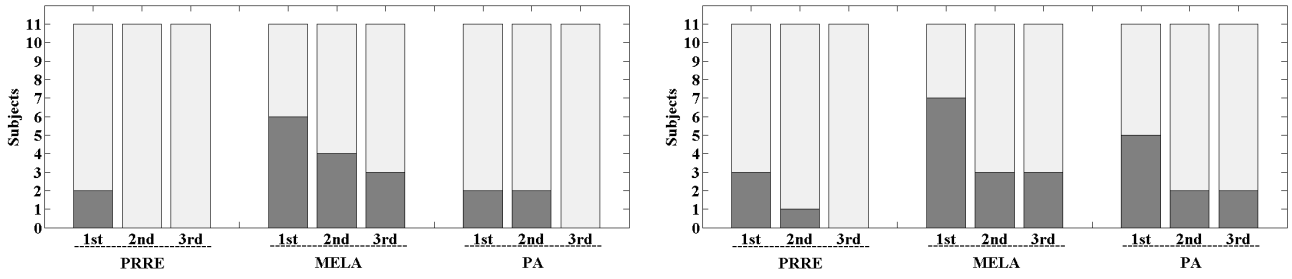

FIGURE 1. Results for CMC_1 in FE (left) and AA (right): dark-grey and light-grey bars represent the n° of subjects with CMC_1 value respectively below or above the threshold of similarity (0.95).

Results for CMC_2 (question Q2), are reported in Figure 2 and show that there is a general increase in the similarity between the affected and sound SHR over sessions. A greater increase in similarity can be observed for the AA movement, while FE appears more critical. In general, however, for more than half of the patients the affected side SHR remains different from the controlateral; ME-

LA and PR-RE appears to be the scapula angles for which the recovery is slower: in the last session 10/11 and 9/11 patients have significant differences between sides during FE, respectively.

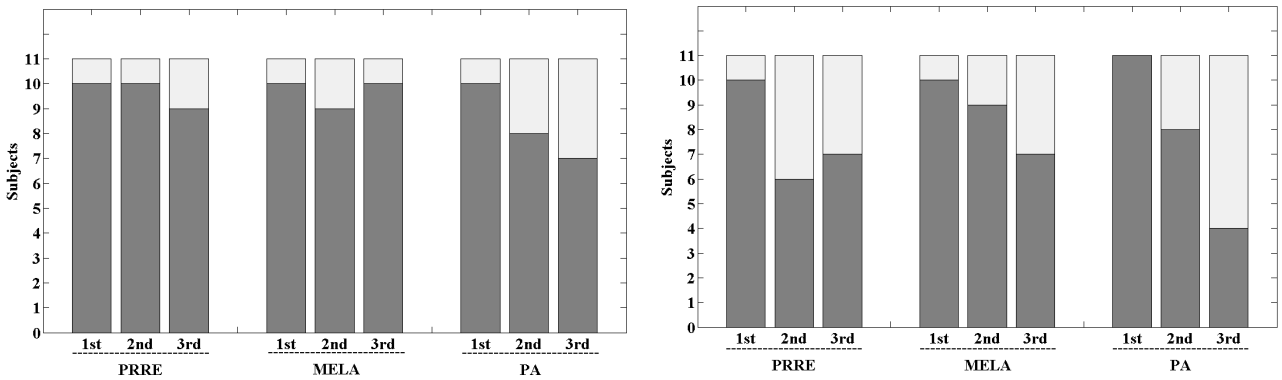

FIGURE 2. Results for CMC_2 in FE (left) and AA (right): dark-grey and light-grey bars represent the n° of subjects with CMC_2 value respectively below or above the threshold of similarity (0.95 for ME-LA and P-A, 0.85 for PR-RE).

Regarding Q3, the Friedman test indicates that there are significant differences in ΔROM_H among sessions. In particular, post-hoc tests indicate that there is a statistically significant difference between session 1 vs 3 and 2 vs 3 both for FE and AA, with an increase between 1 and 3 of 37.54°±25.52° for FE and 42.51°±23.60° for AA.

Results for ΔROM_S are reported in Figure 2 and show that the difference between affected and controlateral side decreases over sessions. A greater decrease can be observed for the AA's ΔROM_S, while those during FE appear more critical. ΔROM_S of ME-LA in FE and AA and ΔROM_S of P-A in FE suggest that these scapula angles present a slower recovery-time: in the last session 9/11 and 8/11 patients have significant differences between sides for ME-LA respectively during FE and AA, and 8/11 for P-A in FE.

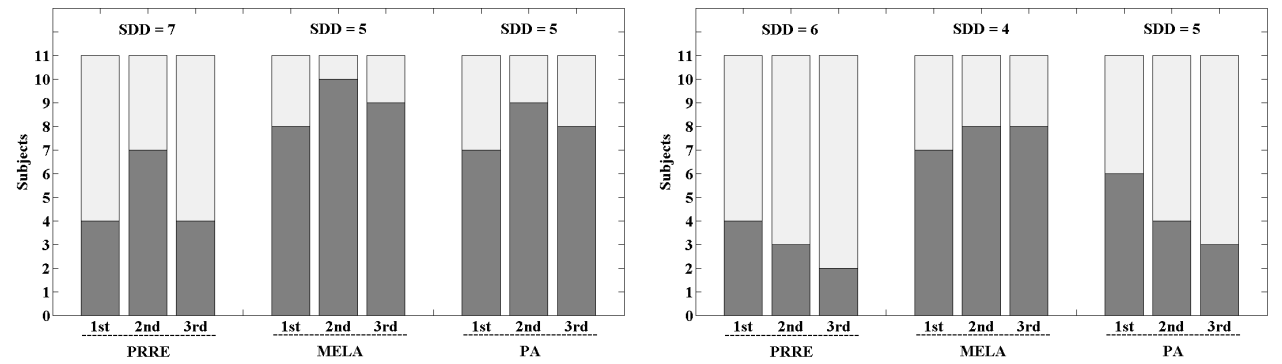

FIGURE 3. Results for ΔROM_S in FE (left) and AA (right): dark-grey and light-grey bars represent the n° of subjects with ΔROM_S value respectively above and below the specific SDD.

CONCLUSIONS

The aim of this study was to measure the changes of the SHR of the affected side of patients arthroscopically treated for rotator-cuff tear, over 90 days. Results show that over time the consistency of the SHR curves of the affected side becomes comparable with the consistency of the curves of the sound. Moreover, the ROM of humerus elevation increases considerably. However, relevant differences still exist at 90 days between the SHR curves of the affected and sound both in terms of similarity (CMC_2) and ROMs of the scapula angles (ΔROM_S), in particular during humerus flexions. This suggests that patients gain a repeatable pattern of the SHR with a functionally useful increase in maximum humerus elevation angle, but this is mostly obtained to the expense of compensatory movements of the scapula. This suggests that increased attention with specific exercise, e.g. based on real-time biofeedback, should be introduced to increase the proprioception of the patient and quantitatively support the physical therapist.

Results also suggest that the protocol and parameters are very sensitive to differences in the measure of the SHR of patients over time.

REFERENCES

1. Cutti AG, Giovanardi A, Rocchi L, Davalli A, Sacchetti R. Ambulatory measurement of shoulder and elbow kinematics through inertial and magnetic sensors. Med Bio Eng Comput 2008; 46(2): 169-78
2. Ulrich M, Cutti AG, Van Tuijl B, Parel I, Veeger DJ. Ambulatory measurement of the scapulohumeral rhythm: accuracy of a protocol based on inertial and magnetic sensors. Gait & Posture. Submitted
3. Parel I, Cutti AG, Fiumana G, Porcellini G, Verni G, Accardo AP. Ambulatory measurement of the scapulohumeral rhythm: intra- and inter-operator agreement of a protocol based on inertial and magnetic sensors. Gait Posture. 2012 Apr; 35(4):636-40
4. Melchior M, Roquelaure Y, Evanoff BA, Chastang JF, Ha C. Why are manual workers at high risk of upper limb disorders? The role of physical work factors in a random sample of workers in France (the Pays de la Loire study). Occup Environ Med 2006. 63: 754-761
5. Parel I, Fiumana G, Cutti AG, Porcellini G, Verni G, Accardo AP. Can the scapulo-humeral rhythm of the controlateral side of patients surgically treated for rotator-cuff tear be measured only once in longitudinal studies? Proceeding at ISB XXII, Brussels, Belgium, 2011

Section 4.3

Modifications in the individual relative Constant score to assess alterations of scapula kinematics

Cutti AG, Parel I, Pellegrini A, Petracci E, Porcellini G, Verni G.
International Shoulder Group Conference 2012, Proceeding.

INTRODUCTION

The Constant score has become one of the most popular clinical scales for the assessment of shoulder disorders. It was firstly presented in [1] and then applied in hundreds of research studies. Recently, a review of the scale's application guidelines was published [2] and debate arose about the normalization of the score of the treated shoulder relative to control groups (stratified per gender and age) or the subject's controlateral unaffected side, if any [3]. Whenever possible, the latter solution proved to be superior, both in terms of sensitivity and specificity and, therefore, appears preferable. This solution was named "individual relative Constant scale".

Despite modifications in the normalization approach, the items of the scale remained unchanged: 100 points can be assigned to a shoulder through assessment of its function outcomes in 4 domains, namely movement (40), strength (25), activities of the daily living (20) and pain (15). The assessment in the movement domain requires the clinician to measure the degree of humerus-to-thorax elevation in the sagittal (10) and scapular plane (10) as well and internal (10) and external rotation (10). In the evaluation of elevation the contribution of the scapulohumeral rhythm is completely ignored, despite the relevance in most shoulder pathologies [4]. This limitation, we think, can lead to misclassifications, since the presence of compensatory movements is unscored; in other words, a patient can be assigned 20 points despite alterations in scapula protraction-retraction (PR-RE), medio-lateral rotation (ME-LA) or posterior-anterior tilting (P-A). Not formally assessing alterations in scapula kinematics neither supports the surgeon in evaluating the outcome of the intervention nor the physical medicine expert in planning and optimizing the rehabilitation.

Originally this limitation was due, most probably, to the difficulty in measuring reliably and easily the scapulo-thoracic rotations. The ISEO protocol [5,6], which takes advantage of inertial and magnetic sensors, allows to measure the thorax, scapula, humerus and elbow kinematics in real-time, outside of the lab, in ambulatory settings; as such, it might be useful to overcame this original limitation.

The aim of this study was to propose a modification of the individual relative Constant score (named hereinafter "Constant score" or COS), by introducing 2 new items to assess scapula rotations by considering the data collected by ISEO. This led to the development of a new score, which will be hereinafter referred to as Constant-ISEO score or COI. Moreover, we intended to verify how patients are re-classified by COI, starting from the classification of COS.

METHODS

In formulating the two new items we made the following assumptions:

1) consistently with the assumptions of COS, the kinematics of the sound side is the goal for the affected side; in other words, the kinematics of the sound side is the one that would have been obtained from the affected side before the injury;
2) considering the common humerus elevation for the treated (T) and sound side (S), if the difference between the ROMs of PR-RE between sides is smaller than the smallest detectable difference by ISEO ($PR\text{-}RE_{SDD95}$) [6], the PR-RE kinematics of the treated and the sound side are indistinguishable; in other words, the treated side PR-RE kinematics has reached its goal;
3) point 2) holds for ME-LA and P-A, considering $ME\text{-}LA_{SDD95}$ and $P\text{-}A_{SDD95}$ [6];
4) longitudinally, different raters might be involved in assessing the same patient;
5) since the scapula kinematics is a complex combination of PR-RE, ME-LA and P-A, only the simultaneous restoration of the kinematics of PR-RE, ME-LA and P-A can be considered as the full accomplishment of the rehabilitation goal;
6) ten points should be assigned to each of the new items, consistently with the other items in the movement domain of COS;
7) the overall amount of points assigned to the movement domain should not change with the introduction of the 2 new items, i.e. it should be 40 points; the 60 points coming from the introduction of the new items should then be proportionally scaled to 40.

With these assumptions, the new items are as follows:

1) During sagittal plane elevation:
   A) $|PR\text{-}RE_S - PR\text{-}RE_T| < PR\text{-}RE_{SDD95} = 6.8° \rightarrow$ 2 pts;
   B) $|ME\text{-}LA_S - ME\text{-}LA_T| < ME\text{-}LA_{SDD95} = 5.2° \rightarrow$ 2 pts;
   C) $|P\text{-}A_S - P\text{-}A_T| < P\text{-}A_{SDD95} = 7.7° \rightarrow$ 2 pts;
   D) if A, B and C are all verified → 4 pts.
2) During scapular plane elevation:
   A) $|PR\text{-}RE_S - PR\text{-}RE_T| < PR\text{-}RE_{SDD95} = 8.6° \rightarrow$ 2 pts;
   B) $|ME\text{-}LA_S - ME\text{-}LA_T| < ME\text{-}LA_{SDD95} = 4.4° \rightarrow$ 2 pts;
   C) $|P\text{-}A_S - P\text{-}A_T| < P\text{-}A_{SDD95} = 6.6° \rightarrow$ 2 pts;
   D) if A, B and C are all verified → 4 pts.

The overall amount of points for the movement domain is then computed as follows:

- Movement = (Elevation + Scapular + Intra + Extra + New Item 1 + New Item 2) * 2/3

To evaluate the effect of COI, we considered a group of 13 patients, who were arthroscopically treated for rotator cuff tear and evaluated through COS and ISEO at 45, 70, 90 days and at least 6 months after surgery. We hypothesized that if COS allows to take into account, indirectly, scapula movement disorders, the calculation of COI should not change the number of patients with "satisfactory" results [7], i.e. featuring a score > 80.

RESULTS

The COS and COI scores for the 13 patients over the four assessments are reported in Table 1.

ID	Scale	45°	70°	90°	> 6 m.
1	***COS***	44	60	64	92
	COI	40	53	57	86
2	***COS***	59	65	85	100
	COI	50	53	72	86
3	***COS***	76	82	86	91
	COI	74	81	82	77
4	***COS***	49	79	75	93
	COI	51	76	66	75
5	***COS***	72	84	93	100
	COI	63	74	82	89
6	***COS***	48	61	83	82
	COI	49	52	75	75
7	***COS***	68	73	87	94
	COI	58	60	77	81
8	***COS***	59	79	97	93
	COI	53	71	86	84
9	***COS***	43	50	60	103
	COI	60	55	60	108
10	***COS***	67	81	75	86
	COI	60	69	69	82
11	***COS***	36	64	78	86
	COI	31	63	75	75
12	***COS***	18	44	45	76
	COI	21	42	43	75
13	***COS***	21	56	65	91
	COI	23	51	61	80

TABLE 1. COS and COI scores for the 13 patients assessed. Blue (Yellow) cells highlight patients with satisfactory results for COS (COI).

	COS	COI	(COI-COS) / COS (%)
45°	0	0	0
70°	3	1	-67
90°	6	3	-50
>6 months	12	8	-33

TABLE 2. Summary of patients with satisfactory results based on COS and COI. The last column reports the reclassification percentage.

CONCLUSIONS

At 45 days after surgery, none of the patient is classified as "recovered" neither by COS nor by COI. Differences between the scales begin at 70 days, with a reclassification percentage, which progressively decreases from 67% at 70 days to 50% at 90 days, to 33% at follow-up. This high rate of reclassification highlights the lack of recovery of the scapulohumeral rhythm in most patients. At the crucial milestone of 90 days (especially in the work reintegration perspective), only 3 out of 13 patients (23%) present a satisfactory scapula kinematics, instead of the 46% highlighted by COS. Also at follow-up alterations in scapula rotations persist, with only 8 patients (61%) with a satisfactory recovery, as opposed to the 92% classified by COS. Our hypothesis about the implicit assessment of scapula kinematics alterations by COS could not be confirmed, and therefore COI does have an impact in the reclassification of patients' functional outcome.

In conclusion, we think that current technologies allow an easy, fast and affordable measure of scapula rotations and it seems therefore important to modify the Constant score to take into account the restoration of scapula kinematics. The preliminary results reported here seem to show that the two new items proposed might serve the purpose.

REFERENCES

1. Constant CR, Murley AHG. A clinical method of functional assessment of the shoulder. Clin Orthop Relat Res, 1987; 160-4
2. Constant CR, Gerber C, Emery RJH, Søjbjerg JO, Gohlke F, Boileau P. A review of the Constant score: Modifications and guidelines for its use. J Shoulder Elbow Surg, 2008; 17:355-361
3. Fialka C, Oberleitner G, Stampfl P, Brannath W, Hexel M, Ve´csei V. Modification of the Constant—Murley shoulder score – introduction of the individual relative Constant score Individual shoulder assessment. Injury 2005; 36:1159-1165
4. Ludewig PM, Reynolds JF. The Association of Scapular Kinematics and Glenohumeral Joint Pathologies. J Orthop Sports Phys Ther 2009; 39(2): 90-104
5. Cutti AG, Giovanardi A, Rocchi L, Davalli A, Sacchetti R. Ambulatory measurement of shoulder and elbow kinematics through inertial and magnetic sensors. Med Bio Eng Comput

2008; 46(2): 169-78
6. Parel I, Cutti AG, Fiumana G, Porcellini G, Verni G, Accardo AP. Ambulatory measurement of the scapulohumeral rhythm: intra- and inter-operator agreement of a protocol based on inertial and magnetic sensors. Gait Posture 2012; 35(4):636-40
7. Iannotti JP, Bernot MP, Kuhlman JR, Kelley MJ, Williams GR. Postoperative assessment of shoulder function: a prospective study of full-thickness rotator cuff tears. J Shoulder Elbow Surg 1996; 5(6): 449-57

Chapter 5

Biomechanical assessment of amputees fitted with commercial multi-grip prosthetic hands

Section 5.1

The biomechanical assessment of upper limb kinematics: a motion analysis protocol for trans-radial amputees

Cutti AG, Parel I, Luchetti M, Rossi NC, Verni G.
eBook 2012, "Grasping the future". Pages 59-77. ISBN 978-1-60805-438-1.

INTRODUCTION

In most daily activities, the kinematics of the upper-limb and trunk has the goal to position and orient the hand in such a way that the hand can effectively and efficiently reach/grasp an object and transport it to the desired target. When a prosthetic joint replaces either the end-effector or one of the joints in the upper-limb kinematic chain with intrinsic motor or sensorial limitations compared to the original body-part, the remaining joints perform compensatory movements. At present, the typical prosthetic solution for a transradial amputee does suffer from such limitations: the wrist rarely features the flexion-extension and it does not present the radio-ulnar deviation; the hand just features a tridigital grip pattern; none of the joints or part of the prosthesis offers a direct sensory feedback. Consequently, transradial amputees need to compensate these limitations and a possible reduction in elbow flexion due to the socket, with compensatory movements of the shoulder, trunk and neck. Despite the clinical observations, quantitative evidences about the actual compensatory movements and strategies adopted by trans-radial amputees to complete activities of the daily living (ADLs) are quite limited [1-4], and they generally suggest that compensatory movements depend on the specific task and that the whole body is involved. In addition to being limited in number, four methodological issues exist in the literature. The first and most evident is the lack of information about scapulo-thoracic motion, which is instead of great interest for the existing connection with shoulder pathologies. In particular, Ludewig and Reynolds [5] reported that alterations in the scapulo-humeral rhythm, i.e. the coordinated movements of scapula and humerus when this latter is elevated, exist in pathologies such as shoulder impingement, rotator cuff tendinopathy, rotator cuff tears, glenohumeral instability, adhesive capsulitis and stiff shoulders. Both shoulders of an amputee are at risk: the controlateral side for overuse and the affected side for muscle weakness [6], which has been previously documented [7]. For these reasons, we think that scapulo-thoracic motion should always be analyzed, for instance with the acromion tracker described in [8]. Moreover, we think that the upper-limb assessment of an amputee should always include the measure of the scapulo-humeral rhythm during basic flexion-extension movements in the sagittal and scapular plane. With regard to the effect of new prosthetic hands, it would be relevant to understand if the availability of different gripping patters has an effect on the scapula and humerus kinematics, allowing the amputee to avoid positions known to be related to subacromial or internal impingement, i.e. related to rotator cuff tendinopathy; these positions are, in particular, humerus flexion & abduction with intra-rotation or abduction with external rotation. The second limitation is the lack of information about head and neck kinematics: these motions can be essential to complete a task when upper-limb joints have a limitation in the range of motion (ROM)

[1]. The existence of joint ROM restriction should be always assessed through basic, single plane, single joint motions. In particular, it seems important to identify if the socket is limiting the elbow maximum flexion and ROM. The third limitation is the lack of information and standardization about the motion analysis protocol used, as opposed to recent recommendations [9]. Specific indications about marker placement on the prosthesis are not generally provided as well as the definition of the anatomical Coordinate Systems (CSs), i.e. the CS associated with each body segment whose relative orientation describe the segment/joint kinematics [9]. In particular, the elbow epicondyles, which are commonly used as anatomical landmarks to define the humerus anatomical coordinate system [10], cannot be easily identified, as the lay underneath the socket. Finally, the forth limitation is the long-standing discussion about the lack of standardization of the activities to be tested, both in terms of *tasks selection* and *constraints in the execution of a specific task*, e.g. regarding body posture, objects to manipulate, starting position, ending position, timing. As discuss in [9], the answer lies in the hypothesis to be tested. First of all, it is important to define the ICF domain of interest: impairment or activity? We think that laboratory motion analysis is best suited for impairment assessment, while quantitative information about activity should be acquired by wearable technologies [11-13] that enable measurement outdoor, in the "real" every-day life.

Replication of ADLs in the laboratory with the aim of gathering information about the *typical behavior* of a patient is unrealistic, since the fact that the subject is intensively monitored, unavoidably conditions the individual, who will tend to perform at his/her best. Consequently, the lack of standardization in the execution of a specific task does not bring additional information, but introduces variability in the data, which make difficult to compare a subject over time (longitudinal studies) or a sample of subjects. With this framework, we support the use of tasks from the SHAP scale. Additional tasks might be necessary, depending of the responses that the investigator wants to elicit in the subject, but these additional tasks should be equally clearly defined and should involve standard or easily replicable objects whenever possible, if manipulation is required.

In the following sections, the motion analysis protocol implemented at Centro Protesi INAIL for the assessment of new prosthetic hands in transradial amputees is shown. The description is based on the recommendations provided in [9].

MOTION ANALYSIS PROTOCOL FOR TRANS-RADIAL AMPUTEES

SEGMENTS AND JOINTS OF INTEREST

Both sides of the amputees are measured, to allow a within-subject comparison. The segments of interest are the head, thorax and, for both sides, scapula, humerus, forearm and hand. Neck

kinematics comes from the relative orientation of head and thorax. Scapula and humerus attitude are referred to the thorax, following current standards.

Elbow flexion-extension is computed from the relative orientation of humerus and forearm, while prono-supination differs between the sound and the prosthetic side: for the sound side it is computed between forearm and humerus, while for the prosthetic side between hand and forearm.

ANATOMICAL COORDINATE SYSTEMS

The anatomical landmarks of interest are reported in Table 1 and the anatomical/functional CSs are defined in Table 2.

Abbreviation	Name
NB	Proximal aspect of the nasal
CH	Mental Protuberance
C0	External Occipital
IJ	Incisura Jugularis
PX	Xiphoid Process
C7	7th Cervical Vertebra
T8	8th Thorac Vertebra
AA	Angulus Acromialis
TS	Trigonum Spinae
AI	Angulus Inferior
GH	Centre of Glenohumeral Head
EL	Lateral Epicondyle
EM	Medial Epicondyle
RS	Radial Styloid; *for the prosthetic side*: identified during the static calibration trial to replicate controlateral side;
US	Ulnar Styloid; *for the prosthetic side*: opposite to the RS;
M3	3rd Metacarpus; *for the prosthetic side*: just proximal to the 3rd finger knuckle.
V_{flex}	Direction of the elbow flexion-extension axis
V_{ps}	Direction of the forearm prono-supination axis
V_{flexW}	Direction of the prosthetic wrist flexion-extension axis

TABLE 1. Anatomical landmarks used for the definition of the anatomical/functional coordinate systems.

Segment	Axes
Head (HD)	$Y_{HD} = (NB - CH)/\| NB - CH \|$: longitudinal $X_{HD} = Y_{HD} \wedge (CO - NB)/\| Y_{HD} \wedge (CO - NB) \|$: medio-lateral $Z_{HD} = (X_{HD} \wedge Y_{HD})/\|\cdot\|$:antero-posterior Origin: *NB*
Thorax (THX)	$Y_{THX} = ((IJ + C7)/2 - (PX + T8)/2)/ \| (IJ + C7)/2 - (PX + T8)/2 \|$: longitudinal $X_{THX} = Y_{THX} \wedge (T8 - PX)/\| Y_{THX} \wedge (T8 - PX) \|$: medio-lateral $Z_{THX} = X_{THX} \wedge Y_{THX}/\|\cdot\|$: antero-posterior Origin: *IJ*
Scapula (SC)	$X_{SC} = (AA - TS)/\| AA - TS \|$: medio-lateral $Z_{SC} = (X_{SC} \wedge (AA - AI)/\| X_{SC} \wedge (AA - AI) \|$: antero-posterior $Y_{SC} = (Z_{SC} \wedge X_{SC})/\|\cdot\|$: longitudinal Origin: *AA*
Proximal humerus (H1)	$Y_{H1} = (GH - E)/\| GH - E \|$: longitudinal $Z_{H1} = \big(Y_{H1} \wedge (EM - EL)\big)/\| Y_{H1} \wedge (EM - EL) \|$: antero-posterior $X_{H1} = Y_{H1} \wedge Z_{H1}/\|\cdot\|$: medio-lateral $E = (EL + EM)/2$ Origin: *GH*
Proximal humerus (H2) (for internal-external rotation assessments only)	$Y_{H2} = (GH - E)/\| GH - E \|$: longitudinal $X_{H2} = (Y_{H1} \wedge Y_{PS})/\| Y_{H1} \wedge V_{PS} \|$: antero-posterior $Z_{H2} = X_{H2} \wedge Y_{H2}/\|\cdot\|$: medio-lateral Origin: *GH*
Distal humerus (H3)	$X_{H2} = V_{FLEX}/\| V_{FLEX} \|$: medio-lateral $Z_{H2} = X_{H2} \wedge (GH - E)/\| X_{H2} \wedge (GH - E)$: antero-posterior $Y_{H2} = (Z_{H2} \wedge X_{H2})/\| Z_{H2} \wedge X_{H2} \|$: longitudinal $E = (EL + EM)/2$ Origin: *E*
Forearm (F)	$Y_F = V_{PS}/\| V_{PS} \|$: longitudinal $Z_F = ((RS - US) \wedge Y_F/\| (RS - SU) \wedge Y_F \|$: antero-posterior $X_F = (Y_F \wedge Z_F)/\|\cdot\|$: medio-lateral $S = (US + RS)/2$ Origin: *S*
Hand – sound side and prosthesis without wrist flexion (HN)	$Y_{HN} = (S - M3)/\| S - M3 \|$: longitudinal $Z_{HN} = (Y_{HN} \wedge (US - RS))/\| Y_{HN} \wedge (US - RS) \|$: anterior-posterior $X_{HN} = (Y_{HN} \wedge Z_{HN})/\|\cdot\|$: medio-lateral Origin: *M3*
Hand – prosthesis with wrist flexion (HW)	$X_{HW} = V_{FLEXW}/\| V_{FLEXW} \|$: medio-lateral $Z_{HW} = (X_{HW} \wedge (S - M3))/\| X_{Hw} \wedge (S - M3) \|$: anterior-posterior $Y_{HW} = (Z_{HW} \wedge X_{HW})/\|\cdot\|$: longitudinal Origin: *M3*

TABLE 2. Definition of the anatomical and functional coordinate systems.

For thorax and scapula, definitions follow the ISB-ISG recommendations [10].

As proposed in [9], for the humerus two coordinate systems are defined: 1) a proximal CS (normally H1, H2 only for the assessment of the internal-external ROM only) to describe the

attitude of the humerus relative to the thorax, i.e. for the computation of the scapulo-humeral rhythm, and 2) a distal CS (H3) to describe the elbow kinematics. The proximal CS follows the ISB-ISG recommendations, with the epicondyles "calibrated" when the amputee is not wearing the prosthesis, as further detailed in the Section "Marker-set and landmark palpation". The distal CS, instead, is based on the estimation of the elbow functional flexion-extension axis of rotation [9], which allows to minimize the kinematic cross-talk with the prono-supination.

For the forearm, the CS is based on the estimation of the functional prono-supination axis, obtained, for the sound side, from the relative motion of humerus and forearm during a pure prono-supination task. For the prosthetic side, instead, the functional axis is obtained from the relative movement of hand and forearm. In both cases, the functional axis is referred to the forearm segment. For the definition of the forearm CS, two anatomical landmarks are also required, namely RS and US. For the prosthetic side, it is proposed to ask the amputee to adjust the prono-supination so that the hands can join and the forearms can touch each other (named hereinafter "styloid calibration posture"). RS on the prosthetic side is then identified by replicating the position of the sound side RS on the prosthesis. The prosthetic side US is obtained as opposed to RS on the wrist circumference. For the sound side hand, the CS (named HN) is based on anatomical landmarks. HN is used for the prosthetic side when the wrist does not feature the flexion-extension. When the wrist does feature the flexion-extension, instead, a functional axis describing this hinge joint is estimated using a functional method [9] and becomes the basis for the construction of the prosthetic hand CS (named HW). An exception to this approach is when the comparison of the radio-ulnar deviation is of interest between different hand models. In this case it is suggested to measure a static trial and perform the radio-ulnar deviation analysis on this trial using HN for both hands.

JOINT OR SEGMENT ANGLES

Joint or segment angles are obtained following [9], as reported in Table 3. In particular, for the elbow joint the Euler sequence XZ'Y'' is applied to decompose the relative orientation of the forearm and humerus orientation matrices. The first rotation provides the elbow flexion-extension angle. The third rotation provides the prono-supination angle for the sound side and a constant value for the prosthetic side, since the prosthetic forearm does not feature the prono-supination (which is between hand and forearm). By applying the Euler sequence YZ'X'' to decompose the hand to forearm orientation matrices of the prosthetic side, the first rotation provides the prono-supination, the second the radio-ulnar deviation and the third the flexion-extension. The same

sequence is applied to the sound side, but the first rotation reports a theoretically constant value (in the ideal case of absence of soft-tissue artifact [9]).

Joint /Segments	Euler Sequence (positive sign)
Head *relative to* Thorax	XZ'Y'' (flexion-abduction-internal rotation)
Thorax *relative to* Global CS	XZ'Y'' (flexion-abduction-internal rotation)
Scapula *relative to* Thorax	YZ'X'' (protraction-lateral rotation-posterior tilt)
Humerus *relative to* Thorax	*Mostly sagittal plane movements:* XZ'Y'' (flexion-abduction-internal rotation) *Mostly frontal plane movements:* ZX'Y'' (abduction-flexion-internal rotation)
Forearm *relative to* Humerus	*Sound side:* XZ'Y'' (flexion-carrying angle-pronation) *Prosthetic side:* XZ'Y'' (flexion-carrying angle-*dummy*)
Hand *relative to* Forearm	*Sound side:* Y'Z'X' (*dummy* – radial deviation-flexion) *Prosthetic side:* Y'Z'X' (pronation – radial deviation-flexion)

TABLE 3. Sequence of Euler angles for each joint/segment kinematics of interest

MARKER-SET AND LANDMARK PALPATION

Assuming that the system of measurement is an optoelectronic system, the marker-set is based on the CAST approach [14], with a few exceptions. Four markers are positioned over an elastic band around the head to form a cluster of markers, and the anatomical landmarks of the head are calibrated with respect to the cluster during a static trial. Similarly, for scapula and humerus, for which the clusters are positioned, respectively, on an acromion cluster and in the central part of the bony segment, slightly posterior. For the humerus, the cluster can be based on 5 makers, in case of visibility issues. The humerus epicondyles must be calibrated relative to the humerus cluster when the amputee is not wearing the prosthesis. For the estimation of the center of the humerus head, a functional task as suggested in [15] is performed, and the method by Gamage et al [16] is applied [17]. For the sound side forearm, the cluster must be as close as possible to the wrist, while for the prosthetic side it must be proximal, outside of the prosthetic glove. For the hand, a three-marker cluster is used, with markers positioned over M3 (Table 1) and on the middle of the 1st and 5th metacarpal bones. Two additional, small markers are place on the index and thumb tip, to have

information about hand opening. All the objects to manipulate should bring a marker, to allow the temporal segmentation of the activity (Figure (1)).

FIGURE 1. Marker set for the motion analysis based on an optoelectronic system. The acromion cluster was realized in Centro Protesi through rapid prototyping.

TASKS

Firstly, a set of static trials are measured:

1. styloid calibration trial, as described previously;
2. upright, elbow flexed 90°, humerus alongside the body perpendicular to the ground: this trial is useful to check the overall scapula posture and for the analysis of the radio-ulnar deviation of the prosthetic side.

Secondly, a set of functional tasks is required, to complete the definition of the CSs:

1. a start arc task [15] with the humerus, for the estimation of the glenohumeral center of rotation;
2. pure elbow flexion-extensions, to estimate the relative functional axes;
3. pure prono-supinations, to estimate the relative functional axes;
4. pure wrist flexion-extensions, to estimate the relative functional axes.

Functional movements 2)-4) should be repeated at least 5 times and the estimation of the axis is through the Woltring algorithm [18].

Then, a set of tasks to assess the condition of the elbow ROM and shoulder scapulo-humeral rhythm are performed, with the subject standing still in upright position:

1. a full ROM elbow flexion-extension;
2. a pure flexion-extension of the shoulder in the sagittal and scapular planes;
3. a pure humerus internal-external rotation with the elbow flexed 90°; the humerus anatomical frame named H2 is used for an accurate measure [19].

Also these movements should be repeated 5 times, to consider at least the central 3 repetitions.

The subject is then asked to sit-down on a stood in front of a table, in the following reference position (RP):

- joint knee flexed at 90°;
- mid-line of the subject aligned with the mid-line of the table, placed in front of him/her;
- the distance of the thorax from the table fixed such that the subject can stand with the elbows flexed at 90°, neural rotation of the shoulders and the wrists aligned with the edge of the table.

Five technical areas (10x15 cm) are then marked on the table, considering the subject in the RP (Figure (2)):

- A0 – frontal area (aligned with the midline), horizontally aligned with the table edge closest to the subject;
- A1 – lateral area, aligned with the right hand of the subject, just placed in front of the hand;
- A2 – in front of the subject, aligned with the body's midline at the maximum reachable distance of the arm under investigation (without moving the thorax);
- A3 – lateral area, aligned with the left hand placed just in front of the hand;
- A4 – frontal area, placed on a shelf, above A2; the height of the shelf must be chosen to aligning it with the mouth of the subject.

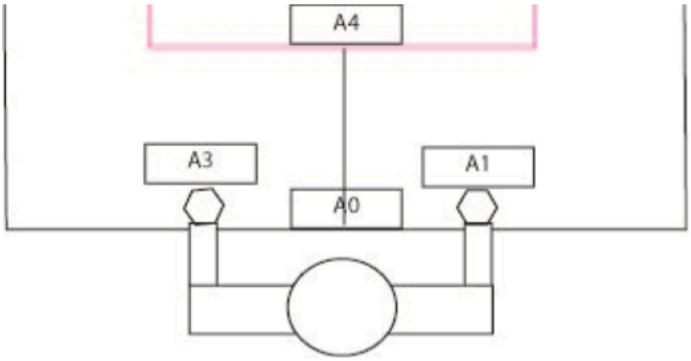

FIGURE 2. Marker set for the motion analysis based on an optoelectronic system. The acromion cluster was realized in Centro Protesi through rapid prototyping.

Once the RP is defined and the technical areas marked, the subject completes the following activities at least three times, at self-selected speed:

1. Jar task – Unilateral task

   Setup: Position the jar (SHAP object) over A2 and place a marker on the cap of the jar;

   Task: Starting from the RP, the subject reaches the jar placed over A2, carries it to A0, returns to RP, brings back the jar from A0 to A2 and returns to RP;

   Motivation: observe the reach-to-grasp, transport and release sequence of a cylindrical object (power-grip) of large diameter; shoulder kinematics and inter-joint coordination can be analyzed.

2. Carton pouring task – Unilateral task

   Setup: Position the SHAP board on the table, aligned with the midline, at a distance of 8 cm from the proximal edge. Position the carton (filled with 200 ml of water) and the jar (without the cap) in the designed areas (SHAP guidelines);

   Task: Starting from the RP, the subject first pours the water from the carton into the jar, brings the carton back on the board and returns to RP;

   Motivation: observe the reach-to-grasp & hold of a squared squeezable object. Shoulder compensatory movements can be analyzed.

3. Drinking task – Unilateral task

   Setup: Position a plastic glass (filled with water) over an area located midway between A0 and A2;

   Task: Starting from the RP, the subject brings the glass to the mouth, drinks the water, brings back the glass on the starting position and returns to RP;

Motivation: observe the reach-to-grasp & hold of a small conic squeezable object. Since the amputee is asked to drink the water, neck and trunk compensatory movements can be analyzed, as they might be essential to complete the task while not spilling the water.

4. Tray task – Bilateral task

   Setup: Position the SHAP tray and the SHAP case over the table, following SHAP guidelines. Place 3 markers on the board making a triangular shape;

   Task: Starting from the RP, the subject reaches the board and moves the tray from one side of the case to the other, using both hands;

   Motivation: observe the strategy adopted to grasping a flat object lying on the plane, which would be better performed with a lateral pinch.

5. Disk tasks – Unilateral task

   Setup: The disks used in the standard Minnesota test are used for this task. Place a disk (with a marker on top) over A1 if the right hand is assessed (A3, if the left hand is assessed);

   Task: Starting from RP the subject completes three exercises:

   1) the subject carries the disk from A1 (A3) to A2, returns to RP, brings the disk back to A1 (A3) and returns to RP;
   2) the subject carries the disk from A1 (A3) to A3 (A1), returns to RP, brings the disk back to A1 (A3) and returns to RP;
   3) the subject carries the disk from A1 (A3) to A4, returns to RP, brings the disk back to A1 (A3) and returns to RP.

   Motivation: observe the strategy adopted to reach-grasp-hold-transport a flat small object, which requires a fine pinch.

REPORT

Ranges of motions are reported as max-min scalar values. Scapulo-humeral rhythm is represented as 3 angle-angle plots for each movement, reporting the scapula protraction-retraction, medio-lateral rotation and anterior-posterior tilting relative to the humerus-thoracic flexion-extension or ab-adduction. Functional tasks kinematics is reported as a percentage of motion, possibly with additional time normalizations for sub-activities (reaching, grasping, transport, return to starting position).

REFERENCES

1. S.L. Carey, M.J. Highsmith, M.E. Maitland and R.V. Dubey. Compensatory movements of transradial prosthesis users during common tasks. Clin Biomech, 23(9):1128-35, 2008.
2. S.L. Carey, R.V. Dubey, G.S. Bauer and M.J. Highsmith. Kinematic comparison of myoelectric and body powered prostheses while performing common activities. Prosthet Orthot Int., 33(2):179-86, 2009.
3. T. Bertels, T. Schmalz and E. Ludwigs. Objectifying the Functional Advantages of Prosthetic Wrist Flexion. JPO, 21(2):74-78, 2009.
4. A. Zinck, P. Kyberd, W. Hill, G. Bush, Ø. Stavdahl, E. Biden and K. Fraser. A study of the use of compensation motions when using prosthetic wrists. Proceedings of the MEC ’08 Measuring Success in Upper Limb Prosthetics, Fredericton, Canada, 2008.
5. P.M. Ludewig and J.F. Reynolds. The association of scapular kinematics and glenohumeral joint pathologies. J Orthop Sports Phys Ther., 39(2):90-104, 2009.
6. L.U. Bigliani and W.N. Levine. Current Concepts Review - Subacromial Impingement Syndrome. The Journal of Bone & Joint Surgery, 79:1854-68, 1997.
7. B. Greitemann, V. Güth and R. Baumgartner. Asymmetry of posture and truncal musculature following unilateral arm amputation--a clinical, electromyographic, posture analytical and photogrammetric study. Z Orthop Ihre Grenzgeb, 134(6):498-510, 1996.
8. P.M. Ludewig and T.M. Cook. Alterations in Shoulder Kinematics and Associated Muscle Activity in People With Symptoms of Shoulder Impingement. Physical Therapy, 80(3):271-291, 2000.
9. A. Kontaxis, A.G. Cutti, G.R. Johnson and H.E. Veeger. A framework for the definition of standardized protocols for measuring upper-extremity kinematics. Clin Biomech, 24(3):246-53, 2009.
10. G. Wu, F.C. van der Helm FC, H.E. Veeger, M. Makhsous, P. Van Roy, C. Anglin, J. Nagels, A.R. Karduna, K. McQuade, X. Wang, F.W. Werner and B. Buchholz. ISB recommendation on definitions of joint coordinate systems of various joints for the reporting of human joint motion--Part II: shoulder, elbow, wrist and hand. J Biomech, 38(5):981-992, 2005.
11. B. Coley, B.M. Jolles, A. Farron and A.K. Aminian. Detection of the movement of the humerus during daily activity. Med Biol Eng Comput., 47(5):467-74, 2009.
12. A.G. Cutti, A. Giovanardi, L. Rocchi, A. Davalli and R. Sacchetti. Ambulatory measurement of shoulder and elbow kinematics through inertial and magnetic sensors. Med Biol Eng Comput, 46:169-178, 2008.
13. I. Parel, A.G. Cutti, G. Fiumana, G. Porcellini, G. Verni and A.P. Accardo. Ambulatory measurement of the scapulohumeral rhythm: intra- and inter-operator agreement of a protocol based on inertial and magnetic sensors. Gait Posture. 2012 Apr; 35(4):636-40
14. A. Cappozzo, U. Della Croce, A. Leardini and L. Chiari. Human movement analysis using stereophotogrammetry. Part 1: theoretical background. Gait Posture, 21(2):186-96, 2005.
15. V. Camomilla, A. Cereatti, G. Vannozzi and A. Cappozzo. An optimized protocol for hip joint centre determination using the functional method. J Biomech, 39(6):1096-106, 2006.
16. S.S. Gamage and J. Lasenby. New least squares solutions for estimating the average centre of rotation and the axis of rotation. J Biomech., 35(1):87-93, 2002.

17. M. Lempereur, F. Leboeuf, S. Brochard, J. Rousset, V. Burdin and O. Rémy-Néris. In vivo estimation of the glenohumeral joint centre by functional methods: accuracy and repeatability assessment. J Biomech., 43(2):370-4, 2010.
18. H.J. Woltring. 3-D attitude representation of human joints: a standardization proposal. J Biomech., 27(12):1399-414, 1994.
19. A.G. Cutti, A. Cappello and A. Davalli. In vivo validation of a new technique that compensates for soft tissue artefact in the upper-arm: preliminary results. Clin Biomech (Bristol, Avon), 21 (Suppl 1):S13-9, 2006.

Section 5.2

Case study: Otto-Bock “Michelangelo”

Cutti AG, Parel I, Luchetti M, Rossi NC, Verni G.
eBook 2012, “Grasping the future”. Pages 59-77. ISBN 978-1-60805-438-1.

INTRODUCTION

In most daily activities upper limb and trunk have the goal to position and orient the hand in such a way that the hand can effectively and efficiently reach/grasp a desired object and transport it to the aimed target. When a prosthetic joint with intrinsic motor or sensorial limitations replaces either the end-effector or one of the joints in the upper-limb chain, compensatory movements take place in the remaining joints. Commonly, transradial amputees using a myoelectric prosthesis need to compensate the loss of the wrist flexion-extension movement and the availability of a single "tri-digital" pinch, resulting in non-physiological movements of elbow, shoulder, trunk and neck [1]. It is questioned to which extent the availability of more gripping patterns in the prosthetic hand can restore a more physiological shoulder kinematics during the execution of common activities.

Centro Protesi INAIL is active in the clinical assessment of all commercial multi-articulated hands. In this context, the biomechanics protocol presented in the previous sections is currently applied for the assessment of the prosthetic hand named Michelangelo, developed by Otto-Bock (D). After an overview of this new technology, we present the results from a case study involving an amputee who had the opportunity to use Michelangelo for a period of 3 months.

MATERIALS AND METHODS

A case study was conducted assessing the upper limb kinematics of a transradial amputee fitted with both a standard Otto-Bock Digital Twin hand (DT) and the novel Otto-Bock prosthetic hand named "Michelangelo" (M). The Michelangelo hand features are the wrist flexion-extension kinematics through a passive frictioned joint and three gripping patterns (i.e. lateral, tri-digital and pinch grip).

A 50-year-old male transradial amputee (GS) participated in this experiment after giving his informed consent. He has been using a myoelectric prosthesis for more than 15 years, for about 8 hours a day.

His affected side scapulo-thoracic, girdle-thoracic, humero-thoracic, elbow and wrist kinematics was measured in two sessions, applying the motion analysis protocol described in Section 5.1: the first session with DT and the second session with M, after 3 months of exclusive use. Among the ADLs, the subject performed a1) Jar transfer activity and 2) a Carton pouring task based on the SHAP scale [2]; 3) a task named Disk task, which consists in moving back and forth 3 times a Minnesota test disk over the table, from an area in front of the prosthetic hand to an area in front of the controlateral side. In order to have a reference for the kinematics, the sound side was collected too, in a third session.

RESULTS

Regarding the elbow pure movement assessment, the maximum flexion with the sound side was 134°, while it was limited to 108° and 115° with the socket for DT and Michelangelo hands, respectively. The range of motion was 135° for the sound side, while it was the same for the prosthetic side, namely 112°. The socket, therefore, limits the maximum flexion of the elbow, in a similar way between prostheses.

The graphical representation of the scapulo-humeral rhythm is reported in Figure 1 for the sound and affected side (using the M hand). Substantial differences exist both in terms of shapes and range of motion, for the same range of humerus elevation. In particular, the affected side features an increased retraction, lateral rotation and tilting, which are indicative of compensatory movements that might be due to muscle weakness or a degeneration of the rotator cuff, compared to the sound side. This suggests the need for a dynamic ecographic screening.

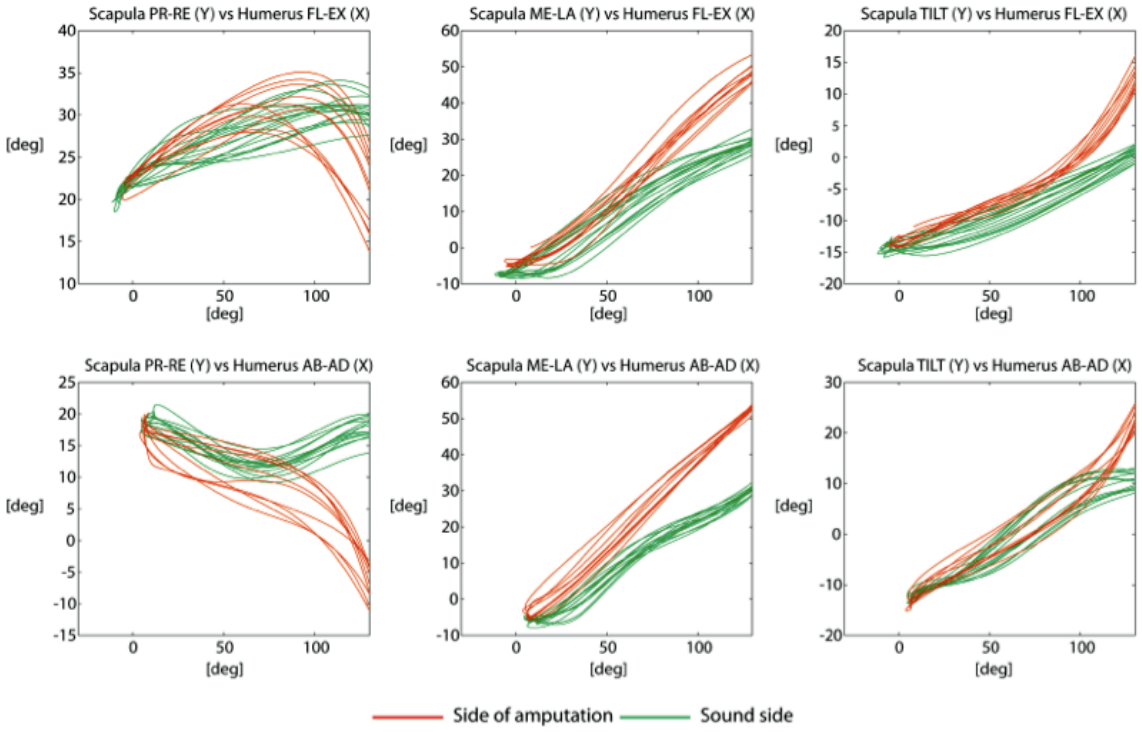

FIGURE 1. Graphical representation of the scapulo-humeral rhythm for the side with (red) and without (green) amputation.

Regarding the Jar task, scapula and humerus kinematic patterns are reported in Figure 2. The whole movement was divided into 6 phases, which were time-normalized: 1) reaching, 2) holding and

transport, 3) back to starting position, 4) reaching, 5) holding and transport, and 6) back to starting position. The percentages of movements were based on the sound side timing.

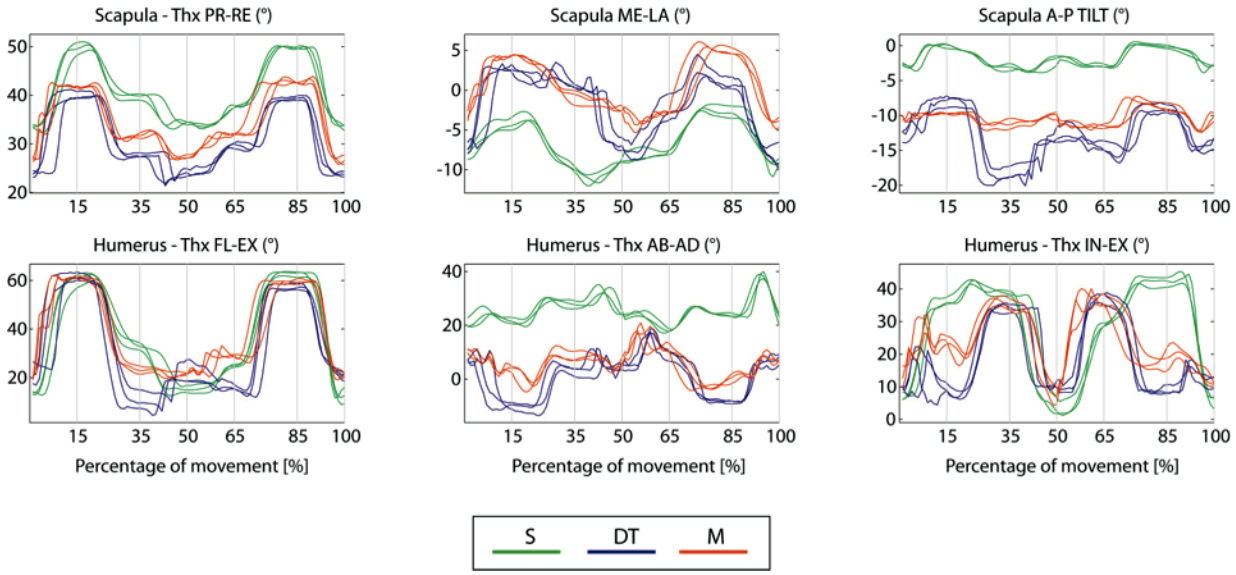

FIGURE 2. Kinematic patterns for the Jar task.

The most noticeable differences are that with the DT hand the patient approaches the object in adduction and with a relevant posterior tilting (Figure 3). On the contrary, with the sound and the M hand, the patient approaches the object in abduction and without almost relying on scapula tilting. Regarding the overall time taken to perform the activity, with the sound side the mean duration was 7s, while it was about 15s with both DT and M hands.

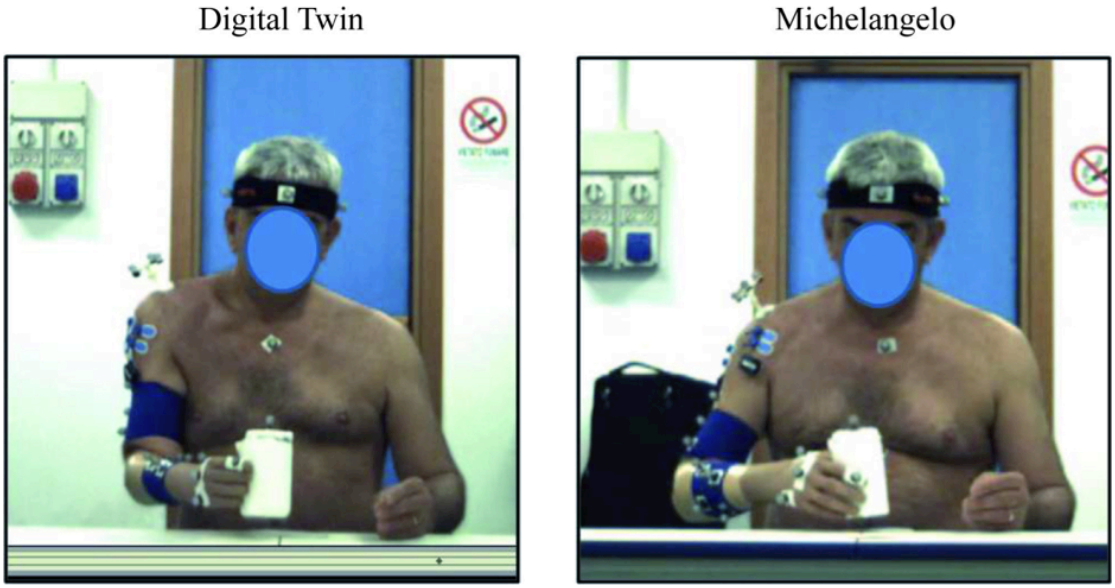

FIGURE 3. Snapshots from the sagittal video tape showing patient during the Jar task, with the DT and Michelangelo hands. A relevant change in scapula kinematics and humerus adduction can be noticed.

Regarding the Drinking task, Figure 4a reports the neck and thorax kinematics, Figure 4b scapula, humerus and elbow kinematics, while Figure 4c the movement of the chin marker (CH) over the percentage of movement in the anterior-posterior and cranio-caudal direction.

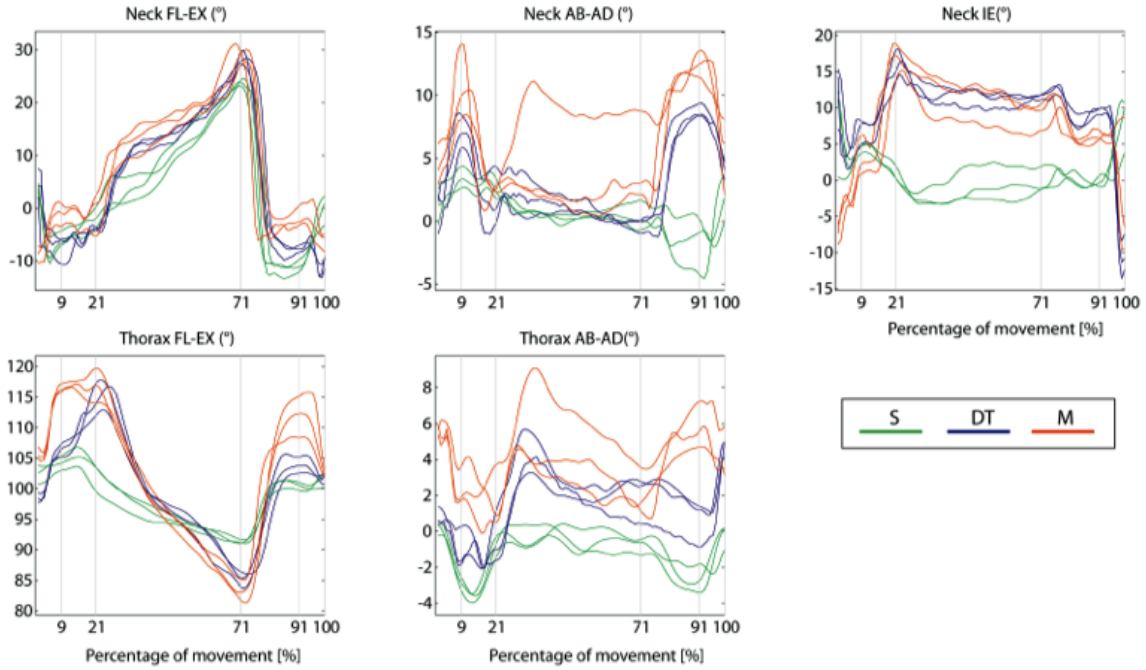

(a)

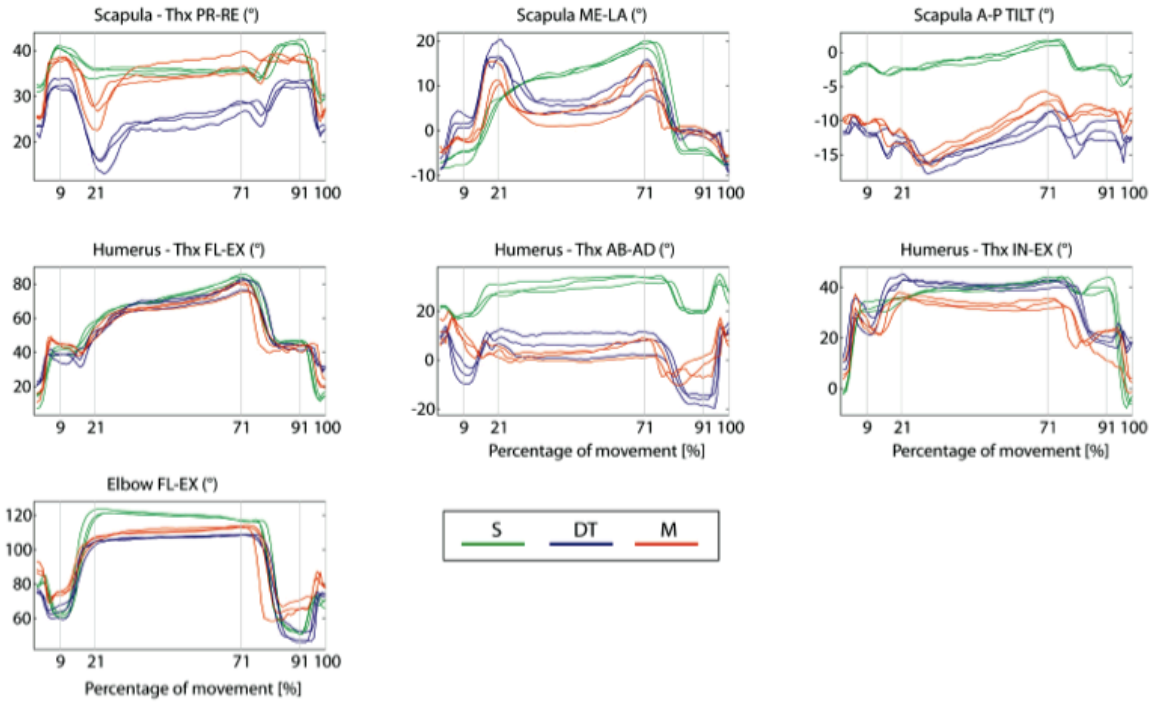

(b)

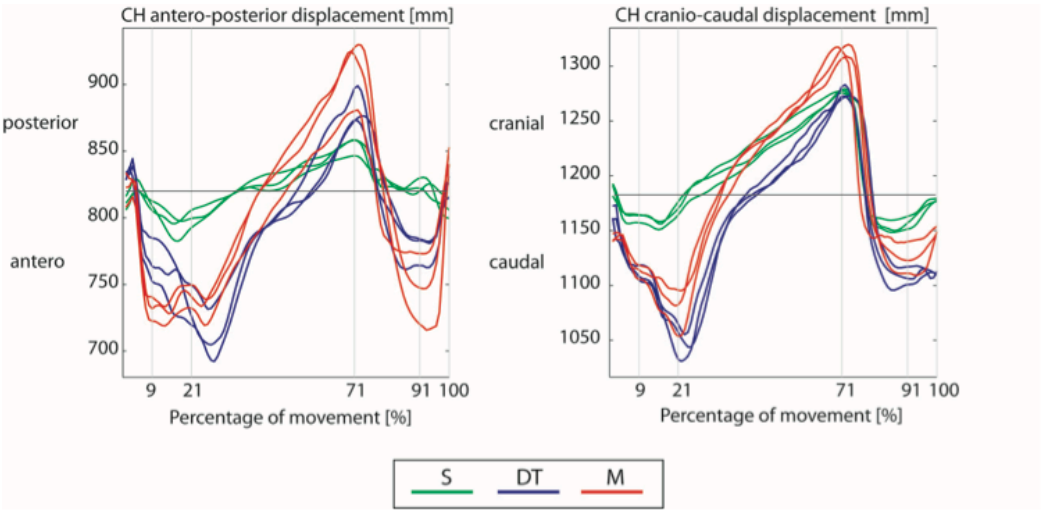

(c)

FIGURE 4. Kinematic patterns of thorax, neck (a), scapula, humerus, elbow (b) during the Drink task. The trajectory of the CH landmark (c) is also reported.

The task was divided into 5 phases, namely: 1) reaching the glass of water, 2) bringing it to the mouth, 3) drinking the water, 4) bringing back the glass to its original position, and 5) returning to the starting position. The percentages of movements were based on the sound side timing. The first relevant set of differences takes place when the glass touches the mouth (Figure 5). Due to limitations in elbow flexion and radio-ulna deviation in the prosthetic side (both with DT and M hands), the patient uses a different strategy to reach the target and not to spill water, namely moving into humerus adduction with scapula retraction, lateral rotation, anterior tilting and, most of all, head anteposition and thorax flexion. It is interesting to notice that neck flexion alone is not indicative of the strategy adopted by the patient. All other differences follow from this initial set.

FIGURE 5. Snapshots from the sagittal video tape showing the patient while drinking, with the sound and prosthetic side. A very relevant anteposition of the head can be observed, as quantified by the trajectory of CH in Figure 4c.

Regarding the Carton pouring task, Figure 6 reports the scapula and humerus kinematics, with the movement divided into 4 phases, namely: 1) reaching the carton, 2) pouring the water, 3) bringing back the carton to its original position, and 4) returning to the starting position. Percentages of movements were based on the sound side timing. Due to the lack of the active wrist prono-supination, the patient is forced to complete the pouring activity relying on increased scapula lateral rotation and humerus internal-external rotation compared to the sound side, both with the M and DT hand. However, with the M hand the amputee is able to reach the carton in abduction, similarity to the sound side, as seen with the Jar task. For what concerns the timing, the activity required about 11s for the sound side and about 20s with the prosthetic side.

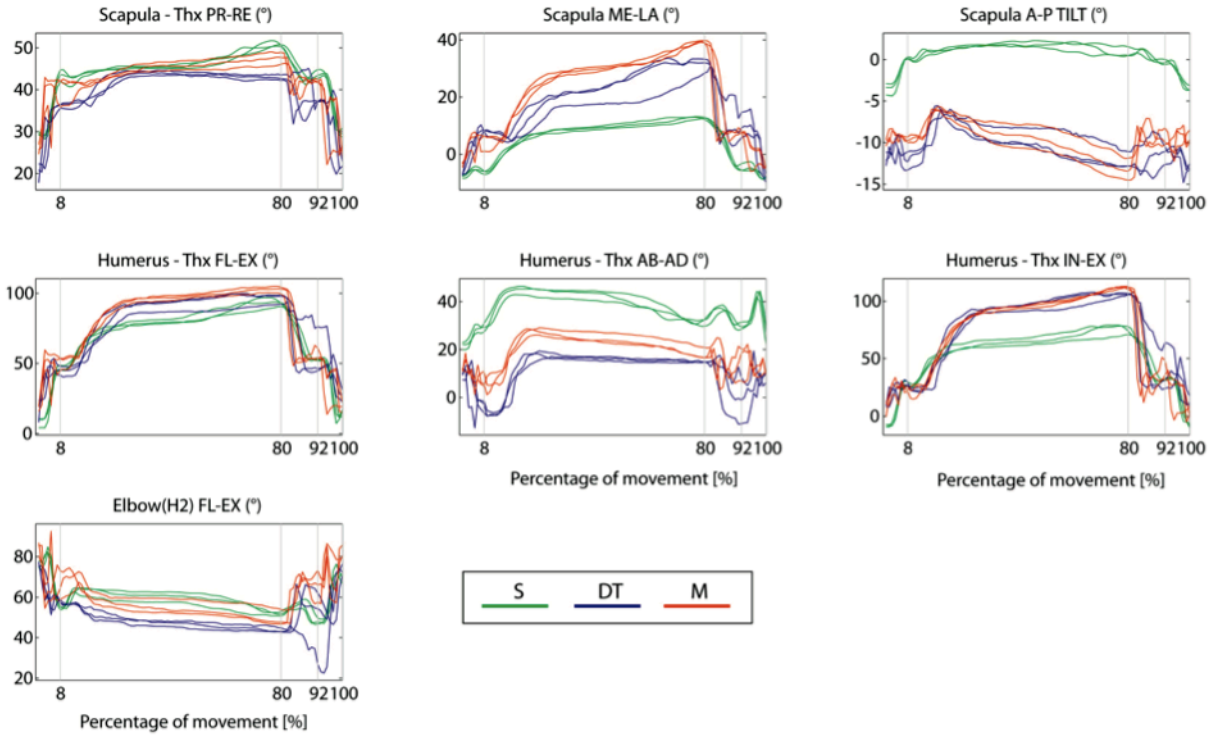

FIGURE 6. Kinematic patterns from the Pouring task.

Finally, results from the Disk task are similar between the different variations of the task, and therefore we will present only the case of the movement between position 1 and 3, i.e. from one side to the body to the other, on the same level. Figure 7 reports the kinematics for scapula and humerus.

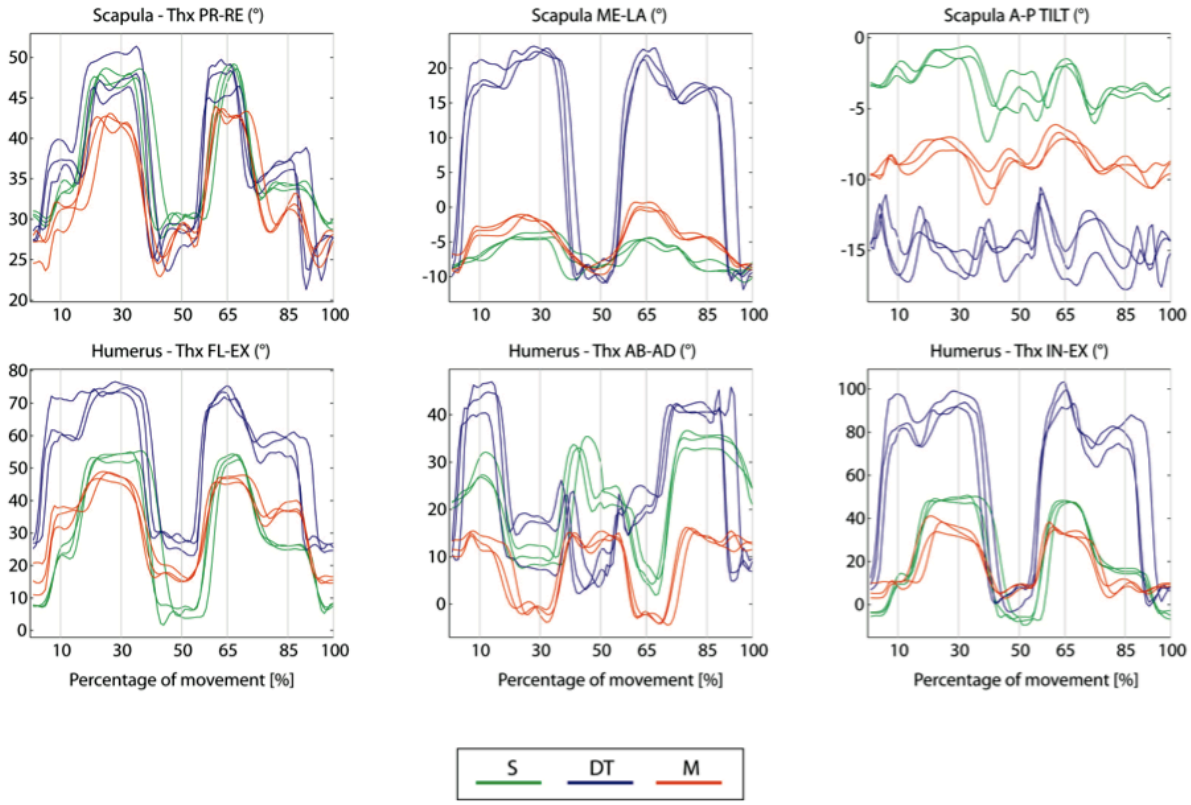

FIGURE 7. Kinematic patterns from the Disk task (from A1 to A3).

The movement was divided into 6 phases, namely: 1) reaching the disk in position 1, 2) grasping and moving the disk to position 3, 3) returning to the starting position, 4) reaching the disk in position 3, 5) grasping and moving the disk to position 1, 6) returning to the starting position. Percentages of movements were based on the sound side timing. For this task, the patient used the lateral grasping with the M hand. Due to this reason, major difference can be observed compared to the movement while using the DT hand (Figure 8). With this latter, the amputee is forced to perform the movement relaying on humerus flexion, abduction, internal rotation, and scapula lateral rotation. With the M hand and the sound side, the amputee avoids the subacromial impingement position. Timing is equally informative of the change between DT and M hands. With the DT hand the whole movement took 11s on average, while it took 7s with both the M hand and the sound side.

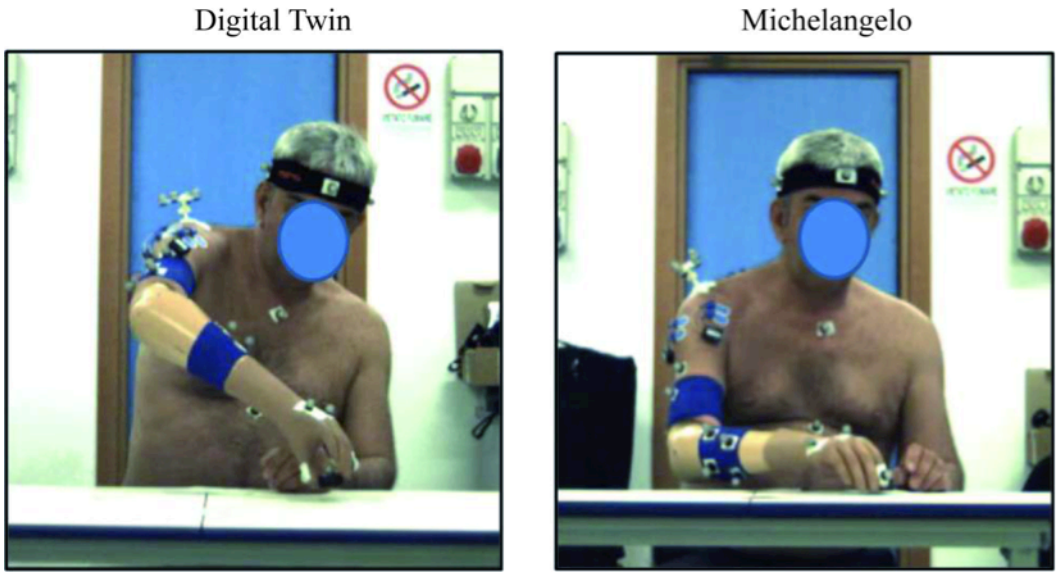

FIGURE 8. Snapshots from the frontal video tape showing the different approach following by G.S. to complete the Disk 13 task.

DISCUSSION

The biomechanical analysis brought in evidence differences between the upper-limb motion strategies while the patient uses DT, M hands and the sound side. Firstly, the amputee has to face an elbow flexion restriction, which most noticeably affected the drinking, with relevant compensatory movements. Secondly, the analysis of the scapulo-humeral rhythm revealed that the shoulder on the side of the amputation is probably affected as well. Further image-based analysis might lead to the set-up of specific rehabilitation exercises and treatments. Similarly to the Drinking task, the Pouring task highlighted differences between the prosthetic side and the sound side, with advantages for M hand in the more natural approach to the object, as also highlighted by the Jar task. The Jar task also showed that M hand allows the amputee to reduce the scapula tilting motion, with the scapula working in a more physiological way. Among the tasks, the Disk showed the most relevant improvements of M hand over DT hand in comparison with the sound side. The Disk task reproduces a very common working-place activity. M hand can thus lead to a major advantage over DT hand in terms of preservation of the shoulder joint by avoiding subacromial impingement positions.

CONCLUSIONS

Great changes are occurring in the upper-arm prosthetic field: innovative solutions are coming out from the laboratories to be used by patients in everyday life.

In order to offer successful solutions to patients and justify higher costs, it is necessary to intensify the activities of technology assessment, based on scientific evidences, which is possible only through the planning and execution of appropriate clinical trials. INAIL is moving in this direction by means of the research projects in progress at Centro Protesi INAIL.

The presented proposal is intended as a base for discussion within the community of professionals involved in prosthetics.

REFERENCES

1. S.L. Carey, M.J. Highsmith, M.E. Maitland and R.V. Dubey. Compensatory movements of transradial prosthesis users during common tasks. Clin Biomech, 2008. 23: 1128-1135.
2. C. M. Light, P. H. Chappell and P. J. Kyberd. Establishing a standardized clinical assessment tool of pathologic and prosthetic hand function: Normative data, reliability, and validity. Arch Phys Med Rehabil 2002. 83: 776-783.

PART 3

Applications of ISEO for performance assessments

In this section studies about the application of ISEO in sport contexts are reported. The purpose of these studies was to understand if the application of ISEO was feasible in specific contexts of interest, i.e. Formula 1 pit-stop (Chapter 6) and baseball pitching (Chapters 7 and 8).

Chapter 6 shows how ISEO was used in a feasibility study for the assessment of upper limb kinematics of a Formula 1 pit-crew during the pit-stop, assessing the kinematics of shoulder and elbow.

Chapters 7 and 8 report studies about the application of ISEO for upper limb assessment in baseball pitchers. Chapter 7 shows a pilot study that aims at applying ISEO for the evaluation of the scapulo-humeral coordination, looking for early predictive sign of shoulder injuries in the 3D kinematics. Chapter 8 reports a study on a larger group of pitchers and the aim was to find predictive scapula kinematic factors that can help for the prevention of possible shoulder injuries.

Chapter 6

A pilot study about the upper limb kinematics of a pit crew of a F1 racing team during the pit stop

Parel I, Cutti AG, Borra F, Verni G.
International Shoulder Group Conference 2012, Proceeding.

INTRODUCTION

The pit stop phase represents a crucial part of the Formula 1 (F1) race competition. During the pit stop a group of about 20 mechanics, called “pit crew”, provides services to the racing car, most commonly refueling and tires changing. During the tires changing the mechanics should execute fast, synchronized and stereotyped movements in order to reduce the service time and to lead to quicker and repeatable performances. Quantitative analysis of movements could support in better understanding the work requirements and in setting up a physical training to prepare each mechanic to the specific activity, reducing the risk of injuries. The aim of the present study was to verify the feasibility of this new approach by collecting and analyzing the whole body kinematics of a pit crew during the tires changing in a pit stop simulation. In this abstract we will report, in particular, about shoulder and elbow kinematics.

METHODS

The pit crew involved in the tires changing of a F1 racing team was considered during repeated pit stop simulations. A replica of the pit stop workplace was installed in a covered hangar. A F1 car was available. For the simulation, the car was initially positioned 20 m away from the workplace with a driver inside. Then a group of 4 mechanics hand-pushed the car to mimic the arrival of the car to the workspace. When approaching the pit stall, the driver brake and the pit-crew performed the tire-change as fast as possible. The whole body kinematics of one mechanic per each role was assessed, namely: the gunman; the front and rear jack men (JM); the front and rear tire carriers assigned to the removal of the old tire (RC); the front and rear tire carriers assigned to the insertion of the new tire (IC). For each mechanics three pit stop simulations were measured and the best one was considered for the further analysis. To collect the shoulder (humerus relative to the thorax) and elbow (forearm relative to the humerus) kinematics of both sides of each subject, the ISEO protocol was used [1,2], which is based on a portable acquisition system (Xsens Technologies, NL). Five MTx inertial and magnetic sensors were placed on the sternum, humerus and forearm, through elastic cuffs that embed specific sensors holders (Figure 1). The sensors warm up (30 s) and the anatomical calibrations were performed in a magnetic disturbance-free area of the hangar. Shoulder kinematics was assessed considering the XZY Euler decomposition because the main elevation plane was the sagittal plane: flexion-extension (sh_FlexExt), abduction-adduction (sh_AbAd) and internal external rotation (sh_IntraExtra). Elbow kinematics was assessed considering the XZY Euler decomposition: flexion-extension (el_FlexExt), carrying angle (el_CA) and pronation-supination (el_ProSup).

FIGURE 1. Sensors placement for the motion analysis.

All angles were described with respect to time. Before, during and after the pit stop, the cross-talk in joint angles was checked to verify the effect of possible magnetic interferences. Video recordings were also used in order to collect a visual feedback of the movements. The kinematics was segmented in sub-phases by means of both the kinematic and the video signals. Then, the largest ROMs and the corresponding video frames where identified by means of visual inspection.

RESULTS

The kinematics was interpreted assessing the largest ROMs and the time required for their execution, role-by-role. For the front JM the largest ROMs took place during the "swing phase", i.e. when the jack was taken away form the front wing: 90° variation for sh_Ext in 640 ms for both sides; 100° for sh_Extra in 800 ms for the right side; 90° for el_Flex in 450 ms for the right side and in 250 ms for the left (Figure 2).

For the rear JM the most critical phase was when he had to push down the jack in order to raise the car. The largest ROMs were found for the right side: 100° for sh_Flex and sh_Intra in 300 ms followed by the opposite movements with the same range in other 300 ms; 50° for sh_Ad in 500 ms; 110° in el_Ext in 360 ms.

For the front RC the largest ROMs were during the removal of the old tire: 80° for sh_Ext in 800 ms for the right side; 55° for sh_Ext in 550 ms for the left side.

For the front IC assigned to the new tire the most critical events was the insertion of the tire: 65° of sh_Flex in 350 s and 50° of el_Ext in 300 ms.

For the rear RC the most critical ROMs were during the removal of the old tire: for the left side, 55° for sh_Ad in 440 ms, 50° for el_Ext in 390 ms and 60° for el_Sup in 350 ms; for the right side 50° for sh_Flex in 270 ms.

For the rear IC the most critical phase is the insertion of the tire: 100° and 75° for respectively left and right sh_Flex, in 500 ms; 50° of el_FlexExt in 500 ms for the left side; 50° for el_Sup for the right side in 350 ms. For the gunman there largest ROM is 65° of sh_Ext in 600 ms for both sides.

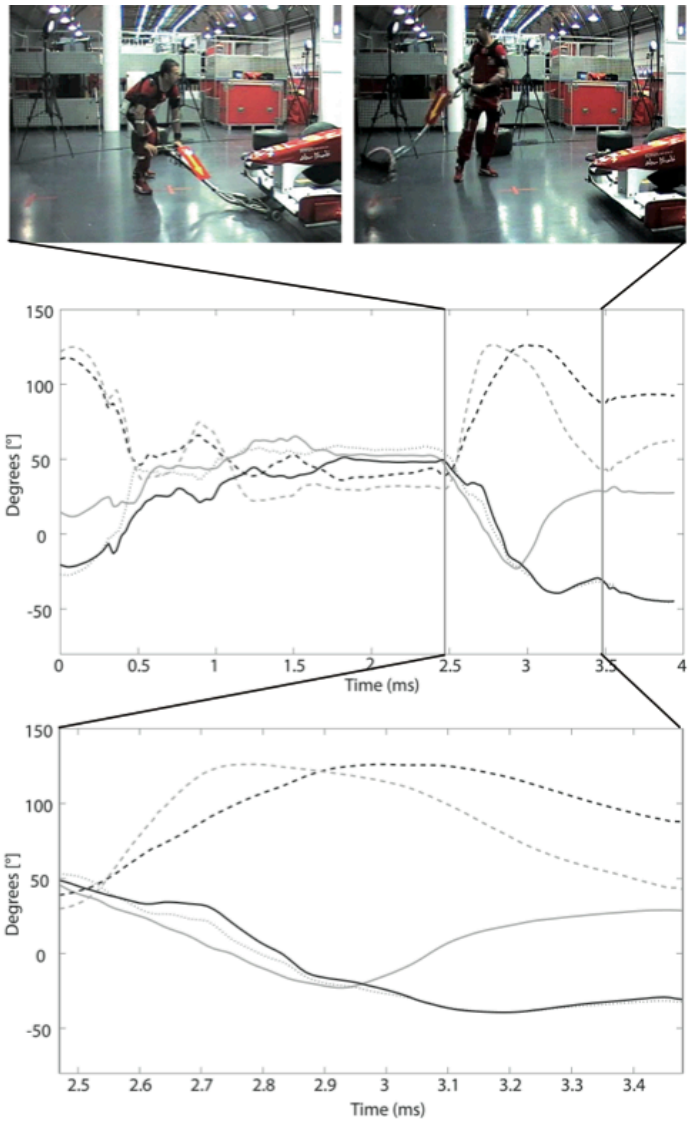

FIGURE 2 Analysis of the kinematics of the front JM. At the top, the two frames of start and end of the swing phase, which is the most critical. At the center, the kinematic angles of the whole activity of the JM: black solid line, sh_FlexExt right side; gray solid line, sh_FlexExt left side; black dotted line, sh_IntraExtra right side; black dashed line, el_FlexExt right side; gray dashed line, el_FlexExt left side. At the bottom, the

detail about the kinematics during the swing phase.

CONCLUSIONS

A study about the kinematics of the upper limb was conducted for a pit stop crew. The members with the highest shoulder kinematic demands were assessed, i.e. the jack men, the gunman and the tires carriers. The purpose of the study was to test the applicability of ISEO for the collection and assessment of the shoulder and elbow kinematics and to start identifying the most critical sub-phases of the movement for each mechanic. The response was positive, thanks to the fast set-up of the system and the possibility to have kinematic data in real-time: the whole-body kinematics of 7 mechanics was acquired and processed in 5.5 hours, without working environment adaptations. Moreover, the magnetic disturbance resulted not to interfere with the data collection. Kinematic tests performed before, during and after the pit stop showed that there was an acceptable cross-talk, similar to the calibration condition. Synchronized video captures and kinematic data are relevant for a proper analysis of the technical gestures: a shoulder and elbow kinematics visual feedback is necessary in order to understand the complex kinematics of the movement sequences. The data collected during this study permitted to identify, so far, the largest single-joint ROMs, which were typically associated to short time intervals and acceleration/decelerations. On these bases, future efforts will be toward the description of:

1) whole-body kinematic-chain critical events;
2) definition of an optimized movement, aiming to reduce the risk of injury and to obtain fast and consistent performances;
3) the set-up of a role-specific neuromuscular physical training program.

REFERENCES

1. Cutti AG, Giovanardi A, Rocchi L, Davalli A, Sacchetti R. (2008) Ambulatory measurement of shoulder and elbow kinematics through inertial and magnetic sensors. *MBEC*. 46: 169-78
2. Parel I, Cutti AG, Fiumana G, Porcellini G, Verni G, Accardo AP. (2012) Ambulatory measurement of the scapulohumeral rhythm: intra- and inter-operator agreement of a protocol based on inertial and magnetic sensors. *Gait & Posture*. 35(4): 636-40

Chapter 7

Upper limb functional evaluation on baseball pitchers through a portable 3D tracking system based on inertial sensors

Pellegrini A, Garofalo P, Cutti AG, Parel I, Tonino P, Paladini P, Campi F, Porcellini G.
Journal of Biomechanics 2012, 43, S69.

INTRODUCTION

During baseball pitching, the shoulder is exposed to micro traumatic stress. Due to traumatic events, baseball can lead to severe and debilitating upper limb diseases and shoulder injury is a potentially career-ending cause. For this reason, the prevention of injuries, through the upper limb clinical assessment of pitchers is important as well as to reach optimal performance. Recently, an upper limb clinical protocol [1] was developed and validated on patients with shoulder pathologies [2]. The protocol allows the measurement and the functional evaluation by means of 3D kinematics analysis of scapulo-thoracic, humero-thoracic and elbow joints. The aim of this work was to apply the same clinical protocol for the evaluation of baseball pitchers, looking for early predictive sign of shoulder injuries in the 3D kinematics.

METHODS

Three pitchers (20 ± 2.6 years-old) participated to the study, after having signed informed consent. The protocol described in [1] was adopted. Four MTx (Xsens Technologies) units were positioned as described in Figure 1.

FIGURE 1. Positioning of MTx units on the upper limb

The scapulo-humeral rhythm (SHR) was assessed considering the medio-lateral rotation (ME-LA) and protraction-retraction (PR-RE) of the scapula during flexion-extension (FE) and abduction-adduction (AA) movements of the shoulder. The humero-thoracic external rotation (EXT) was

calculated during internal-external rotation movements (IE) when the humerus is 90 degrees abducted. The evaluations were repeated before (S1) and after 60 pitches (S2) and then after 24 hours (S3). Ranges of motion (ROM) and patterns (Figure 2) of SHR and EXT for each session of measurement (S1, S2, S3) were *qualitatively* compared each other.

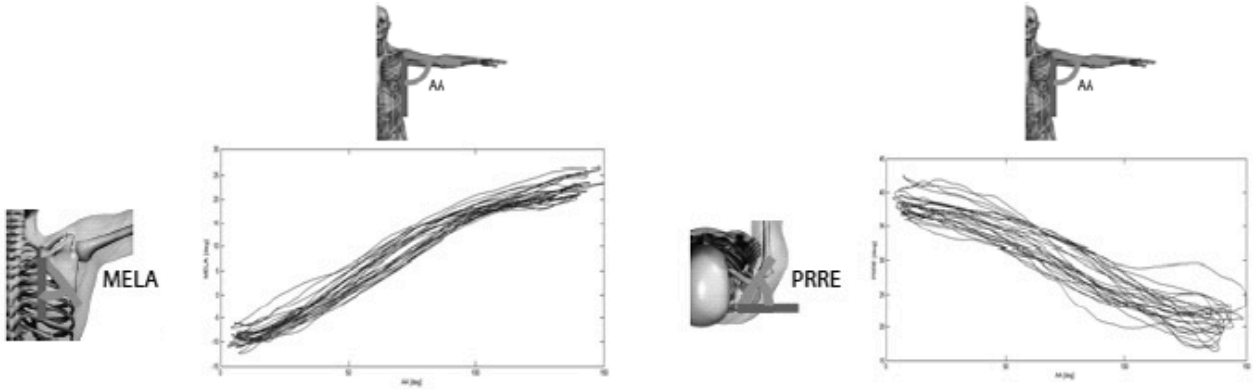

FIGURE 2. Coordination between scapulo-thoracic and humerothoracic joints during ab-adduction movements. Medio-lateral rotation (ME-LA) and protraction-retraction (PR-RE) of the scapulothoracic joint are visualized in the ordinates.

RESULTS

All the subjects showed good repeatability in the SHR pattern, indicating stereotyped movements. The low smoothness of the curves indicated fatigue.

Subject 1 presented consistent ROM in all the degrees and movements examined, indicating no particular shoulder alterations due to the pitching. Subject 2 presented higher range in IE in S2 compared with S1, during IE movements. However, the starting range was restored in S3 and similarly, during AA movements, for the ROM of AA. Moreover, the movements of the scapula (ME-LA and PR-RE) were reduced in S3 with respect to S2, indicating alterations occurring between S1 and S2, and an improvement in the SHR after 24 hours (S3). Differently from the others, in Subject 3 the external rotation was still reduced after 24 hours. Furthermore, FE and AA were reduced in S2 in the attempt to compensate this effect increasing the scapula movements. This behavior is maintained after 24 hours (although the ROM increased), indicating an evident alteration in the shoulder kinematics.

DISCUSSION

Larger population of pitchers is needed to draw conclusions. Results indicate the system is able to visualize and monitor alterations in shoulder kinematics, measuring simple shoulder movements. Real-time pitching measurement could augment the knowledge about the behavior of the shoulder during training, for performance and injury prevention purposes.

REFERENCES

1. Cutti AG, Giovanardi A, Rocchi L, Davalli A, Sacchetti R. Ambulatory measurement of shoulder and elbow kinematics through inertial and magnetic sensors. Med Biol Eng Comput 2008. 46(2): 169–178.
2. Cutti A, Garofalo P, Parel I, Fiumana G, Porcellini G. Intra- and inter-rater reliability of the scapulohumeral rhythm measured by a protocol based on inertial and magnetic sensors. Gait & Posture 2009. 30: S17.

Chapter 8

Jobe's test and motion analysis evaluation in pre and post training of baseball pitchers

Pellegrini A, Tonino P, Parel I, Palladini P, Campi F, Porcellini G.
International Convention on Science, Education and Medicine In Sport 2012, Proceeding.

INTRODUCTION

Baseball pitching injuries are due to micro-traumas and repetitive motion. Altered scapular orientation has been implicated in shoulder injury [1].

An upper limb functional evaluation protocol based on MTx (Xsens Technologies NL) was developed [2] for the kinematics analysis of the scapulo-humeral rhythm (SHR). The aim of this work was to apply the protocol on a larger population of baseball pitchers, looking for indications to prevent possible shoulder injuries.

METHODS

Thirteen collegiate baseball pitchers (age 20±2.6) participated in this study. All pitchers signed informed consent. SHR was evaluated before and after 60 pitches by evaluating elevation (AA) of the humerus in the frontal plane, repeated after 24 hours. In particular, the subsequent parameters were calculated: the maximum Range of Motion (ROM) of the humerus, the maximum ROM of the scapula upward-backward rotation, protraction-retraction and posterior-anterior tilting. SHR during each session of measurement (S1, S2, S3) were compared. In the same way, Jobe's test (90° of forward shoulder elevation in the scapular plane in maximal internal rotation) was performed, looking for supraspinatus weakness.

RESULTS

Subjects were divided into 3 groups. Results from three representative subjects are presented in Table 1.

GROUP-SESSION	MAX Lateral elevation (deg)	MAX Scapula Upward-Backward rotation (deg)	MAX Scapula Protraction-Retraction (deg)	MAX Scapula Posterior-Anterior tilting (deg)	JOBE TEST
Group1-S1	143.0	24.0	35.3	35.7	0
Group1-S2	153.0	27.1	36.7	39.3	1
Group1-S3	157.0	26.2	37.5	42.0	0
Group2-S1	163.0	35.8	28.4	12.3	0
Group2-S2	151.0	23.9	24.3	20.9	1
Group2-S3	176.0	31.9	29.4	15.2	0
Group3-S1	163.0	33.9	33.9	20.5	0
Group3-S2	156.0	39.0	33.7	17.4	1
Group3-S3	161.0	35.5	40.5	21.7	0.5

TABLE 1. Results from three representative subjects.

Group A did not demonstrate any changes between the three sessions, suggesting no particular shoulder alterations. Group B presented alterations from S1 to S2, and an improvement after 24 hours but the early SHR was not completely restored. Group C showed an improvement between S1 and S2, kept at 24 hours (S3).

DISCUSSION

Outcome from Jobe's test was not supported by results from motion analysis. Pitchers manifested a different behavior in the recovery time. Group 2 may be at an increased risk for developing injuries associated with decreased scapular upward rotation, such as subacromial impingement and glenohumeral instability.

The monitoring here described can explain the behavior of the shoulder during training, and provide support for injury prevention.

REFERENCES

1. Jobe CM, Pink MM, Jobe FW, Shaffer B. Anterior shoulder instability, impingement, and rotator cuff tear: theories and concepts. In: Jobe FW, ed. Operative Techniques MO: Mosby; 1996:164–176.
2. Parel I, Cutti AG, Fiumana G, Porcellini G, Verni G, Accardo AP. Ambulatory measurement of the scapulohumeral rhythm: Intra- and inter-operator agreement of a protocol based on inertial and magnetic sensors. Gait & Posture 2012; 35(4):636-40.

CONCLUSIONS

The aim of this thesis was to validate and assess the applicability of a shoulder ambulatory motion analysis protocol for clinical investigations.

In order to reach these goals several investigations were needed and the following results were obtained:

- ISEO inter-sessions agreement was generally acceptable for all scapula rotations (limitations exist for PR-RE) and results obtained were comparable or even better than those reported in the literature. These high intra- and inter-operator agreement support the use of ISEO for an every-day clinical application;

- "monolateral" and "differential" prediction bands and intervals were computed based on a large sample of asymptomatic subjects. For the first time the Bootstrap technique was applied for this type of data and results highlighted the superiority of this technique over parametric methods. In addition, for the first time age-stratified reference data for the scapulo-humeral coordination were provided;

- the agreement between two motion analysis protocols was investigated, comparing ISEO to a protocol currently in use in another motion analysis laboratory and based on the current gold-standards, i.e. scapula tracker and ISB anatomical frame definition. Results obtained might be interpreted based on the aim of the clinical study. However, the best results were obtained for the analysis of the interchangeability of the two protocols for the acquisition of ME-LA;

- regarding the application of ISEO for clinical assessments, a longitudinal study was conducted to analyze the recovery of patients surgically treated for rotator cuff tear. The investigations led to important results: the definition of a set of 3 criteria for the identification of a single controlateral asymptomatic side session that can be assumed as reference; at 90 days from the surgery most patients increase humerus elevation at the expense of scapula compensatory movements, especially during humerus flexion; measures of scapula rotations can be used to modify the Constant score in order to introduce, in this clinical scale, information about the restoration of scapula kinematics;

- regarding the application of ISEO for performance assessments, the studies conducted showed that ISEO can be applied for the collection of kinematic data in sport contexts, such as the tires changing in a pit stop simulation, and that ISEO is suitable for the analysis of shoulder kinematic alterations in baseball pitchers, providing support for injury prevention in athletes.

Results were presented at national and international conferences and were submitted to scientific journals, receiving good responses from reviewers.

The aim of this thesis was to carry on a scientific project started a few years ago, when ISEO was created and the main goal was to develop a tool that could provide quantitative measures, helping clinicians in better understanding a pathology or make them change opinion on the treatment of a patient. This thesis falls in line with this proposal, providing a scientific support for an effective application of ISEO in clinics.

In order to ease the application of ISEO in the clinical practice, further investigations can be conducted to create a *performance index* that summarize all the quantitative information provided by the protocol and, possibly, information from other evaluation scales, designing a unique parameter for shoulder assessment.

RINGRAZIAMENTI

Ed ora i ringraziamenti..

Ai miei genitori che adoro e che mi hanno sempre sostenuta senza alcuna riserva.
Le mie zie e i miei cugini, che ogni giorno mi ricordano l'importanza della famiglia e della condivisione delle esperienze positive ed anche negative.
I miei amici, colonna portante della mia vita. Un "ufficiale" ringraziamento da capitan Parel a tutta la ciurma: Lalla, Vale, Eli, Giuly, Leo e Giek.
La mia super squadra di pallavolo. Compagne in campo ma anche nella vita!
Ringraziamento alla mia amica "per sempre", la Fede, ti voglio un'immensità di bene!
Andrea, l'uomo invincibile, un amico, il mio riferimento. Grazie per il sapere che mi hai trasmesso e il sostegno e la fiducia che hai sempre riposto in me!
Il Prof. Accardo, per avermi dato quest'opportunità e per tutto l'appoggio ricevuto.
A special thanks to Andreas and Howard, for the unique opportunity that you gave me. You have been very inspiring to me and you gave me the chance to prove myself. Thank you so much!
Un doveroso ringraziamento a tutto lo staff clinico con cui ho collaborato: il Dott. Porcellini, Gabriele Fiumana, Andrea Pellegrini e la Manu.
Infine un grazie speciale a tutti i miei colleghi dell'EX ricerca INAIL: Andrea (ancora), Michi, Aurora, Davide, Biagio, Gruppio, Enrico, Nino, Marti (psycho), Marti (ing), Betta e Diego (ci siete tutti vero??). Quanti bei momenti passati insieme. Siamo stati proprio bene e soprattutto avevamo creato un bellissimo gruppo affiatato. E' stato bello lavorare con voi e vi auguro tutto il bene del mondo…!